



This is to certify that the

dissertation entitled


GAS SEPARATION AND PERVAPORATION OF CHEMICALLY MODIFIED  
POLY[1-TRIMETHYLSILYL-1-PROPYLENE] MEMBRANES

presented by

Jingpin Jia

has been accepted towards fulfillment  
of the requirements for

Ph.D. degree in Chemistry

  
Major professor

Date 17 April 1997



3 1293 01579 6026



**PLACE IN RETURN BOX** to remove this checkout from your record.  
**TO AVOID FINES** return on or before date due.

DATE DUE	DATE DUE	DATE DUE
<div> <div>_____</div> <div> <div>APR 08 2003</div> <div>08 01 06</div> </div> <div>_____</div> </div>	<div>_____</div>	<div>_____</div>
<div>_____</div>	<div>_____</div>	<div>_____</div>
<div>_____</div>	<div>_____</div>	<div>_____</div>
<div>_____</div>	<div>_____</div>	<div>_____</div>
<div>_____</div>	<div>_____</div>	<div>_____</div>
<div>_____</div>	<div>_____</div>	<div>_____</div>

MSU Is An Affirmative Action/Equal Opportunity Institution

c:\pic\datedue.pm3-p.

**GAS SEPARATION AND PERVAPORATION OF CHEMICALLY MODIFIED  
POLY[1-TRIMETHYLSILYL-1-PROPENE] MEMBRANES**

**By**

**Jingpin Jia**

**A DISSERTATION**

**submitted to**

**Michigan State University**

**in partial fulfillment of the requirements**

**for the degree of**

**DOCTOR OF PHILOSOPHY**

**Department of Chemistry**

**1997**



## ABSTRACT

### GAS SEPARATION AND PERVAPORATION OF CHEMICALLY MODIFIED POLY[1-TRIMETHYLSILYL-1-PROPYNE] MEMBRANES

By

Jingpin Jia

Poly[1-trimethylsilyl-1-propyne] (PTMSP) has the highest gas permeability coefficient of any known polymer. It is a potential high productivity membrane material when used for gas separation and it is also one of the few polymers that permeates ethanol preferentially against water. Thus it is potentially useful for separating ethanol from dilute aqueous solution. However, its selectivity for gas separation and liquid separation is relatively low, and the high gas permeability has been reported to be unstable with time, with the permeability coefficient of oxygen decreasing to 1/10 of the original value after 100 days when stored under vacuum.

We believe the permeability decline is caused by the slow interdiffusion of polymer coils in the solid state. Several methods were attempted in this study to cross-link the PTMSP membranes in order to stabilize the permeability. PTMSP membranes were successfully cross-linked via addition of bis(aryl azides) and by preparing copolymers that contain azide groups poly[1-trimethylsilyl-1-propyne-*co*-1-(4-azidobutyldimethylsilyl)-1-propyne]. Both photo irradiation and thermal treatment initiated the cross-linking. Photo-

crosslinked membranes (either by bis(aryl azides) or copolymerization) showed higher selectivity for oxygen/nitrogen separation with lower permeability than PTMSP membranes. Photo-crosslinked membranes with certain cross-linking degrees showed higher selectivities than the commercial membranes with comparable permeabilities. Thermal-crosslinked membranes showed little changes in permeability and selectivity. All cross-linked membranes resulted in a stabilized permeability compared to PTMSP membranes when stored in vacuum. This is believed due to the restriction of inter-chain diffusion caused by the cross-linking, which helped to maintain the high free volume and therefore stabilized the permeability.

In studies of ethanol/water separation through PTMSP membranes, we attempted to use solubility parameters,  $\delta$ , as a guide in the synthesis and modification of ethanol-selective membranes. A variety of modified PTMSP membranes were used as pervaporation membranes for ethanol/water separation. The solubility parameters of these membranes were obtained by inverse gas chromatography, swelling measurements, and the group contribution method. There is difficulty in achieving a quantitative relationship between the solubility parameter of polymer membranes and pervaporation results of ethanol/water separation, and both the free volume and solubility parameters of the membranes must be considered in the design of membranes. Some modified membranes showed higher separation factors compared to PTMSP membranes when used for ethanol/water separation.

## ACKNOWLEDGMENTS

I would like to express thanks to Professor Gregory L. Baker for his guidance, encouragement, and patience on my research. A work such as this would not be possible without his assistance. It has been my privilege to have had him as my preceptor. What I have learned from him is far beyond chemistry itself, and it will continue to influence me in the future.

I would also like to thank Professors John Allison, Gary Blanchard, Jeffrey Ledford, Alec Scranton and Victoria McGuffin for their assistance. I would like to thank professor Peter Wagner for allowing me to use the photo reactors and UV spectrometer in his lab. Many thanks go to the members in Professor Baker's group, present and past, who helped me out of the hard times and made my experience at MSU enjoyable.

I owe a great deal to the many friends with whom I shared lots of frustration and happiness.

I wish to thank my parents for the love and support they have provided in my life. I want to thank my husband, Jian, for his love and patience, and I thank my daughter, Jacqueline, for so much joy she brings to me.

## TABLE OF CONTENTS

List of Tables.....	viii
List of Figures.....	x
List of Schemes.....	xiii
<b>Chapter 1. Introduction.....</b>	<b>1</b>
1.1. Membrane separation processes.....	2
1.2. Features of poly[1-trimethylsilyl-1-propyne].....	12
1.3. References.....	17
<b>Chapter 2. Cross-linking of Poly[1-trimethylsilyl-1-propyne] Membranes using bis(aryl azides).....</b>	<b>21</b>
2.1. Introduction.....	21
2.2. Experimental.....	23
2.3. Results and Discussion.....	36
2.4. Conclusions.....	51
2.5. References.....	52
<b>Chapter 3. Cross-linking of Poly[(1-trimethylsilyl)-1-propyne] Membranes through the Functionalization of Allylic Methyl Group.....</b>	<b>54</b>

3.1. Introduction.....	54
3.2. Experimental.....	58
3.3. Results and Discussion.....	61
3.4. Conclusions.....	74
3.5. References.....	75
 <b>Chapter 4. Cross-linking of Poly[1-trimethylsilyl]-1-propyne] Membranes by Introducing Cross-linking Sites through Co-Polymerization.....</b>	 <b>76</b>
4.1. Introduction.....	76
4.2. Experimental.....	77
4.3. Results and Discussion.....	83
4.4. Conclusions.....	100
4.5. References.....	101
 <b>Chapter 5. Study of Ethanol / Water Pervaporation Through Modified PTMSP Membranes.....</b>	 <b>102</b>
5.1. Introduction.....	102
5.2. Experimental.....	109
5.3. Results and Discussion.....	113
5.4. Conclusions.....	128
5.5. References.....	128

<b>Chapter 6. Summary and Future Work.....</b>	<b>132</b>
6.1. Summary.....	132
6.2. Future work.....	136
6.3. References.....	137
 <b>APPENDIX.....</b>	 <b>138</b>

## LIST OF TABLES

Table	Page
Table 2.1. Permeability coefficients of oxygen, $P(O_2)$ , nitrogen, $P(N_2)$ , and the oxygen/nitrogen separation factor, $\alpha$ , at $23 \pm 1$ °C, for PTMSP and photo-crosslinked PTMSP membranes.....	40
Table 2.2. Permeability coefficients of oxygen, $P(O_2)$ , nitrogen, $P(N_2)$ , and the oxygen/nitrogen separation factor, $\alpha$ , at $23 \pm 1$ °C, for PTMSP and thermal-crosslinked PTMSP membranes.....	43
Table 2.3. Swelling and density of the membranes.....	44
Table 2.5. Temporal stability of the membranes stored under vacuum.....	50
Table 3.1. Summary of methods used for introducing azide into PTMSP at allylic position.....	73
Table 4.1. Elemental analysis results of poly[1-trimethylsilyl-1-propyne-co-1-(4-azidobutyldimethylsilyl)-1-propyne] with various contents of $N_3$ .....	82
Table 4.2. Permeability coefficients of oxygen, $P(O_2)$ , nitrogen, $P(N_2)$ , and the oxygen/nitrogen separation factor, $\alpha$ , at $23 \pm 1$ °C, for thermally crosslinked poly[1-trimethylsilyl-1-propyne-co-1-(4-azidobutyldimethylsilyl)-1-propyne] copolymer membranes.....	95
Table 4.3. Permeability coefficients of oxygen, $P(O_2)$ , nitrogen, $P(N_2)$ , and the oxygen/nitrogen separation factor, $\alpha$ , at $23 \pm 1$ °C, of photo-crosslinked poly[1-trimethylsilyl-1-propyne-co-1-(4-azidobutyldimethylsilyl)-1-propyne] copolymer membranes.....	96
Table 4.4. The pycnometric densities of poly[1-trimethylsilyl-1-propyne-co-1-(4-azidobutyldimethylsilyl)-1-propyne] copolymer membranes under various treatment.....	98
Table 4.5. Temporal stability of the crosslinked copolymer membranes stored under vacuum.....	99
Table 5.1. Stationary Phases and Column Parameters.....	113

<b>Table 5.2.</b>	<b>Pervaporation Results of Dilute Ethanol Aqueous Solution Through PTMSP and Modified Membranes at 25 °C.....</b>	<b>116</b>
<b>Table 5.3.</b>	<b>Specific retention volumes of probes as a function of temperature on PTMSP and 20 % brominated PTMSP.....</b>	<b>118</b>
<b>Table 5.4.</b>	<b>Probe parameters as a function of temperature.....</b>	<b>118</b>
<b>Table 5.5.</b>	<b>Calculated Flory-Huggins interaction parameters <math>\chi</math> of probes on PTMSP and 20% allyl brominated PTMSP.....</b>	<b>120</b>
<b>Table 5.6.</b>	<b>The solubility parameters <math>\delta_2</math> of PTMSP and 20% allyl brominated PTMSP at different temperatures.....</b>	<b>122</b>
<b>Table 5.7.</b>	<b>Temperature dependence of the parameter of probes in PTMSP and 20 % allyl brominated PTMSP.....</b>	<b>122</b>
<b>Table 5.8.</b>	<b>Solubility parameters of polymer membranes used for ethanol/water pervaporation.....</b>	<b>127</b>



## LIST OF FIGURES

Figures	page
Figure 1.1. Model of separation with a polymer membrane.....	4
Figure 1.2. Chemical structure of poly[1-trimethylsilyl-1-propyne].....	13
Figure 1.3. Hypothetical rotational barriers for 1,2-disubstituted <i>trans</i> -polyacetylenes .....	13
Figure 1.4. Two possible senses of rotation about a single bond in the PTMSP backbone .....	16
Figure 1.5. Model for the formation of a porous PTMSP film and its densification....	16
Figure 2.1. NMR spectrum of PTMSP.....	25
Figure 2.2. IR spectrum of PTMSP.....	26
Figure 2.3. Crosslinking agents for PTMSP.....	28
Figure 2.4. NMR spectra of azide BAA (4,4'-diazidobenzophenone) and its corresponding amine (4,4'-diaminobenzophenone).....	30
Figure 2.5. IR spectra of azide BAA (4,4'-diazidobenzophenone) and its corresponding amine (4,4'-diaminobenzophenone).....	31
Figure 2.6. NMR spectra of azide HFBA (4,4'- (hexafluoroisopropylidene)diphenylazide) and its corresponding amine (4,4'-(hexafluoroisopropylidene)dianiline).....	32
Figure 2.7. IR spectra of azide HFBA (4,4'- (hexafluoroisopropylidene)diphenylazide) and its corresponding amine (4,4'-(hexafluoroisopropylidene)dianiline).....	33
Figure 2.8. Schematic diagram of gas permeation cell.....	36
Figure 2.9. UV-vis absorption spectra of bis-azide crosslinking agents.....	37
Figure 2.10. IR spectra of PTMSP with 3% azide HFBA.....	38

Figure 2.11.	DSC of PTMSP containing 3.0 mol % azide <b>HFBA</b> .....	42
Figure 2.12.	Arrhenius plot of the oxygen and nitrogen permeability coefficients for PTMSP and a crosslinked PTMSP membrane.....	46
Figure 2.13.	Temporal stability of the membranes stored in air.....	49
Figure 3.1.	<sup>1</sup> H NMR of PTMSP and brominated PTMSP.....	62
Figure 3.2.	IR spectra of PTMSP and brominated PTMSP.....	63
Figure 3.3.	Thermogravimetric analysis of PTMSP and brominated PTMSP.....	64
Figure 3.4.	DSC of PTMSP and brominated PTMSP.....	65
Figure 3.5.	<sup>1</sup> H NMR spectra of: a. reaction of brominated PTMSP with <i>n</i> -BuLi and epichlorohydrin; b. reaction of brominated PTMSP with <i>t</i> -BuLi and epichlorohydrin.....	67
Figure 3.6.	NMR spectrum of polymer product obtained by reacting brominated PTMSP with azides.....	70
Figure 3.7.	IR spectra of <b>1</b> , brominated PTMSP; <b>2</b> , the polymer resulting from brominated PTMSP reacting with azides.....	71
Figure 4.1.	Synthetic procedure for preparing poly[1-trimethylsilyl-1-propyne- <i>co</i> -1-(4-azidobutyldimethylsilyl)-1-propyne] from 4-bromo-1-butene.....	79
Figure 4.2.	<sup>1</sup> H NMR spectra of reaction mixtures during the reaction of poly[1-trimethylsilyl-1-propyne- <i>co</i> -1-(4-bromobutyldimethylsilyl)-1-propyne (10 mol% Br) to poly[1-trimethylsilyl-1-propyne- <i>co</i> -1-(4-azidobutyldimethylsilyl)-1-propyne] (10 mol% N <sub>3</sub> ).....	85
Figure 4.3.	FTIR spectra of poly[1-trimethylsilyl-1-propyne- <i>co</i> -1-(4-bromobutyldimethylsilyl)-1-propyne] (10 mol % Br) and poly[1-trimethylsilyl-1-propyne- <i>co</i> -1-(4-azidobutyldimethylsilyl)-1-propyne] (10 mol% N <sub>3</sub> ).....	86
Figure 4.4.	UV-visible spectra of: <b>1</b> , poly[1-trimethylsilyl-1-propyne]; <b>2</b> , poly[1-trimethylsilyl-1-propyne- <i>co</i> -1-(4-bromobutyldimethylsilyl)-1-propyne] (10 mol% N <sub>3</sub> ) (in cyclohexane).....	87

Figure 4.5.	DSC curves: 1, poly[1-trimethylsilyl-1-propyne- <i>co</i> -1-(4-azidobutyldimethylsilyl)-1-propyne]; 2, poly[1-trimethylsilyl-1-propyne- <i>co</i> -1-(4-bromobutyldimethylsilyl)-1-propyne] ( in nitrogen, heating rate: 20 °C/min).....	89
Figure 4.6.	TGA curves: 1, poly[1-trimethylsilyl-1-propyne- <i>co</i> -1-(4-azidobutyldimethylsilyl)-1-propyne]; 2, poly[1-trimethylsilyl-1-propyne- <i>co</i> -1-(4-bromobutyldimethylsilyl)-1-propyne] ( in nitrogen, heating rate: 10° C/min).....	90
Figure 4.7.	The plot of the measured enthalpy change of various poly[1-trimethylsilyl-1-propyne- <i>co</i> -1-(4-azidobutyldimethylsilyl)-1-propyne] copolymers vs. the theoretical N <sub>3</sub> content in the copolymers.....	91
Figure 4.8.	FTIR spectra of poly[1-trimethylsilyl-1-propyne- <i>co</i> -1-(4-azidobutyldimethylsilyl)-1-propyne](10 mol% N <sub>3</sub> ).....	92
Figure 5.1.	Pervaporation apparatus.....	111
Figure 5.2.	Pervaporation cell.....	112
Figure 5.3.	Composition curves for separation of ethanol/water mixture.....	114
Figure 5.4.	Estimation of the solubility parameters of PTMSP and 20% brominated PTMSP from Flory-Huggins parameters.....	121
Figure 5.5.	The plot of the swelling coefficient, Q, for HFBA (2%) crosslinked PTMSP as a function of the solubility parameter of various solvents.....	124
Figure 5.6.	The plot of swelling coefficient Q of crosslinked poly[1-trimethylsilyl-1-propyne- <i>co</i> -1-4-azidobutyldimethylsilyl-1-propyne] (2% N <sub>3</sub> ) as a function of the solubility parameter of various solvents.....	125
Figure 6.1.	Literature data for O <sub>2</sub> /N <sub>2</sub> separation factor versus O <sub>2</sub> permeability.....	135
Figure 6.2.	Possible synthetic routes to N <sub>3</sub> CH <sub>2</sub> C≡CSiMe <sub>3</sub> .....	136

## LIST OF SCHEMES

<b>Scheme</b>	<b>Page</b>
Scheme 2-I .....	21
Scheme 2-II .....	25
Scheme 2-III .....	29
Scheme 2-IV .....	29
Scheme 3-I .....	56
Scheme 3-II .....	57
Scheme 3-III .....	69

# Chapter 1

## Introduction

Since it was first synthesized,<sup>1</sup> poly[1-(trimethylsilyl)-1-propyne] (PTMSP) has been a material of particular interest for gas and liquid separations because of two unique properties. First, its gas permeability is higher than commercial polymeric materials. Oxygen permeability through PTMSP is ten times that of polydimethylsiloxane (PDMS), which was previously known to have highest oxygen permeability among polymers.<sup>2</sup> Using PTMSP as a gas separation membrane should improve productivity for the enrichment of oxygen from air. Second, when used for liquid-liquid separations, PTMSP is one of the few polymers that permeates ethanol preferentially against water. This property is very useful for separating ethanol from dilute aqueous solutions. However, PTMSP has two drawbacks. Its selectivity in gas separation and liquid separation is relatively low and the high gas permeability has been reported to be unstable with time, with the permeability coefficient of oxygen decreasing to 1/10 of the original value after 100 days of storage under vacuum.<sup>3</sup> Numerous studies over the past decade have aimed improving the selectivity<sup>4-12</sup> and stability<sup>13-16</sup> of PTMSP membranes. The goal of this research is to understand the unique structure and properties of PTMSP and improve its performance as a membrane material.

## **1.1. Membrane Separation Processes**

In recent years, separations using synthetic membranes have become increasingly important processes in the chemical manufacturing industry, in food and waste water processing, and in medical treatment.<sup>17</sup> When substituted for conventional separation systems, membranes can potentially save enormous amounts of energy in the processing industry, because membranes separate mixtures into components by discriminating on the basis of a physical or chemical attribute, such as molecular size, charge or solubility rather than thermal energy.<sup>18</sup>

Among all membrane processes, gas separation and pervaporation have received the most attention. In gas separation, a mixed gas feed at an elevated pressure is passed across the surface of a membrane that is selectively permeable to one component of the feed. A membrane separation process produces a permeate enriched in the more permeable species and a residue enriched in the less permeable species. Particularly important target applications in gas separation are the separation of oxygen and nitrogen from air and the separation of carbon dioxide and hydrogen from natural gas and chemical-process streams. Since the low cost availability of oxygen-enriched air would dramatically alter the economics of many combustion processes, the discovery of a stable, intermediate permeability membrane with a high oxygen/nitrogen selectivity is a high priority research topic for DOE.<sup>18</sup>

In pervaporation, a liquid mixture is placed in contact with one side of the membrane and the permeate is removed as a vapor from the other side. There are three

current applications for pervaporation: solvent dehydration, water purification, and organic-organic separation as an alternative to distillation. Current pervaporation membranes are sufficiently permselective for relatively hydrophobic solvents, but are inadequate for handling hydrophilic solvents such as ethanol and methanol. However, for solvent recovery, water purification, or pollution control, hydrophilic solvents must be removed from aqueous streams. The development of membranes able to separate hydrophilic polar solvents would allow membrane processes to be much more widely used. For example, membranes with a high selectivity for polar organic solvents over water could find substantial applications in fermentation and solvent recovery if they can be made on a large scale.

#### **1.1.1. Solution-diffusion model of membrane processes**

Separations of gases and liquids with polymeric membranes are usually solution-diffusion based processes where the difference in solubility and diffusion of the gas or liquid molecules in the polymer membranes is the driving force for the separation, as illustrated in Fig. 1.1. In this mechanism, permeation involves three steps: (a) adsorption of the permeating species into the polymer membrane; (b) diffusion of the permeating species through the polymer membrane, traveling, on average, along the concentration gradient; and (c) desorption of the permeating species from the membrane surface and evaporation or removal by other mechanisms.<sup>19,20</sup>

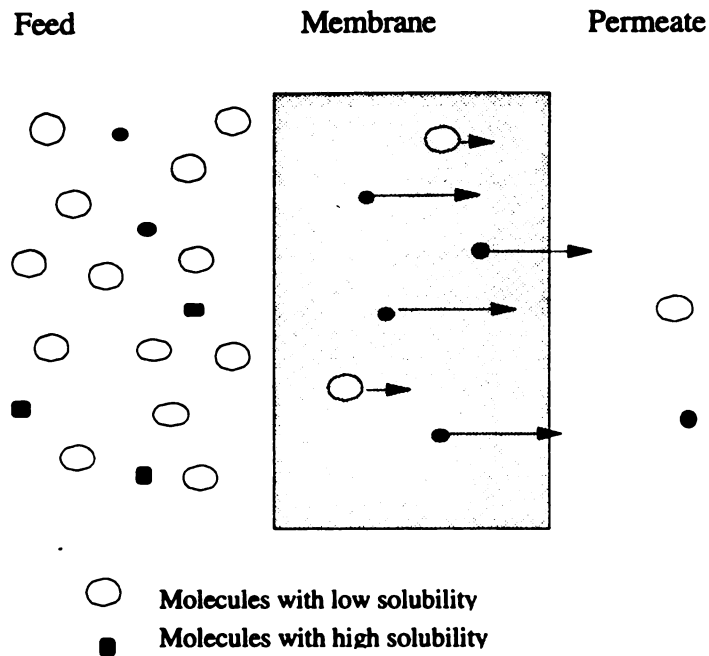


**Figure 1.1.** Model of separation with a polymer membrane.

Diffusion of a penetrant substance in a flat sheet (one-dimensional) membrane can be described by Fick's first law:<sup>17,21</sup>

$$J = - D(C) \left( \frac{dC}{dx} \right) \quad (1.1)$$

where  $J$  is the flux of the permeating species in terms of the amount passing in unit time through a unit-area of cross section in the direction of the gradient of concentration,  $dC/dx$ ,  $D$  is the local diffusion coefficient for the penetrant-membrane system, and  $C$  is the local concentration of the penetrant species. The interfacial equilibrium for sorption and desorption can be expressed by:<sup>21</sup>



$$C = S(C) p \quad (1.2)$$

where  $S(C)$  is the solubility coefficient as a function of concentration, and  $p$  is the gas or vapor pressure. Therefore, the steady-state permeation flux can be expressed as

$$J = D(C) S(C) (p_1 - p_2)/l \quad (1.3)$$

where  $P$  is the permeability coefficient,  $p_1$  and  $p_2$  are the upstream and downstream penetrant pressures, respectively, across the membrane of thickness  $l$ . Generally, the permeability coefficient,  $P$  is used to describe a normalized flux represented by eq. 1.4,<sup>22</sup>

$$P = [\text{flux}]/[D(\text{driving force})/l] \quad (1.4)$$

Therefore,<sup>19,22</sup>

$$P = D(C) S(C) \quad (1.5)$$

In experiments, the measured values of  $D$ ,  $S$ , and therefore  $P$  are average (effective) values, and Eq. 1.5 can be expressed as

$$P = D S \quad (1.6)$$

The permeability coefficient,  $P$  is defined as the volume of vapor passing per unit time through unit area of a polymer membrane having unit thickness, with a unit pressure difference across the membrane. While there are many dimensions and units used in the literature for permeability, the preferred dimensions currently are<sup>19</sup>

$$P = \frac{(\text{volume of permeate}) (\text{film thickness})}{(\text{area}) (\text{time}) (\text{pressure drop across film})} \quad (1.7)$$

In the pervaporation of liquid mixtures, the permeation rate,  $R$ , is used instead of  $P$ , where the driving force term is dropped from the definition

$$R = \frac{(F \cdot \theta)}{(a \cdot t)} \quad (1.8)$$

where  $F$ ,  $q$ ,  $a$ , and  $t$  are the permeate flux (g), membrane thickness (m), membrane area ( $\text{m}^2$ ), and time (h), respectively.

The coefficients in eq. 1.6 can be complex functions of many variables. The primary nature of polymer, however, determines these coefficients in most cases.<sup>22</sup> It was observed that both sorption and diffusion mechanisms strongly depend on the relationship between the temperature,  $T$ , and the glass transition temperature,  $T_g$ , of the polymer.<sup>21,23</sup> Above  $T_g$ , the segmental motion of the rubbery polymer chains is rapid, and they respond quickly to the environmental changes of the polymer. As a result, solution equilibrium between a rubbery polymer and a penetrant species is established in a short time compared to the time required for the diffusion. Accordingly, all penetrant molecules are believed to

follow a single model. In contrast, at temperatures below  $T_g$ , segmental motion of glassy polymer chains is restricted and the environment of a penetrant molecule cannot be completely homogenized. The glassy polymer itself is not in a true equilibrium state within the experimental time scale and unrelaxed volume segments called "holes" or "microvoids" of different sizes are believed to introduce inhomogeneity at a molecular scale. This leads to different or multiple solution and diffusion models.<sup>21,23</sup>

The sorption behavior of gases and liquids in a rubbery polymer usually obeys either Henry's law (eq. 1.9) or the Flory-Huggins equation (eq. 1.10):

$$C = S(0) p \quad (1.9)$$

$$\ln (p/p_0) = \ln (v) = \ln (1-v) + \chi (1-v)^2 \quad (1.10)$$

where  $p$  is the pressure of the substance,  $p_0$  is its vapor pressure of the pure liquid or gas at the temperature,  $v$  is the volume fraction of the substance in the polymer, and  $\chi$  is the Flory-Huggins parameter. The sorption behavior in glassy polymers, due to the inhomogeneous environment in the polymer, is described by a dual-mode model composed of Henry's law and Langmuir terms.<sup>21</sup>

$$\begin{aligned} C &= C_D + C_H \\ &= k_D p + C_H \quad bp / (1 + bp) \end{aligned} \quad (1.11)$$

where  $C_D$  and  $C_H$  are the penetrant concentrations resulting from ordinary dissolution (Henry's law mode) and by the Langmuir equation (Langmuir mode), respectively;  $k_D$  is Henry's law parameter corresponding to  $S(0)$ ;  $C_H$  and  $b$  are the maximum penetrant concentration and the affinity constant of the penetrant in the Langmuir mode.

The diffusion of a penetrant in a polymer occurs as a result of random motions of individual penetrant molecules and cooperative motion of polymer chain segments surrounding these molecules.<sup>21</sup> The variation of the diffusion coefficient with concentration, temperature,  $T_g$ , and penetrant size can be rationalized in terms of the free volume theory of diffusion.<sup>17</sup> This theory assumes that a diffusing molecule can move from site to site when the local specific volume, and hence the local amount of empty space (free volume) around the diffusing molecule, exceeds a critical value. The free volume of any system increases with increasing temperature, and for a fixed temperature, decreases with increasing  $T_g$  in polymer systems. Because penetrants have more free volume than polymers, free volume increases with increasing concentration of penetrant. It follows that the diffusion coefficient will increase with increasing concentration, with increasing temperature, with decreasing glass transition temperature, and with decreasing size of diffusant.

### **1.1.2. Separation factor**

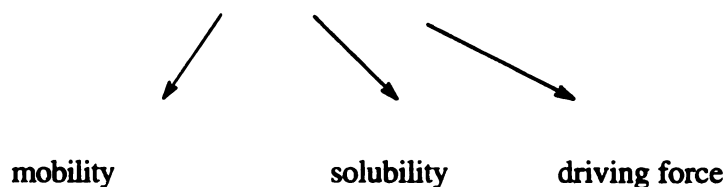
When gas or liquid mixtures pass through nonporous polymer membranes, separation of the mixture occurs more or less during the permeation process. The selectivity of a polymer membrane for component  $i$  relative component  $j$ , is characterized

by the ideal separation factor,  $\alpha_{ij}$ , defined by equation 1.12 in terms of the downstream (1) and upstream (2) mole fractions (X) of components (i) and (j), respectively

$$\alpha_{ij} = [X_{i1}/X_{j1}]/[X_{i2}/X_{j2}] \quad (1.12)$$

One can arrange eq. 1.12 in terms of the ratio of effective (average) diffusion  $[D_i/D_j]$  and solubility  $[S_i/S_j]$  coefficients as well as the differences in partial pressures of the two components existing across the membrane, viz.,

$$\alpha_{ij} = \frac{[D_i]}{[D_j]} \cdot \frac{[S_i]}{[S_j]} \cdot \frac{[\Delta p_i / X_{i2}]}{[\Delta p_j / X_{j2}]} \quad (1.13)$$



Usually, if the downstream pressure is held at vacuum, the driving force term becomes equal to unity and the separation factor becomes equation 1.14,<sup>24</sup>

$$\alpha_{ij} = P_i/P_j = [D_i/D_j] [S_i/S_j] \quad (1.14)$$

As indicated in equation 1.14, one can conveniently consider the overall selectivity to have two parts, a solubility and a mobility contribution.

The mobility term in equation 1.14 is based on the inherent ability of polymer matrices to function as molecular size- and shape-selective media. This is governed by such factors as chain backbone rigidity and intersegmental packing. Solubility selectivity is determined by interactions between the penetrants and the polymer composing the membrane for both liquid and gas systems.<sup>21,22,25</sup>

### 1.1.3. Gas separation and pervaporation

In gas separation, a good measure of the relative solubility of two permanent gases is given by their respective boiling point i.e., condensibility.<sup>26</sup> Subtle effects due to interactions between the membrane material and gases are occasionally seen, but they tend to be small and can be ignored in most cases. In general, solubility increases with molecular size, but the increase in  $S$  usually is much less than the decrease of  $D$ , and so increasing the size of the diffusant causes the permeabilities to decrease almost as much as the diffusion coefficient. For a wide range of temperatures, gases, or polymers, the changes in the solubility coefficient are much less than the changes in the diffusion coefficient and thus variations in the diffusion coefficient are the main factor affecting gas permeability.

The principles guiding the search for significantly improved membrane materials are based on the mobility term in equation 1.13.<sup>18,22</sup> It can be distilled to two rules of thumb, summarized below.

- (i) Structural modifications that simultaneously inhibit chain packing and the torsional mobility around flexible linkages in the polymer backbone tend to cause either: a)

simultaneous increases in both the permeability and selectivity, or b) a significant increase in permeability with negligible losses in selectivity.

(ii) Modifications that reduce the concentration of the most mobile linkages in a polymer backbone tend to increase selectivity without undesirable reductions in permeability.

The above principles apply to materials for liquid and vapor separation as well as for gases. Unfortunately, the much higher swelling levels typically encountered in vapor and liquid systems inevitably complicate their use. Generally, discussions of membrane optimization are based on solubility effects.<sup>27</sup> In the ethanol/water separation system, the diffusion coefficient of ethanol is less than that of water because of the size difference. Thus, to obtain ethanol selectivity, one must retain a large free volume and increase the solubility of ethanol in the polymer membrane. Most work in this field focuses on the membrane permeability and rejection properties of a candidate material, rather than understanding the sorption and transport properties as a function of polymer structure. Few explicit analyses have been made of the solubility and mobility contributions to the separation factors observed in most cases for polymer materials.<sup>10,22</sup> The relationship between transport and polymer structure must be resolved for this field to advance significantly.

## 1.2. Features of Poly[1-trimethylsilyl]-1-propyne]

Depending on temperature and structure, amorphous polymers exhibit widely different physical and mechanical behavior patterns. At low temperatures, amorphous polymers are glassy, hard, and brittle. As the temperature is raised, they go through the glass-rubber transition ( $T_g$ ) and enter the rubbery state.

Rubbery polymers, such as polydimethylsiloxane around room temperature, usually have a high gas permeability that is attributed to its flexible backbone and resultant high free volumes.<sup>19,28</sup> On the other hand, glassy polymers usually have low gas permeabilities. PTMSP is amorphous according to x-ray diffraction<sup>28</sup> and thermal analysis,<sup>29</sup> and shows no evidence of a glass transition temperature to the upper limit of its chemical stability, usually 300°C. Mechanical measurements<sup>13,29</sup> place the modulus between that of typical glassy and rubbery materials. Nevertheless, it has the highest gas permeability reported among conventional polymers. It is believed that these properties are due to the unique structural features of the PTMSP backbone.<sup>22,29,30</sup>

Usually, flexible polymers in solution have coiled backbones while rigid polymers are associated with rod-like geometries.<sup>30</sup> The correspondence between chain rigidity and rod-like conformation, however, apparently breaks down for substituted polyacetylenes. The reported solution properties suggest a stiff polymer chain, yet the polymers are highly soluble and amorphous with no report of liquid crystalline behavior. It is deduced that PTMSP has a rigid but disordered backbone contour, i.e., a rigid random coil conformation.



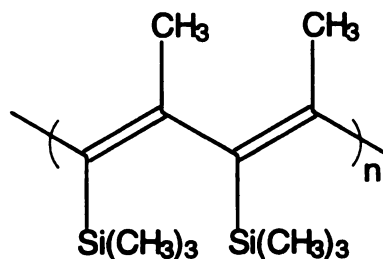


**Figure 1.2.** Chemical structure of poly[1-(trimethylsilyl)-1-propyne].

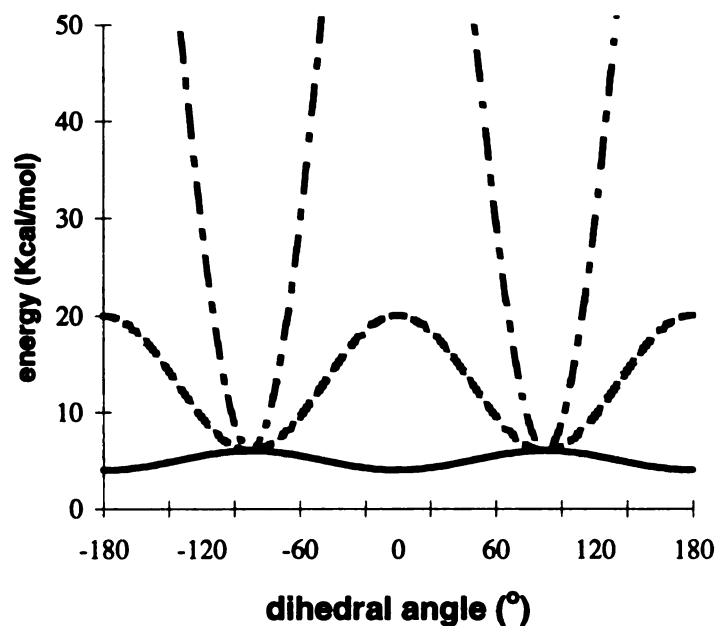


**Figure 1.3.** Hypothetical rotational barriers for 1,2-disubstituted trans-polyacetylenes.

0 corresponds to the planar conformation shown in figure 1.2. solid line: *trans*-polyacetylene, 6 kcal/mol  $\pi$  barrier; dashed line: 20 kcal/mol rotational barrier that simulates significant 1,3 steric interactions; dot-dash line: 100 kcal/mol barrier that simulates polyenes with bulky substitutes.

For PTMSP (shown in Figure 1.2), simple molecular mechanics calculations suggest that steric interactions between the substituents on adjacent carbon atoms can cause significant deviations from planarity. Because of the shorter distances between carbon atoms in the  $sp^2$  skeleton, the magnitude of the interactions are expected to be much larger than for their saturated analogs and there should be a large barrier to rotation.

Plotted schematically in Figure 1.3, is a potential energy diagram for rotation about single bonds in substituted *trans*-polyacetylenes. The rotational barrier has two energy terms; one with a  $\cos^2 \theta$  dependence that accounts for the  $\pi$  contribution to the rotational barrier, and a second term with a  $\cos 2\theta$  dependence that corresponds to the steric barriers to rotation. Based on results for butadiene,<sup>31</sup> the  $\pi$  barrier is set at 6 kcal/mol. With small substituents (H, Cl, ...), the combination of a small  $\pi$  energy term and limited 1,3 steric interactions leads to a broad shallow potential well with the most stable conformations being those that are nearly planar. As the magnitude of the steric interactions is increased, a double well potential becomes well-defined and the  $\pi$  contribution becomes a minor perturbation to the total energy. For large substituents (*t*-butyl, trimethylsilyl, ...), the barrier to rotation at room temperature may be large enough to make planar conformations so unfavorable that the polymer is driven into one of two sharply defined potential wells. With these bulky substituents, the barrier to rotation may become large enough to limit access to a single well. Thus, the polymer conformation is fixed, and overall changes in the shape of the polymer are limited to oscillations within a single well.

Thermal annealing experiments provide an illustration of the polymer's inability to change conformations.<sup>32</sup> Depending on the catalyst used to prepare the polymer, different amounts of *cis* and *trans* double bonds are found in the polymer. For polyacetylenes in the solid state, isomerization of *cis* double bonds to *trans* double bonds occurs readily at temperatures above 100 °C. At 180 °C for example, the isomerization of semicrystalline films of *cis*-polyacetylene to the *trans* isomer is completed in one minute.<sup>32</sup> Similar experiments on PTMSP show no signs of isomerization.<sup>33</sup> For annealing at temperatures above 200°C <sup>13</sup>C NMR spectra show that the isomer content is unchanged after 24 hours, and instead random chain scission leads to lower molecular weight polymers with the original *cis/trans* ratios preserved. Remarkably, the barrier to isomerization apparently exceeds the energy required to break the polymer backbone. The barrier calculated from molecular dynamics simulations (40 kcal/mol) is in accord with such behavior. Thus, PTMSP fits well the model of a rigid chain with a highly disordered backbone contour.

The random coil shape is a consequence of rotation around single bonds in both (+) and (-) senses that causes the deviation from planarity.<sup>30</sup> Figure 1.4 shows these two possible rotations. During the polymerization process, if a number of consecutive monomer units are linked with the same direction of deviation, it will lead to a helical sequence. Since for PTMSP, both directions of deviation should be equally possible, long chains will form a random coil. With its rigid backbone structure and the presence of large bulky substituents (trimethylsilyl group), intersegmental packing is hindered and thus the polymer has a large free volume. Therefore PTMSP has many molecular-scale holes just after its preparation which results in a high gas permeability.

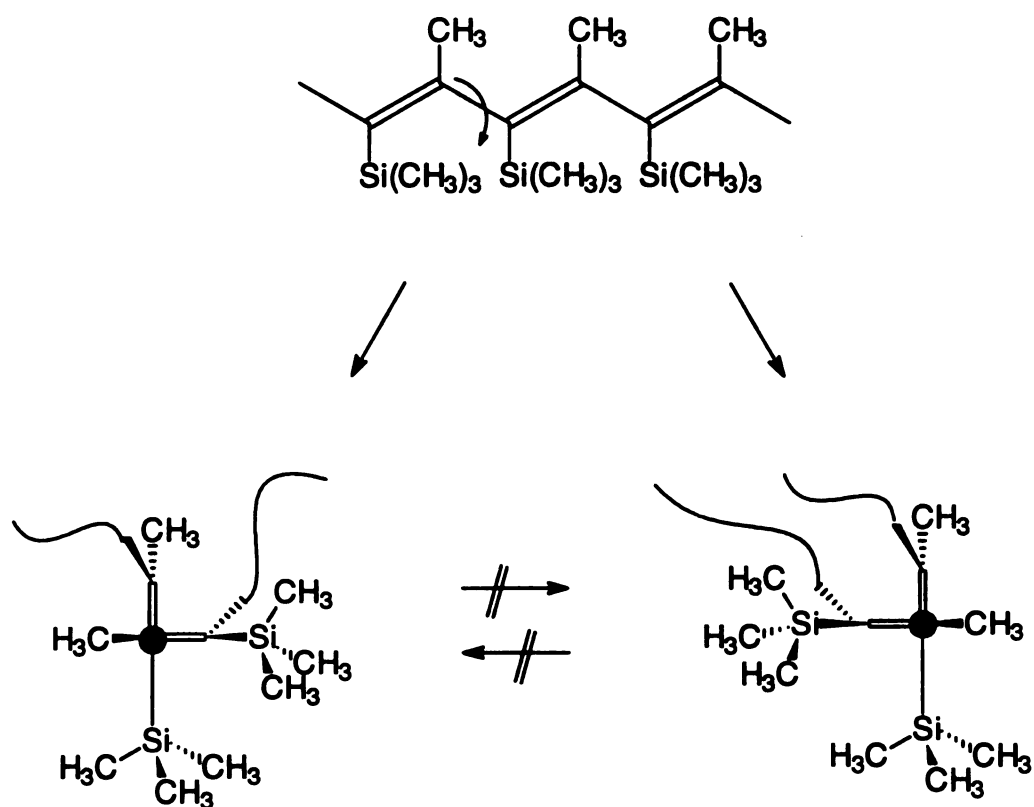


**Figure 1.4.** Two possible senses of rotation about a single bond in the PTMSP backbone.

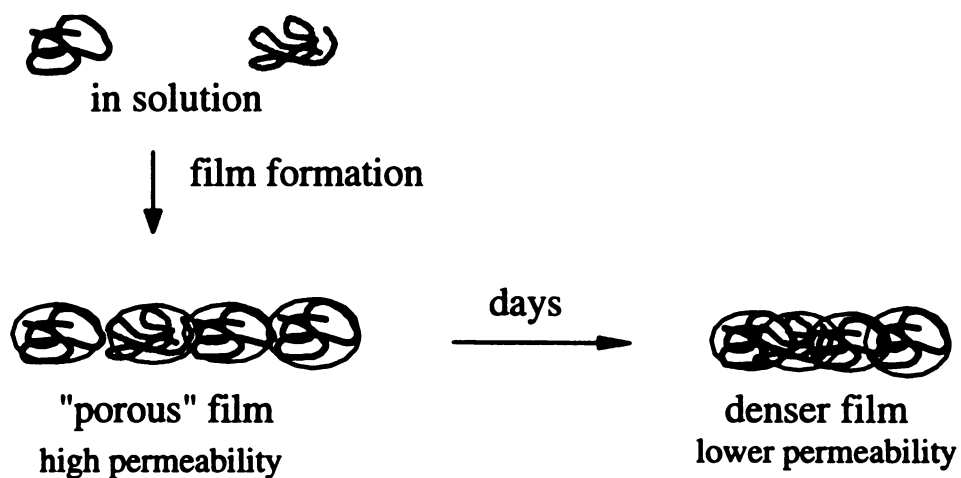


**Figure 1.5.** Model for the formation of a porous PTMSP film and its densification.

The permeability decays with time, dropping to 10 % of its original value after 100 days. One model for the decrease is the slow interdiffusion of polymer coils in the solid state. From solution, the polymer is deposited under kinetic control as an ensemble of rigid spheres. With time, the chains entangle causing an increase in the density and decrease in free-volume and permeability (Figure 1.5). Stabilization of PTMSP in its porous form is needed for PTMSP to be useful.

In this study, we tested this applicability of this model to the PTMSP system. The primary goal was to cross-link the polymer and stabilize the high permeability. In addition, we sought to chemically modify the stabilized structures to enhance the selectivity of the membranes for ethanol/water and gas separations.

### 1.3. References

1. Masuda, T.; Isobe, E.; Higashimura, T.; Takada, K. *J. Am. Chem. Soc.* **1983**, *105*, 7473.
2. Shimomura, H.; Nakanishi, K.; Odani, H.; Kurata, M.; Masuda, T.; Higashimura, T. *Kobunshi Ronbunshu* **1986**, *43*, 747.
3. Masuda, T.; Higashimura, T. in *Silicon Based Polymer Science* Ziegler, J. M.; Fearon, G. F. M., Ed; American Chemical Society, Washington, DC, **1990**: p 641.
4. Langsam, M.; Anand, M.; Karwacki, E. J. *Gas Sep. Purific.* **1988**, *2*, 162.

5. Kita, H.; Sakamoto, T.; Tanka, K.; and Okamoto, K.-I. *Polymer Bulletin*, **1988**, *20*, 349.
6. Aoki, T.; and Oikawa, E. *J. Membr. Sci.*, **1991**, *57*, 207.
7. Nagase, Y.; Ueda, T.; Matsui, K.; and Uchikura, M. *J Polym. Sci., Part B: Polym. Phys.* **1991**, *29*, 171.
8. Chen, G.; Griesser, H. J.; Mau, A. W. H. *J. Membr. Sci.* **1993**, *82*, 99.
9. Lin, X.; Chen J.; Xu, J. *J. Membr. Sci.* **1994**, *90*, 81.
10. Nagase, Y.; Ishihara K.; Matsui, K. *J. Polym. Sci., Part B: Polym. Phys.* **1990**, *28*, 377.
11. Nagase, Y.; Sugimoto, K.; Takamura, Y.; Matsui, K. *J. Appl. Polym. Sci.* **1991**, *43*, 1227.
12. Nagase, Y. ; Takamura, Y.; Matsui, K.; *J. Appl. Polym. Sci.* **1991**, *42*, 185.
13. Langsam, M; and Robeson, L. M. *Polymer Engineering and Science* **1989**, *29*, 44.
14. Withchey-Lakshmanan, L. C.; Hopfenberg, H. B.; Chern, R. T. *J. Membr. Sci.* **1990**, *48*, 32.
15. Nakagawa, T.; Fujisaki, S.; Nakano, H.; Higuchi, A. *J. Membr. Sci.* **1994**, *94*, 183.
16. Nagai, K.; Higuchi, A.; Nakagawa, T. *J. Polym. Sci., Part B: Polym. Phys.* **1995**, *33*, 289.

17. Bungay, P. M.; Lonsdale, H. K.; de Pinho, M. N. *Synthetic Membranes: Science, Engineering and Applications*, Bungay, P. P.; Lonsdale, H. K.; de Pinhol, M. N., Eds., D. Reidel Publishing Company, **1983**.
18. Baker, R. W. et al. *Membrane Separation Systems*, Noyes Data Corporation, Park Ridge, **1991**.
19. Sperling, L. H. *Introduction to Physical Polymer Science*, John Wiley & Sons, Inc., New York; **1992**.
20. Albrecht, R. *Membrane Processes*, John Wiley & Sons, Inc., **1989**; p 50.
21. Kimura, S.; and Hirose, T. "Theory of Membrane Permeation" in *Polymers for Gas Separation*, Toshima, N., Ed., VCH Publishers, Inc., New York; **1992**.
22. Koros, W. J.; Fleming, G. K.; Jordan, S. M.; Kim, T. H.; and Hoehn, H. H. *Progr. Polym. Sci.* **1988**, *13*, 339.
23. Koros, W. J.; and Chern, R. T., "Separation of Gaseous Mixtures Using Polymer Membranes," in *Handbook of Separation Process Technology*, Rousseau, R. W., Ed., Wiley Interscience, New York, **1987**.
24. McCandless, F. P. *Ind. Eng. Chem. Process Des. Develop.* **1972**, *11*, 470.
25. Koros, W. J. *J. Polym. Sci., Polym. Phys. Ed.* **1985**, *23*, 1611.
26. Kim, T. H.; Koros, W. J.; and Husk, G. R. *Sep. Sci. and Tech.* **1988**, *23*, 1611.
27. Mudler, M. H. V.; Kruit, F.; and Smolders, C. A. *J. Membr. Sci.* **1982**, *19*, 1163.
28. Takada, K.; Matsuya, H.; Masuda, T.; and Higashimura, T. *J. Appl. Polym. Sci.* **1985**, *30*, 1605.

29. Masuda, T.; Tang, B.-Z.; Tanaka, A.; Higashimura, T. *Macromolecules* **1986**, *19*, 1459.
30. Clough, S. B.; Sun, X. F.; Tripathy, S. K.; and Baker, G. L. *Macromolecules* **1991**, *24*, 4264.
31. Bock, C. W.; George, P.; Trachtman, M; Zanger, M. *J. Chem. Soc., Perkin Trans.* **1979**, *1*, 26.
32. Rolland, M.; Bernier, P.; Lefrant, S.; Aldissi, M. *Polymer* **1980**, *21*, 1111.
33. Baker, G. L.; Shelburne, III, J. A (unpublished data).

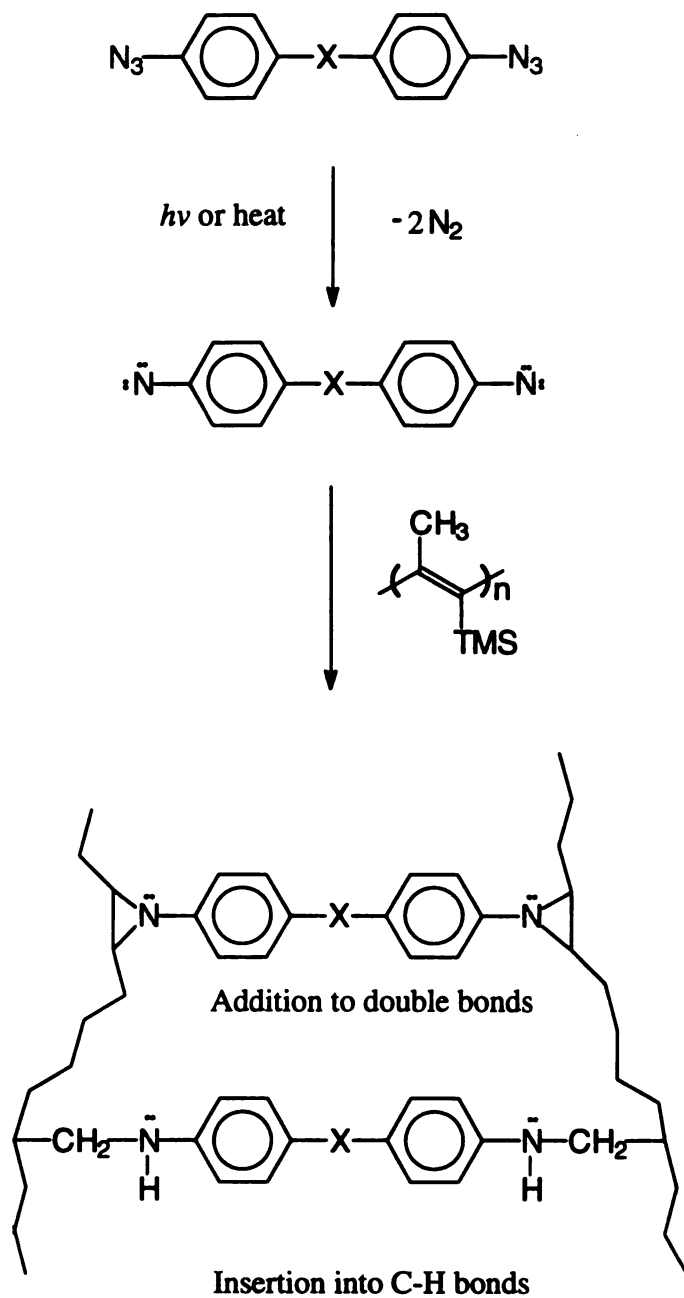


## **Chapter 2**

# **Crosslinking of Poly[1-trimethylsilyl-1-propyne] Membranes using Bis(aryl azides)**

### **2.1. Introduction**

There are various modes for inducing crosslinking in polymers, with the most important ones chemical, thermal and photochemical processes. The UV-irradiation of PTMSP membranes has been studied. Improvements in the oxygen/nitrogen selectivity were found but there was no report of the crosslinking degree.<sup>1</sup> In order to better control the degree of crosslinking, we attempted to chemically cross-link PTMSP membranes. Bis(arylazides) were successful crosslinking agents for an early negative resist system that used poly(butadiene) and poly(isoprene) as the cross-linkable polymer.<sup>2,3</sup> The results encouraged us to use this technique to cross-link PTMSP membranes. Photo irradiation or thermal treatment of azides results in the loss of nitrogen and the formation of a reactive nitrene that can react with double bonds to give aziridines or inset into C-H bonds to give amines. As shown in Scheme 2-I, difunctional azides may be added as a curing agent or alternatively, azides may be chemically bound to PTMSP as latent crosslinking sites.



Scheme 2-I

## 2.2. Experimental

Unless otherwise specified, ACS reagent grade starting materials and solvents were used as received from commercial suppliers without further purification. Proton nuclear resonance ( $^1\text{H}$  NMR) analyses were carried out at room temperature in deuterated chloroform ( $\text{CDCl}_3$ ) on a Varian Gemini-300 spectrometer with the solvent proton signals being used as chemical shift standards. Infrared (IR) spectra of polymer were obtained under nitrogen at room temperature on a Nicolet IR/42 Fourier Transform IR spectrometer. IR measurements before and after thermal or photo treatment were carried out on free standing membranes. The spectra of bis azides and their corresponding amines were obtained from thin films deposited on NaCl plates. A Shimadzu UV-160 spectrometer was used to obtain the UV-visible spectra of the polymers with cyclohexane as solvent. Molecular weights of polymers were determined by gel permeation chromatography (GPC) using a PLgel 20m Mixed A column and a Waters R401 Differential Refractometer detector at room temperature with THF as eluting solvent at a flow rate 1 mL/min. Monodisperse polystyrene standards were used to calibrate the molecular weights. The concentration of the polymer solution was 1 mg/mL.

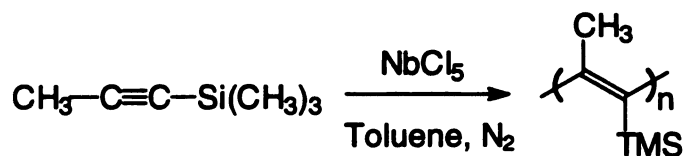
Differential scanning calorimetry (DSC) and thermogravimetric analyses (TGA) of the polymers and polymer/azide mixtures were performed under a nitrogen atmosphere at a heating rate 10  $^{\circ}\text{C}/\text{min}$  on a Perkin Elmer DSC 7 and a Perkin Elmer TGA 7 instrument, respectively. The temperature was calibrated with an indium standard.

Special handling was necessary for the air- and moisture-sensitive polymer synthesis reactions. Solvent (i.e., toluene) was dehydrated by distilling first from calcium hydride and then from sodium benzophenone ketyl under nitrogen. Monomers were dried by refluxing over calcium hydride ( $\text{CaH}_2$ ) under nitrogen for 1 hour. To separate the monomer from the  $\text{CaH}_2$ , the monomer was frozen with liquid nitrogen and connected to a vacuum line. After evacuating the system, the monomer was transferred to a Schlenk flask connected to another end of the vacuum line by warming up the monomer flask and cooling the receiving Schlenk flask. The catalyst ( $\text{TaCl}_5$  or  $\text{NbCl}_5$ ) was weighed and added to reaction vessel in a VAC He-43-4 dry box. Syringes were used to transfer the monomer solution to the catalyst solution to initiate the reaction.

### 2.2.1. Synthesis of Poly[1-trimethylsilyl-1-propyne]

An example of the preparation procedure of PTMSP (Scheme 2-II) follows.<sup>4</sup> A monomer solution was prepared by mixing 1-trimethylsilyl-1-propyne (1.12 g, 10.0 mmol) and toluene (3.2 mL) and the solution was warmed to 80 °C.  $\text{NbCl}_5$  (0.20 mmol) was dissolved in toluene (5 mL) at 80 °C for 10 min, to give a golden yellow solution. The above monomer solution was immediately added to the catalyst solution. As the reaction proceeded, the polymerization system became brown and solidified. After 12 hours, polymerization was terminated by adding a mixture (3 mL) of methanol and toluene (1:4 volume ratio) which led to decolorization. The polymer formed was dissolved in toluene (200 mL) and precipitated into methanol (2L). It was then purified by an additional dissolution/filtration/precipitation step. The typical yield was > 80%. The weight average

molecular weights measured by gel permeation chromatography in THF were  $6\text{-}8 \times 10^5$  with a polydispersity of 1.8-2.2. Figure 2.1 and Figure 2.2 show the NMR and IR spectra of the polymer.



**Scheme 2-II**

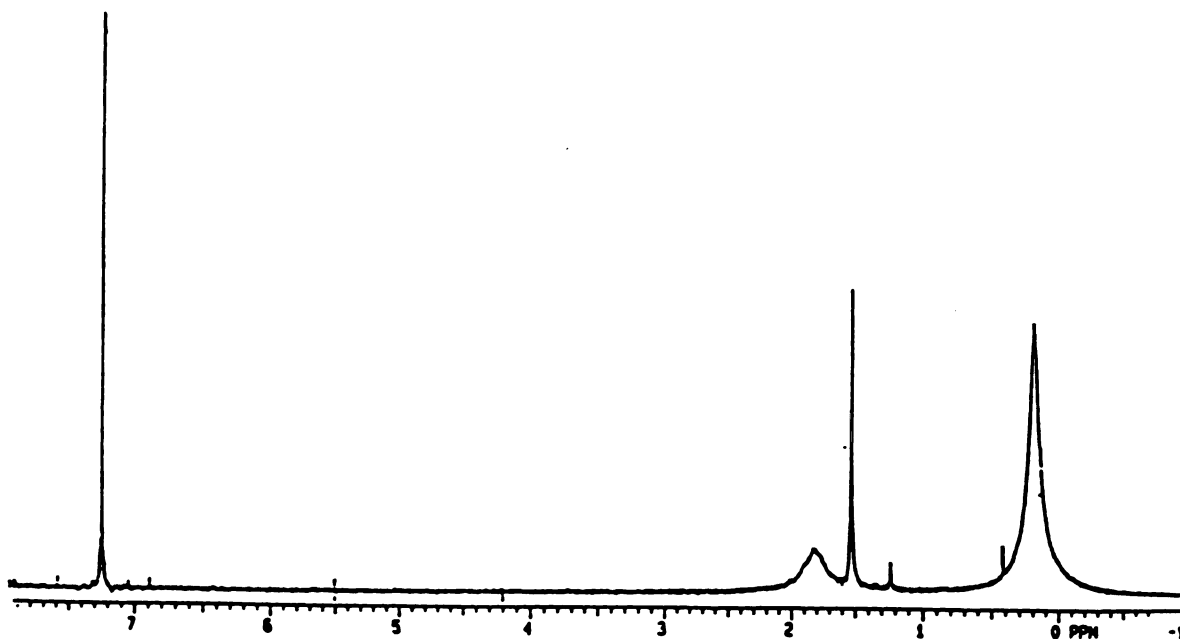


**Figure 2.1.** NMR spectrum of PTMSP. The two broad peaks at 0.2 ppm and 1.8 ppm are from TMS and CH<sub>3</sub> in PTMSP; other sharp peaks are from solvent (CDCl<sub>3</sub>) and solvent impurities.

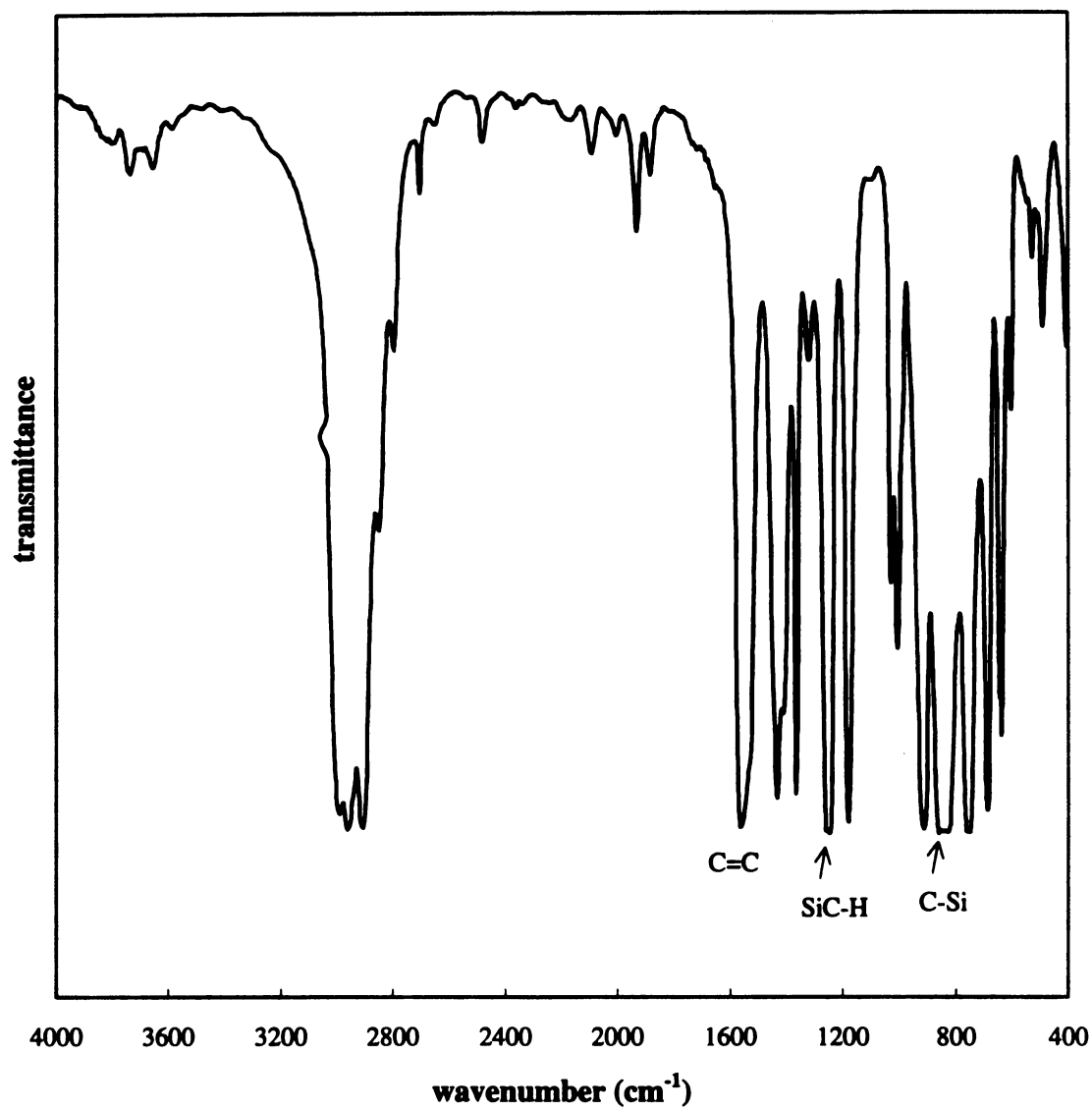
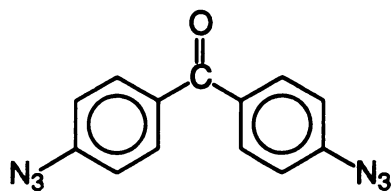


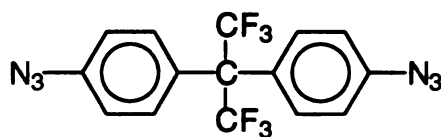
**Figure 2.2.** IR spectrum of PTMSP.

### 2.2.2. Synthesis of bis(aryl azide) crosslinking agents

The bis(aryl azide) crosslinking agents shown in Figure 2.3 (4,4'-diazido benzophenone, **BAA**, and 4,4'-(hexafluoroisopropylidene)diphenylazide, **HFBA**), were obtained by diazotization of the corresponding amines (purchased from Aldrich) followed by nucleophilic displacement of the diazonium salt with  $\text{NaN}_3$  (Scheme 2-III and Scheme 2-IV).<sup>5,6</sup> The synthetic procedures are described using **BAA** as an example. Water (6.3 mL) was placed in a 100 mL three-neck round bottom flask equipped with a thermometer and a mechanical stirrer. With stirring, 1.9 mL of concentrated sulfuric acid ( $\text{H}_2\text{SO}_4$ ) were added, followed by 4,4'-aminobenzophenone (1.0 g, 4.7 mmol). When all the amine had been converted to the white sulfate, 3.2 mL of water was added and the suspension was cooled to 0-5 °C in an ice-salt (sodium acetate) bath. A solution of  $\text{NaNO}_2$  (0.66 g, 9.6 mmol) in 2.5 mL water was then added dropwise over a period of 15 min, and the mixture was stirred for 45 min longer. A yellow precipitate formed. With strong stirring, a solution of  $\text{NaN}_3$  (0.64 g, 9.8 mmol) in 1.9 mL of water was added, and stirring was continued for 40 min longer. The solid was filtered with suction and washed with 100 mL water. The material was allowed to dry in air in a dark place. The purified products were obtained by recrystallization from 95% ethanol. The yield was ~90%. Figures 2.4 and Figure 2.5 show NMR and IR spectra of azide **BAA** in comparison to its corresponding amine. Figures 2.6 and Figure 2.7 show NMR and IR spectra of azide **HFBA** with the corresponding amine.



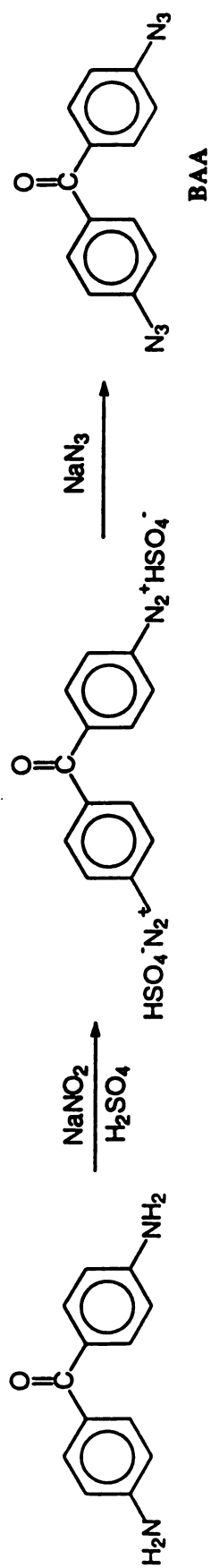
**4,4'-diazidobenzophenone (BAA)**



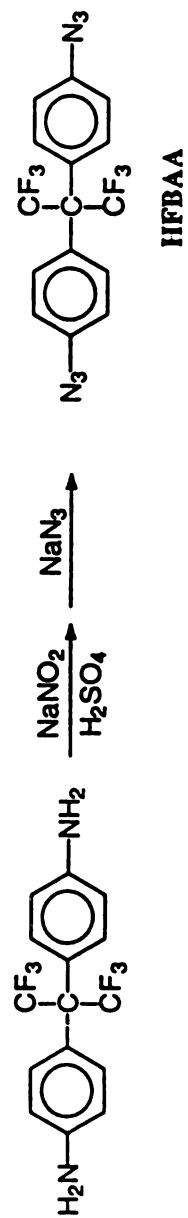
**4,4'-(hexafluoroisopropylidene)diphenylazide (HFBA)**

**Figure 2.3.** Crosslinking agents for PTMSP.





Scheme 2-III



Scheme 2-IV

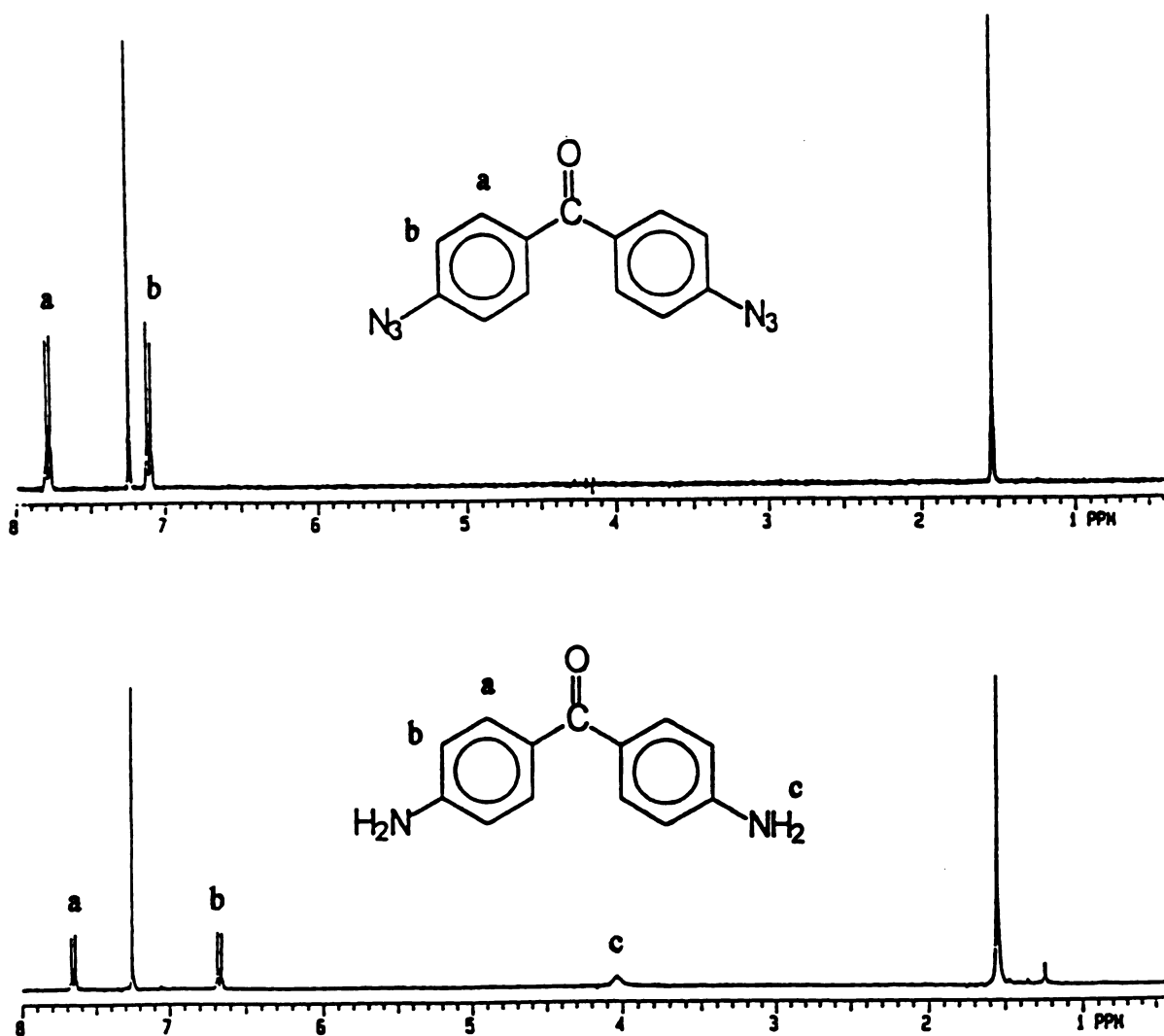


**Figure 2.4** NMR spectra of azide BAA (4,4'-diazidobenzophenone) and its corresponding amine (4,4'-diaminobenzophenone).

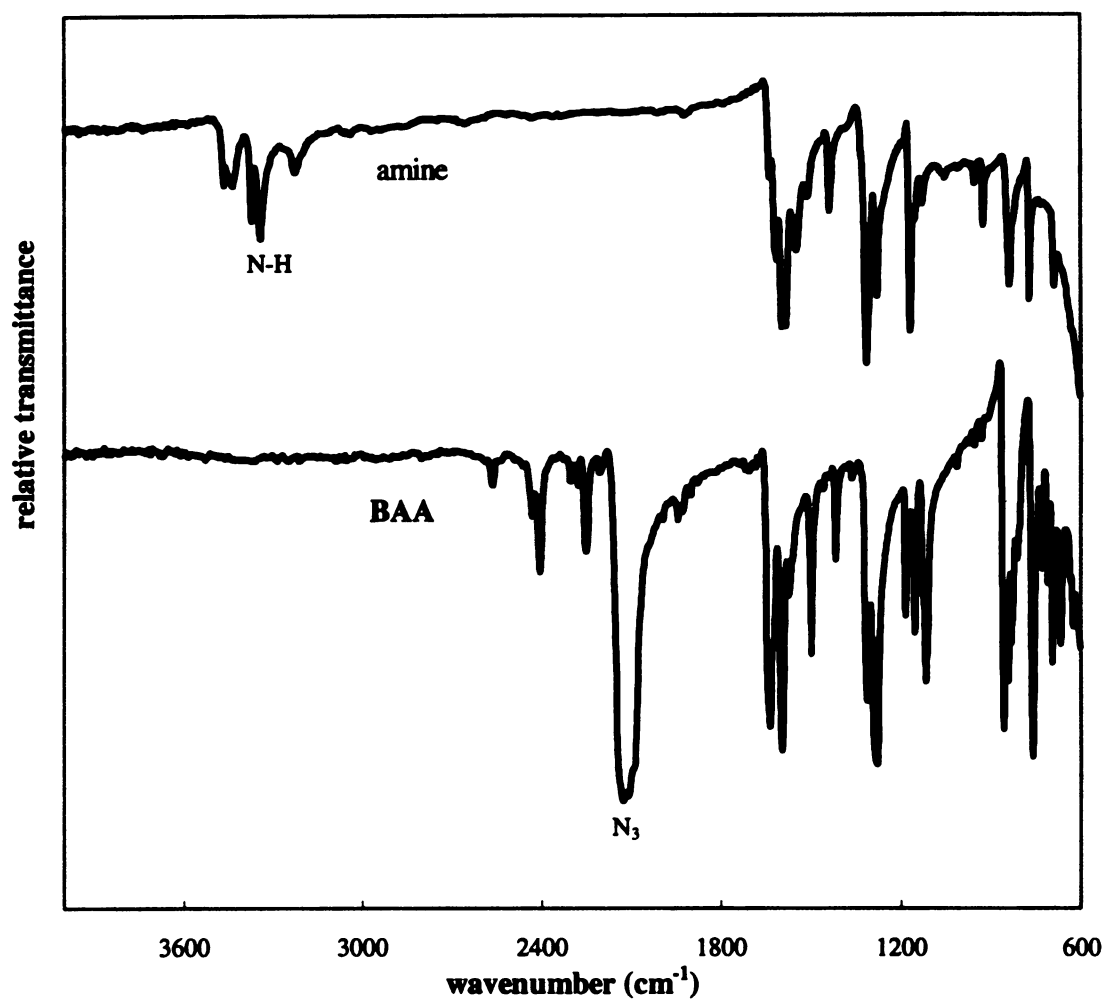


**Figure 2.5** IR spectra of azide **BAA** (4,4'-diazidobenzophenone) and its corresponding amine (4,4'-diaminobenzophenone).

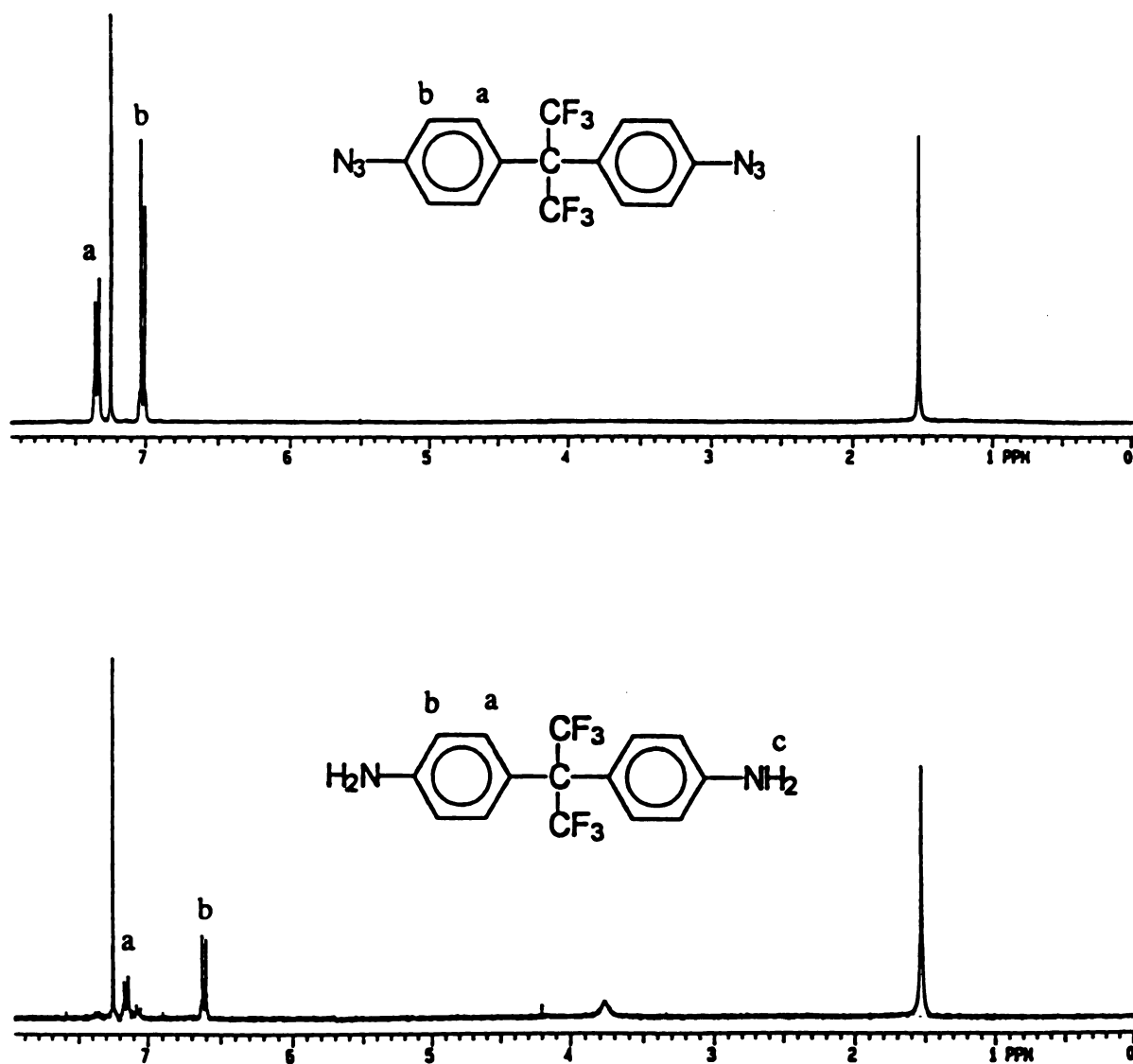


**Figure 2.6.** NMR spectra of azide HFBA (4,4'-(hexafluoroisopropylidene)diphenylazide) and its corresponding amine (4,4'-(hexafluoroisopropylidene)dianiline).

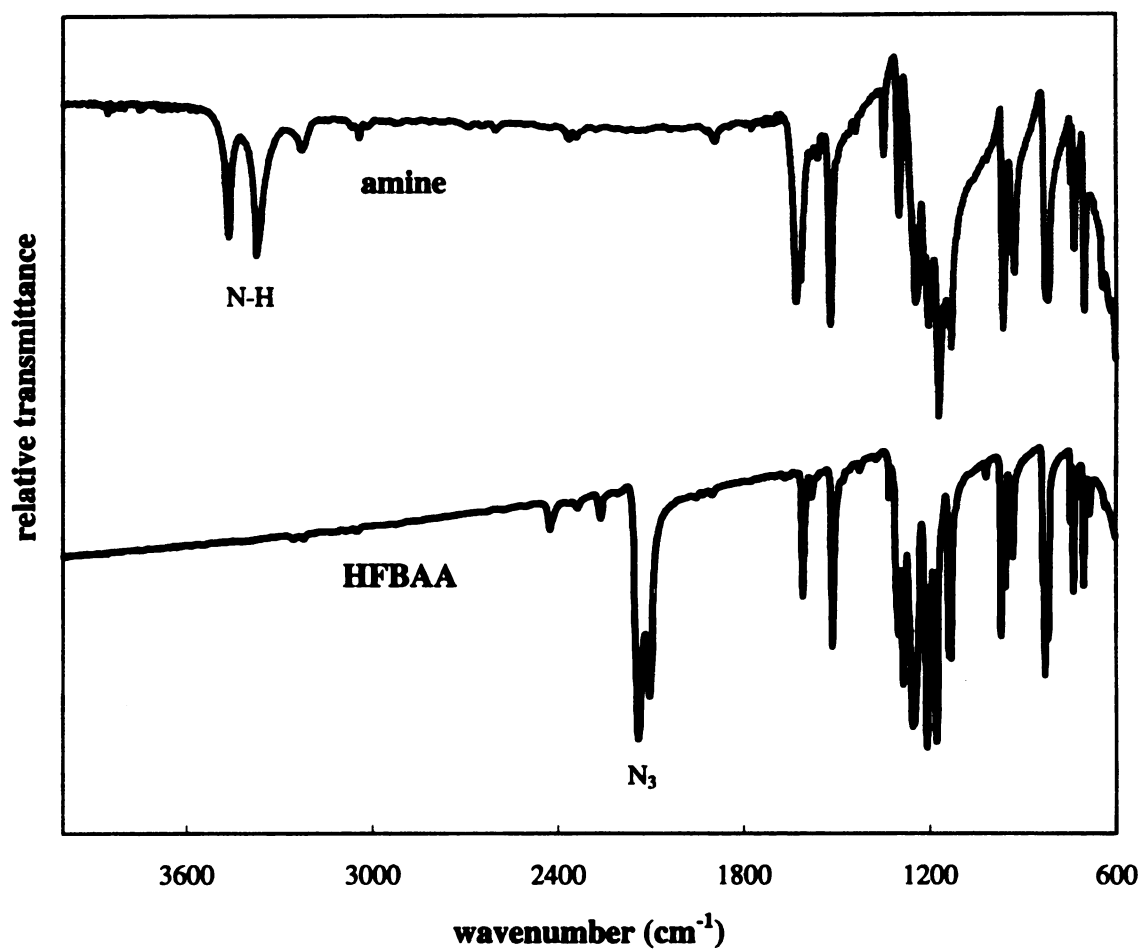


**Figure 2.7.** IR spectra of azide **HFBAZ** (4,4'-(hexafluoroisopropylidene)diphenylazide) and its corresponding amine (4,4'-(hexafluoroisopropylidene)dianiline).

### 2.2.3. Membrane preparation and modification

Membranes were prepared by casting a dilute solution (1-2 wt%) of PTMSP in toluene on a glass plate at room temperature. The solution was allowed to evaporate to dryness for 48 hours, and the membranes were then dried under vacuum for 12 hours. To prepare modified membranes, PTMSP and a small amount of the appropriate bis-azide were co-dissolved in toluene, and membranes were then cast from the solution after filtration.

The crosslinking of the bis(aryl azide) containing membranes was induced by either UV irradiation or thermal treatment. Photo crosslinking of membranes with azide BAA, was carried out at 300 nm in a Rayonet photoreactor with membranes sealed under nitrogen in a wide diameter cylindrical Pyrex container for 3 hours or until the  $N_3$  absorption band in the IR disappeared. Photo crosslinking of membranes with fluorinated azide HFBA, was carried out at 254 nm for a half hour using an Ace-Hanovia quartz high-pressure mercury-vapor lamp with the membranes sealed under in a wide diameter cylindrical quartz container. After photo treatment, membranes were curled toward the side that was exposed to UV light. Thermal crosslinking of the membranes was achieved by heating the flat membranes in a vacuum oven at 175 °C for 3-7 hours depending on the amount of azide in the membranes. Thermally treated membranes remained flat after crosslinking.

#### **2.2.4. Measurement of gas permeability and densities**

Permeability coefficients for O<sub>2</sub> and N<sub>2</sub> were measured by the variable volume method, using ASTM procedure D-1434.<sup>7</sup> The gas permeation cell, as shown in Figure 2.8, measures the flow of a gas or vapor through a polymer film by means of a capillary flow meter. The permeability is calculated by equation 1.7 for which the quantity of permeate, film thickness, film area, permeate time and the pressure drop across film need to be determined. The precision glass capillary, with a calibrated cross-sectional area, has a U-bend to trap the liquid plug and a cajon fitting to make a gas tight connection to the cell. A suitable cathetometer or scale is attached to the capillary for measuring changes in meniscus position. The volume of gas transmitted across the membrane, which represents the quantity of permeate, thus can be calculated after being converted to standard conditions. The pressure drop across the membrane is the pressure reading from the manometer connected to the gas inlet less the atmospheric pressure measured by a barometer. A micrometer is used to measure the membrane thickness to the nearest 1  $\mu\text{m}$  with a minimum of eight points distributed over entire test area. The cell can be put in a temperature-control liquid bath to control the temperature of the cell body to  $\pm 0.1^\circ\text{C}$ .

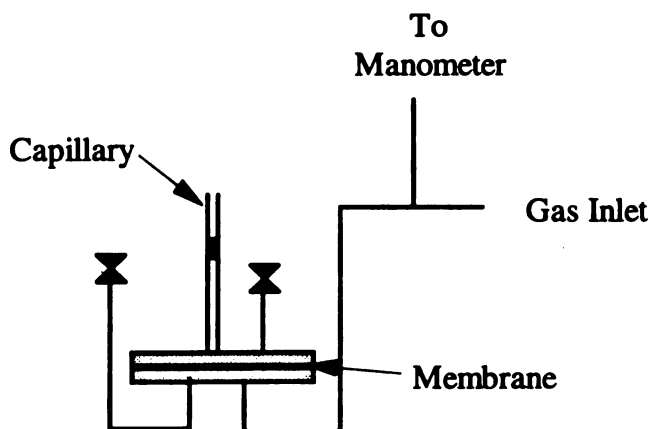


**Figure 2.8.** Schematic diagram of gas permeation cell.

### 2.3. Results and Discussion

The bis(aryl azides) readily dissolved in PTMSP to form homogeneous mixtures. At high loadings, (>3 mol% **BAA** and >5 mol% **HFBA**) signs of phase separation appeared. Optical microscopy confirmed the segregation of cross-linker and polymer. All crosslinking studies reported here were carried out on clear films which showed no apparent signs of phase separation. The dried films were clear, and UV/vis and IR spectra show that the spectra of the as-prepared films are simply the linear combination of the spectrum of PTMSP and that of the azide cross-linker.

Two types of crosslinking experiments were carried out: UV induced crosslinking at room temperature and thermal crosslinking at 175 °C. In both cases, the crosslinking reactions were carried out under an inert atmosphere.



### 2.3.1. Photo-crosslinked and thermal-crosslinked membranes

The irradiating wavelength was set as the peak of the absorption band for the azide. For fluorinated azide **HFBA**, the peak of the absorption is near 254 nm while the absorption spectrum of the benzophenone-based azide **BAA** is red-shifted with a peak near 300 nm (Figure 2.9). Thus we used 254 nm and 300 nm for crosslinking PTMSP/HFBA and PTMSP/BAA composites, respectively. The stretching vibration for the azide at  $2100\text{ cm}^{-1}$  is easily monitored in the IR, and the loss in its intensity can be correlated with the progress of the crosslinking reaction (Figure 2.10). After crosslinking, the membranes became insoluble in THF and toluene, both good solvents for PTMSP. Double bonds on the PTMSP backbone and methyl groups on the side chains are two possible crosslinking sites, but the latter is more likely since access to the double bonds is sterically hindered.<sup>8</sup>

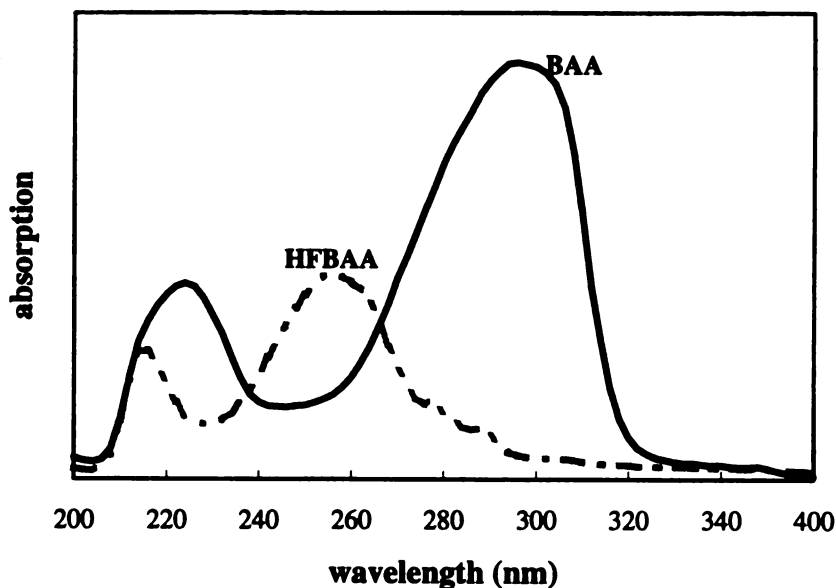


**Figure 2.9.** UV-vis absorption spectra of bis-azide crosslinking agents.

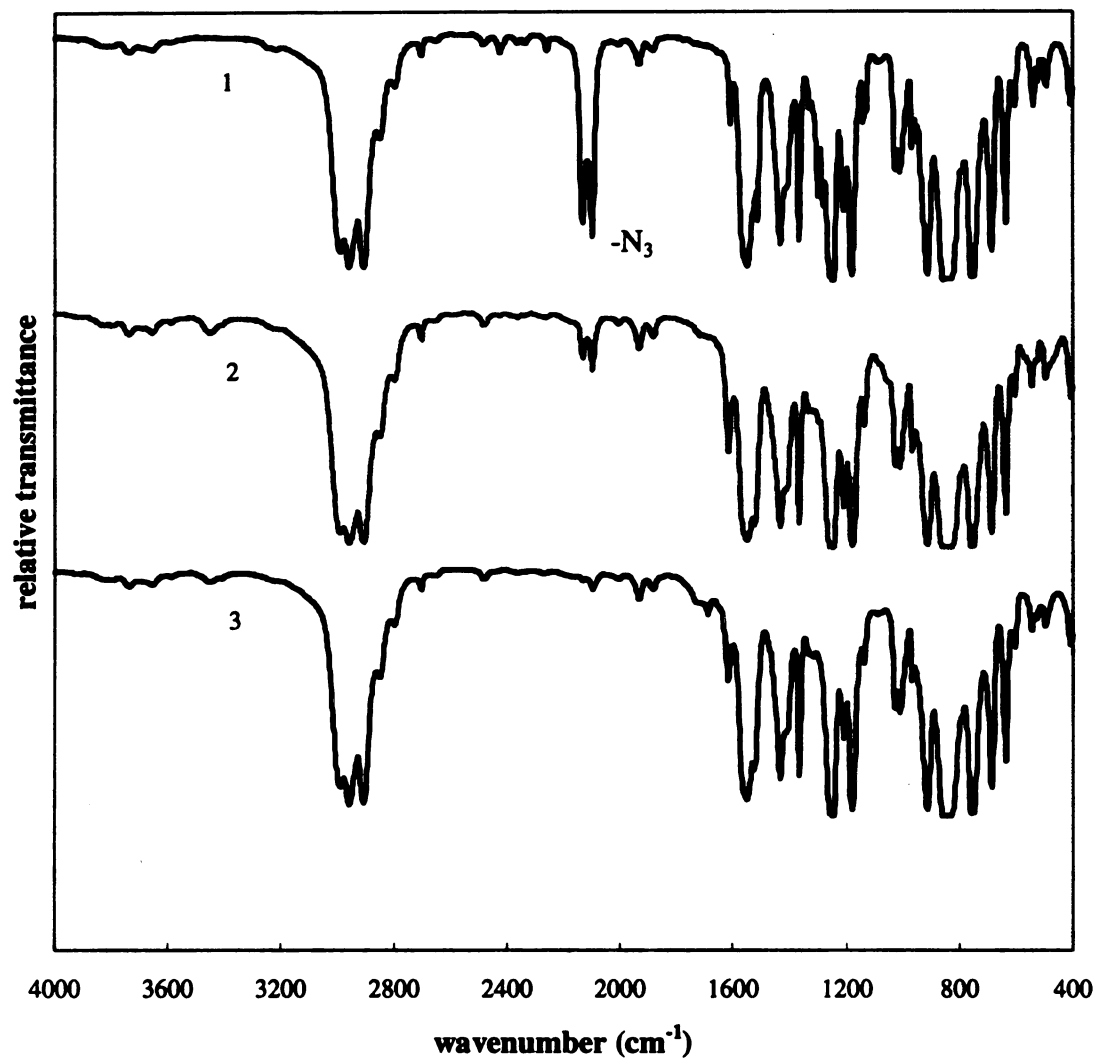


**Figure 2.10.** IR spectra of PTMSP with 3% azide HFBA: 1, PTMSP with 3% azide before treatment; 2, after irradiation; 3, after thermal treatment.

Permeability data were taken for films with different amounts of crosslinker. The addition of bis-azides to PTMSP decreased the permeability slightly before photo irradiation, with no improvement of separation efficiency. Table 2.1 shows that the crosslinking of the bis-azide containing membranes caused decreases in permeability, but the  $O_2/N_2$  separation factors increased slightly. Higher degrees of crosslinking resulted in lower gas permeabilities and higher selectivity. Blanks were run for photochemical reactions to study the effects of irradiation on the properties of PTMSP. When irradiated at 300 nm for 3 hours (the condition used for the irradiation of PTMSP/BAA composite), films showed no significant change in permeability and selectivity. However, when PTMSP membranes were irradiated at 254 nm for a half hour (the condition used for the irradiation of PTMSP/HFBAA), the selectivity improved and the permeability decreased. It is not clear whether the selectivity improvement for PTMSP/HFBAA was caused by the crosslinking of PTMSP or a structure change of PTMSP. One explanation is that some photooxidation occurred during the irradiation of PTMSP that led to decreased porosity and some crosslinking, but not enough to result in an insoluble film. But the fact that the crosslinking with azide BAA led to improvement demonstrated that photo crosslinking played the important role. It is important to note that the irradiated PTMSP membrane (without azides) remained soluble in most solvents while the PTMSP with azide additives became insoluble after irradiation at same condition.

Crosslinked membranes with 1.3% and 2.0% BAA and with 2.0%, 3.0% HFBAA have larger separation factors than PDMS ( $P[O_2] = 0.35 \times 10^{-7} \text{ cm}^3(\text{STP}) \cdot \text{cm}/\text{cm}^2 \cdot \text{s} \cdot \text{cm}$

Hg;  $\alpha[\text{O}_2/\text{N}_2] = 2.0$ ) with comparable permeabilities, making them attractive membrane materials for commercial applications.

**Table 2.1.** Permeability coefficients of oxygen,  $P(\text{O}_2)$ , nitrogen,  $P(\text{N}_2)$ , and the oxygen/nitrogen separation factor,  $\alpha$ , at  $23 \pm 1^\circ\text{C}$ , for PTMSP and photo-crosslinked PTMSP membranes.

crosslinking agent		before		after	
<i>azide</i>	<i>mol% azide</i>	$P(\text{O}_2)$	$\alpha(\text{O}_2/\text{N}_2)$	$P(\text{O}_2)$	$\alpha(\text{O}_2/\text{N}_2)$
none <sup>i</sup>	0	8.05	1.4	7.26	1.4
	1.3	4.47	1.4	1.29	3.0
<b>BAA</b>	2.0	4.11	1.6	0.551	4.3
	3.0	2.01	1.5	0.184	4.2
none <sup>ii</sup>	0	7.91	1.4	0.70	3.2
<b>HFBA</b>	2.0	2.79	1.7	0.543	3.5
	3.0	1.90	2.0	0.559	3.6

$P(\text{O}_2)$  and  $P(\text{N}_2)$  are in units of  $10^{-7} \text{ cm}^3(\text{STP}) \cdot \text{cm}/\text{cm}^2 \cdot \text{s} \cdot \text{cm Hg}$

i irradiated at 300 nm

ii irradiated at 254 nm

The temperature used to initiate the thermal crosslinking, 175 °C, was determined from DSC measurements that show the onset of N<sub>2</sub> loss (Figure 2.11). As shown in Table 2.2, thermal crosslinking had little effect on both the permeability and selectivity. Swelling measurements (Table 2.3) showed higher degrees of swelling for thermal-crosslinked membranes than the corresponding photo-crosslinked membranes, indicating either more free volume in the thermally crosslinked membranes (possibly due to the thermal expansion of the membranes during the crosslinking process) or a lower degree of crosslinking. The densities show a similar trend. Distinct differences in the values of pycnometric and geometric densities were observed. Such behavior is typically seen when these two methods are used to measure the density of glassy polymers.<sup>9</sup> The larger pycnometric densities are related to the filling of the microvoids of glassy polymers by a wetting liquid that is inert with respect to the polymer. The difference between these two groups of density data reflect the amount of preexisting microcavities in glassy polymers. The free volume fraction of the polymer can be estimated by comparing geometric and pycnometric densities of the polymer.<sup>9</sup> Using measured geometric and pycnometric densities of different films, the free volume fractions in the films were estimated. From these data in Table 2.3, one can observe two trends, the free volume fraction in the films decreased after crosslinking and photo-crosslinked membranes have lower free volumes than thermal-crosslinked membranes which results in the lower permeability and higher selectivity. The second trend indicates that film dilation had occurred during thermal crosslinking processes which led to higher free volume for the thermal-crosslinked membranes.

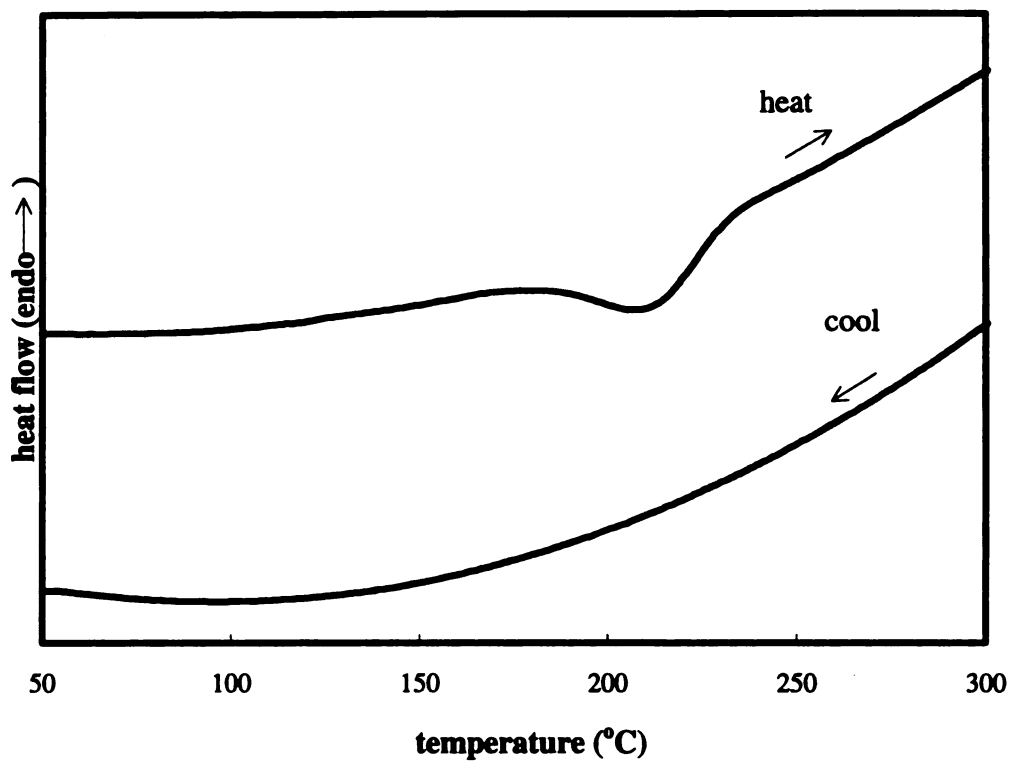


**Figure 2.11.** DSC of PTMSP containing 3.0 mol % azide **HFBAA**. (heating and cooling rate: 10°C/min). The dip in the heating curve corresponds to the decomposition of HFBAA and the loss of nitrogen.

**Table 2.2.** Permeability coefficients of oxygen,  $P(O_2)$ , nitrogen,  $P(N_2)$ , and the oxygen/nitrogen separation factor,  $\alpha$ , at  $23 \pm 1$  °C, for PTMSP and thermal-crosslinked PTMSP membranes.

crosslinking agent		before		after	
<i>azide</i>	<i>mol % azide</i>	$P(O_2)$	$\alpha(O_2/N_2)$	$P(O_2)$	$\alpha(O_2/N_2)$
none	0	7.05	1.7	6.03	1.6
<b>BAA</b>	2.0	3.26	1.6	3.36	1.6
<b>HFBA</b>	0.9	4.80	1.6	4.05	1.5
	2.0	2.88	1.6	2.85	1.6
	3.0	1.13	2.2	1.77	2.3
	4.3	1.05	2.1	2.15	2.2

$P(O_2)$  and  $P(N_2)$  are in units of  $10^{-7} \text{ cm}^3(\text{STP}) \cdot \text{cm}/\text{cm}^2 \cdot \text{s} \cdot \text{cm Hg}$

**Table 2.3.** Swelling and density of the membranes.

Membranes	Density (g/cm <sup>3</sup> )			Degree of Swelling (% in toluene)
	$\rho_g$	$\rho_p$	$(\rho_p - \rho_g) / \rho_g$	
PTMSP	0.70	0.926	0.32	i
2%-BAA-thermal	0.76	0.933	0.23	ii
2%-BAA-photo	0.80	0.935	0.17	ii
2%-HFBA-thermal	0.74	0.938	0.27	224
2%-HFBA-photo	0.80	0.947	0.18	155
3%-HFBA-thermal	0.75	0.947	0.26	191
3%-HFBA-photo	0.80	0.949	0.19	140

$\rho_g$  , geometric density

$\rho_p$  , pycnometric density

i, Swelling experiment not performed because PTMSP is soluble in toluene;

ii, Unable to weigh the film due to highly adhesive property after swelling.



#### 2.3.4. Temperature dependence of permeation

The temperature dependence of the permeability coefficients of oxygen and nitrogen in PTMSP and a crosslinked membrane were studied, and their apparent activation energies for permeation were evaluated using an Arrhenius plot (Figure 2.12). The  $P(O_2)$  and  $P(N_2)$  measurements were carried out from 10-50 °C, a temperature range in which the effect of heat treatment on the films is negligible.

The activation energies for  $P(O_2)$  and  $P(N_2)$  of PTMSP membranes are negative, which are in agreement with the results of other researchers.<sup>10,11</sup> In contrast, the activation energies for  $P(O_2)$  and  $P(N_2)$  of the photo-crosslinked PTMSP membranes are positive, a result typical seen for dense membranes.<sup>12</sup> The apparent activation energy for permeation has two contribution, the activation energy for diffusion  $E_D$ , and the heat of sorption,  $\Delta H$ . The large intersegmental distance in PTMSP (high free volume) is responsible for the low activation energy, and the high solubility coefficient of gases in PTMSP indicates a negative value of heat of sorption. The result is a negative activation energy for permeation.<sup>13</sup> The apparent activation energy for permeation changing to a positive value for crosslinked PTMSP can be interpreted as the decrease of intersegmental distance as well as lower solubility of gases in the membranes.

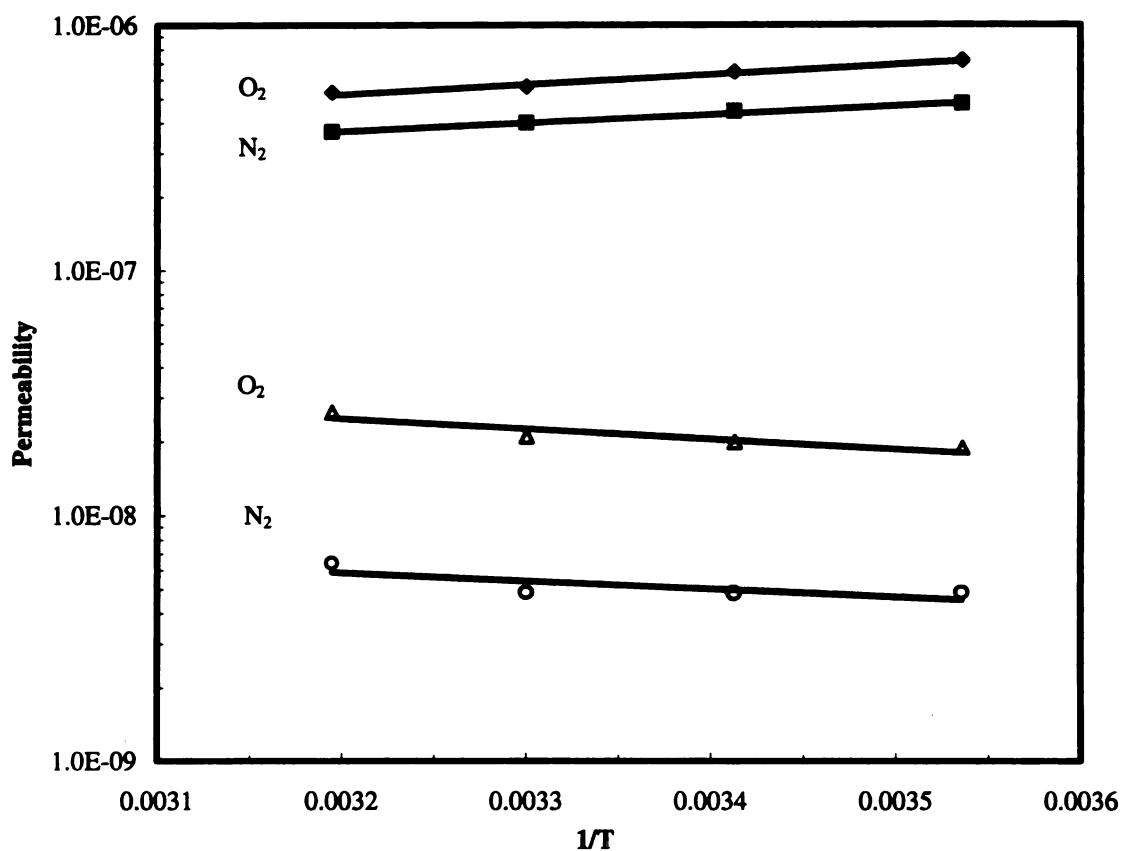


**Figure 2.12.** Arrhenius plot of the oxygen and nitrogen permeability coefficients for PTMSP and a crosslinked PTMSP membrane (2.0% azide **BAA**, photo-crosslinked). Solid patterns, PTMSP,  $E_a(\text{O}_2) = -7.5$  kJ/mol,  $E_a(\text{N}_2) = -6.5$  kJ/mol; Open patterns, crosslinked membranes,  $E_a(\text{O}_2) = 7.6$  kJ/mol,  $E_a(\text{N}_2) = 5.9$  kJ/mol.

### 2.3.5. Effect of fluorination on the permselectivity of O<sub>2</sub>/N<sub>2</sub> separation

It is well known that oxygen has a relatively high solubility in fluorinated polymers.<sup>12</sup> Because the permeability depends on both the diffusion coefficient of the permeant and its solubility, the introduction of fluorine to the PTMSP membranes should increase the selectivity of O<sub>2</sub>/N<sub>2</sub> separation without a significant reduction of the oxygen permeability. In this study, however, the fluorine-containing azide crosslinking agent had no advantages over the non-fluorinated azide except that it has a higher solubility in PTMSP. This result is not surprising, given the low fluorine content in the membranes.

### 2.3.6. Stability of the membranes

We also studied the temporal stability of PTMSP and crosslinked PTMSP membranes (Figure 2.13). Both the unmodified and crosslinked PTMSP membranes showed slight declines in the oxygen permeability over a period of nine months when stored in air. The fact that the permeability decline is independent of crosslinking implies a gradual chemical degradation mechanism intrinsic to the PTMSP structure. Two other groups<sup>12,14</sup> have investigated the long term stability of PTMSP stored in air. Chen *et al.*<sup>12</sup> reported that oxygen permeability changed from 7.87 to  $7.25 \times 10^{-7} \text{ cm}^3(\text{STP}) \cdot \text{cm}/\text{cm}^2 \cdot \text{s} \cdot \text{cm Hg}$  after six month in air at 20 °C. The authors attributed this relative small change to instrument drifts over the time and the measurement uncertainty rather than chemical changes in the samples. Langsam *et al.*<sup>14</sup> studied long term aging effect by heating PTMSP at 60 °C for several hours every one or two months during the 7.5 month storage in air. The starting (day 1) and ending (day 225) oxygen permeability were the same (8.2

$\times 10^{-7} \text{ cm}^3(\text{STP}) \cdot \text{cm}/\text{cm}^2 \cdot \text{s} \cdot \text{cm Hg}$ ), but the permeability initially increase and reached its highest value ( $10.9 \times 10^{-7} \text{ cm}^3(\text{STP}) \cdot \text{cm}/\text{cm}^2 \cdot \text{s} \cdot \text{cm Hg}$ ) on day 49 and decreased thereafter. Although our data and both these two groups' data all showed slight declines in oxygen permeability, the decrease might not be significant from a practical point of view given the long period of time. PTMSP membranes stored in air should be considered stable for the duration of its commercial life time.

When stored in vacuum at 10 mtorr for a month, the crosslinked membranes showed no decline and the PTMSP membrane showed only a slight decline (Table 2.5) in contrast to the results by Nagai et al.<sup>15</sup> It is believed that the PTMSP membranes absorb pump oil vapors when stored in vacuum and the decline in permeability is caused by the hydrocarbon oil contaminating the PTMSP membranes. It was reported that without a cold trap between the vacuum pump and the PTMSP membrane, a gravimetric increase of 20 wt% by oil vapor sorption was found<sup>16</sup> while with a cold trap a gravimetric increase by oil vapor sorption was not observed.<sup>15</sup> We assume that a very small amount of oil vapor would work as an accelerator of the inter-chain diffusion that causes densification and a decrease in the free volume and permeability. This suggests that crosslinking of PTMSP inhibits the inter-chain diffusion and stabilizes the gas permeability.

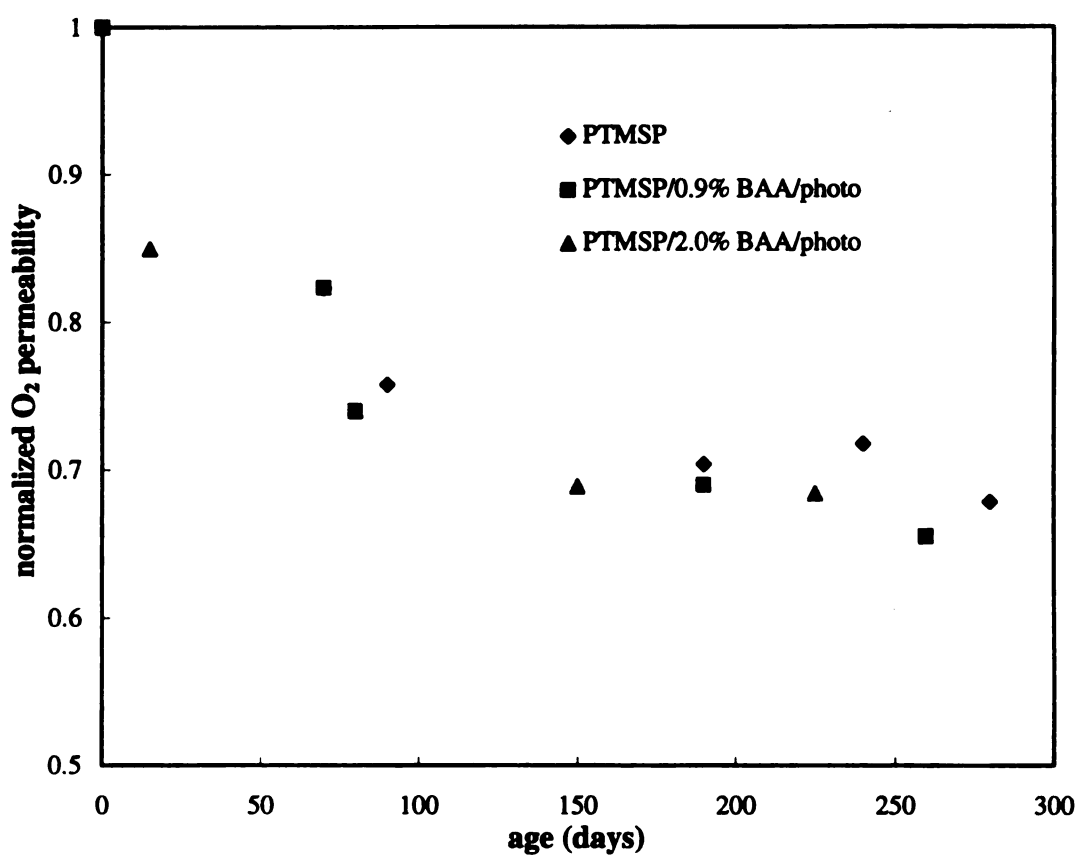


**Figure 2.13.** Temporal stability of the membranes stored in air.

**Table 2.5.** Temporal stability of the membranes stored under vacuum.

<b>Membranes</b>	<b>Days in vacuum</b>	<b>P(O<sub>2</sub>)</b>	<b>Normalized P(O<sub>2</sub>)</b>
<b>PTMSP**</b>	0	8	1
	28	2	0.25
<b>PTMSP*</b>	0	6.95	1
	33	4.88	0.70
<b>3%-BAA-thermal</b>	0	1.31	1
	39	1.20	0.92
<b>2%-BAA-photo</b>	0	0.169	1
	27	0.168	1.0
<b>3%-BAA-photo</b>	0	0.136	1
	31	0.120	0.88
<b>2%-HFBA-thermal</b>	0	2.11	1
	29	2.20	1.0
<b>2%-HFBA-photo</b>	0	0.326	1
	29	0.303	0.93

P(O<sub>2</sub>) and P(N<sub>2</sub>) are in units of 10<sup>-7</sup>cm<sup>3</sup>(STP)•cm/cm<sup>2</sup>•s•cmHg

\*\*Data from Nagai, K.; Higuchi, A.; Nakagawa, T. *J. Polym. Sci. Part B: Polym. Phys.*, 1995, 33, 289.

\*Data from this work.

## 2.4. Conclusions

By the addition of a small amount of bis(aryl azide), PTMSP membranes can be photochemically or thermally crosslinked. The additive resulted in a lower selectivity before crosslinking was initiated, which is believed to be due to the filling of the free volume by the additives. After photo-crosslinking, membranes showed a further increase in selectivity and a lower permeability, with some photo-crosslinked membranes showing higher selectivities than commercial membranes with comparable permeabilities. Thermal-crosslinked membranes showed no changes in permeability and selectivity compared to PTMSP with additive azides in the membranes. Higher degrees of swelling for thermal-crosslinked membranes indicates either more free volume in these membranes (possibly due to the thermal expansion of the membranes during the crosslinking process) or a lower degree of crosslinking. When stored in air, both unmodified and crosslinked PTMSP membranes showed slight permeability declines over nine months, which may be caused by chemical contamination or aging (oxidation). When stored in vacuum for a month, PTMSP membranes showed slight declines while crosslinked membranes had no decline in the oxygen permeability. Crosslinking of PTMSP is thought to restrict inter-chain diffusion which would otherwise be accelerated by small molecules such as pump oil. The restriction of inter-chain diffusion helped to maintain the high free volume therefore stabilized the permeability.

## 2.5. References

1. Hsu, K. K.; Nataraj, S.; Thorogood, R. M.; Puri, P. S. *J. Membr. Sci.* **1993**, *79*, 1.
2. DeForset, W. *Photoresist Materials and Processes*; McGraw Hill, New York, NY, 1975.
3. Willson, C. G. In *Introduction to Microlithography*; Thompson, L. F.; Willson, C. G., Bowden, M. J., Eds.; ACS Symposium Series 219; American Chemical Society, Washington, DC; **1983**, p 87.
4. Masuda, T.; Isobe, E., Higashimura, T. *Macromolecules* **1985**, *18*, 841.
5. Neenan, T. X.; Kumar, U.; Miller, T. M. *Polym. Prepr.* **1994**, *35(1)*, 391.
6. *Organic Syntheses, Collective Volume 5*; Baumgarten, H. E. Ed.; John Wiley and Sons: New York; **1973**, p 829.
7. ASTM, D1434-82 (reapproved 1988), *American Society for Testing and Materials*; 1990 Annual Book of Standards.
8. Clough, S. B.; Sun, X. F.; Tripathy, S. K.; Baker, G. L. *Macromolecules*, 1991, *24*, 4264.
9. Plate, N. A.; Bokarev, A. K.; Kaliuzhnyi, N. E.; Litvinova, E. G.; Khotimskii, V. S., Volkov, V. V.; Yampol'skii, Yu. P. *J. Membr. Sci.* **1991**, *60*, 13.
10. Nakagawa, T.; Fujisaki, S.; Nakano, H.; Higuchi, A. *J. Membr. Sci.* **1994**, *94*, 183.



11. Takada, K.; Matura, H.; Masuda, T.; Higashimura, T. *J. Appl. Polym. Sci.* **1985**, *30*, 1605.
12. Chen, G.; Griesser, H. J.; Mau, A. W. H. *J. Membr. Sci.* **1993**, *82*, 99.
13. Nakagawa, T.; Fujisaki, S.; Nakano, H.; Higuchi, A. *J. Membr. Sci.* **1994**, *94*, 183.
14. Langsam, M.; Robeson L. M. *Polym. Eng. Sci.* **1989**, *29(1)*, 44.
15. Nagai, K.; Higuchi, A.; Nakagawa, T. *J. Polym. Sci. Part B: Polym. Phys.* **1995**, *33*, 289.
16. Witchey-Lakshmanan, L. C.; Hofenberg, H. B.; Chern, R. T. *J. Membr. Sci.* **1990**, *48*, 321.

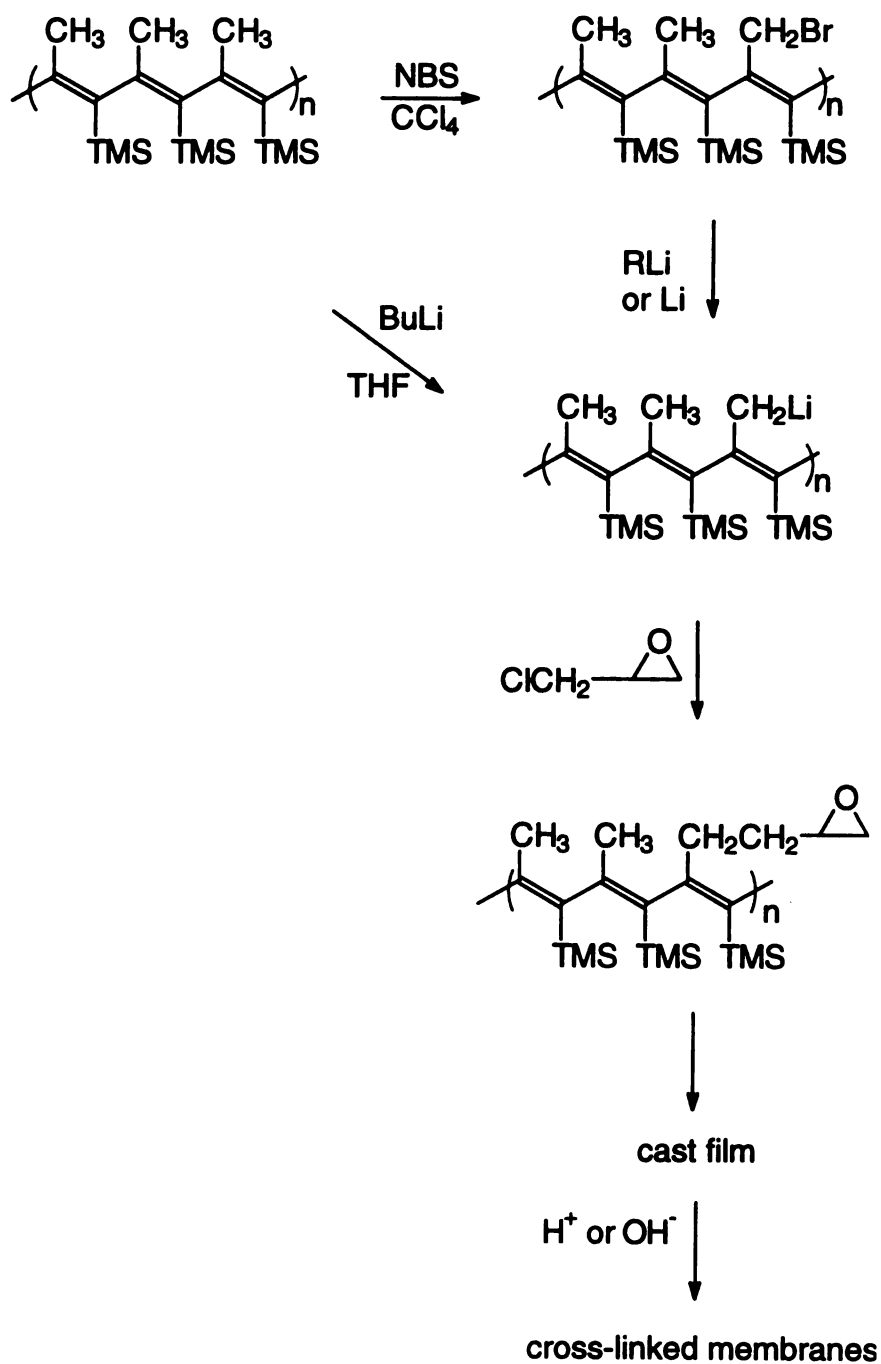
## **Chapter 3**

# **Crosslinking of Poly[1-trimethylsilyl-1-propyne] Membranes through the Functionalization of Allylic Methyl Group**

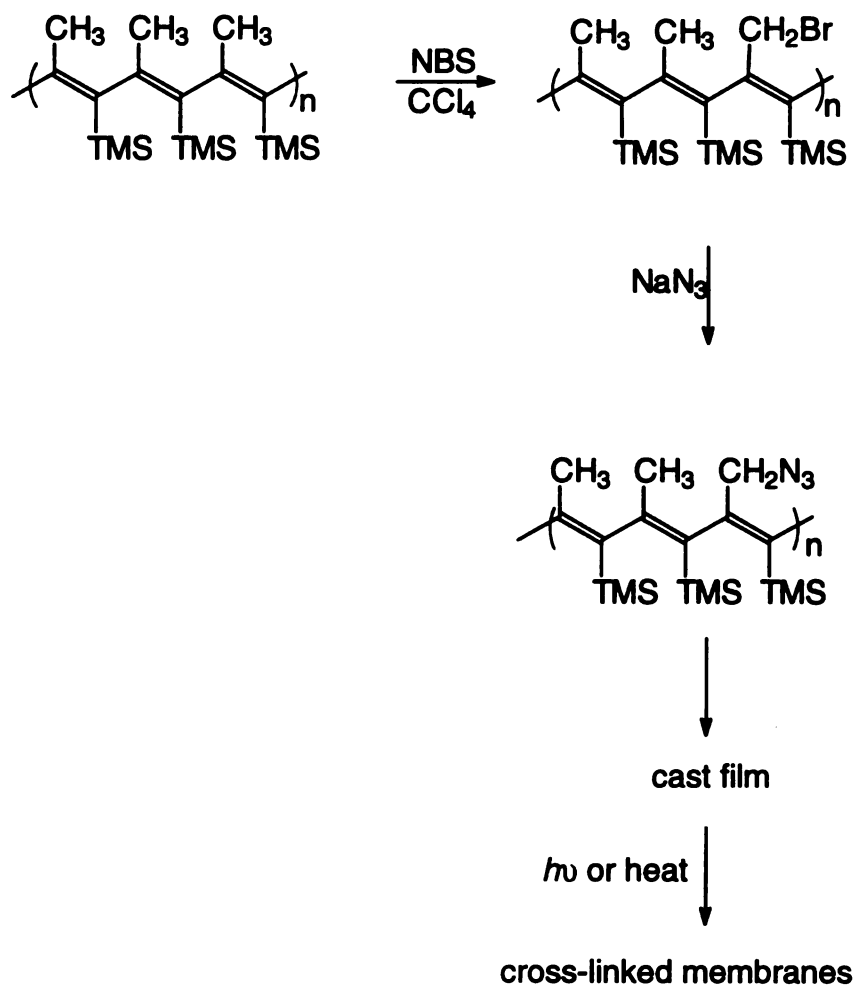
### **3.1. Introduction**

As described in Chapter 2, poly[1-trimethylsilyl-1-propyne] membranes were crosslinked by adding 1-3% of bis-aryl azide crosslinking agents to the polymer. In this scheme, the crosslinking density is limited by the solubility of the crosslinking agents in the polymer matrix. In order to control the crosslinking density over a wider range, it is necessary to generate crosslinking sites attached to the polymer backbone or side chains. To functionalize poly[1-trimethylsilyl-1-propyne] three routes are available: reaction with main chain double bonds, reaction with allylic protons and copolymerization with an acetylenic comonomer having a functionalizable pendant group. Despite numerous attempts and the use of various reaction conditions, it has been shown that the double bonds of the polymer backbone are unreactive.<sup>1,2</sup> Low reactivity for the double bonds of poly[1-trimethylsilyl-1-propyne] should be expected because of its rigid random coil conformation and the severe steric effects caused by the methyl and trimethylsilyl side chain groups. The stability of PTMSP in air, its lack of optical absorption at  $\lambda > 280$  nm,

and an examination of space filling models of the polymer all implied that the double bonds are not conjugated, that the chemistry at double bonds of the polymer would be limited, and that allylic substitution should be favored.<sup>3</sup> Allylic functionalization of PTMSP has been reported to yield brominated PTMSP<sup>4</sup> and a lithiated intermediate.<sup>5</sup> Introducing the crosslinking sites through allylic substitution should be an alternative to crosslinking PTMSP membranes using arylazides. Two schemes were investigated. The first is based on the polymerization of pendant epoxide units,<sup>6</sup> a well-known route to crosslinked polymers that is widely used in photoresist chemistry. As shown in Scheme 3-I, the pendant epoxide units could be introduced via bromination of PTMSP followed by lithiation, or via direct lithiation (metallization) of PTMSP. The second scheme was an attempt to introduce an azide group via brominated polymer as shown in Scheme 3-II.



Scheme 3-I



Scheme 3-II

## 3.2. Experimental

### 3.2.1. Materials and Characterization

PTMSP was prepared by the method described in Chapter 2. The polymer thus obtained was dried in vacuum overnight before use. N-bromosuccinimide, *n*-BuLi, *t*-BuLi, Li, NaN<sub>3</sub>, and epichlorohydrin were purchased from Aldrich. THF and toluene were dried by distillation from sodium to remove trace amounts of water. Proton nuclear resonance (<sup>1</sup>H NMR) analyses were carried out at room temperature in deuterated chloroform (CDCl<sub>3</sub>) on a Varian Gemini-300 spectrometer with the solvent proton signals being used as chemical shift standards. Infrared (IR) spectra of polymer were obtained under nitrogen at room temperature on a Nicolet IR/42 Fourier Transform IR spectrometer. The IR measurements were carried out on thin films deposited on NaCl plates. Differential scanning calorimetry (DSC) and thermogravimetric analyses (TGA) of the polymers were performed under a nitrogen atmosphere at a heating rate 10 °C/min on a Perkin Elmer DSC 7 and a Perkin Elmer TGA 7 instrument, respectively. The temperature was calibrated with an indium standard.

### 3.2.2. Synthesis of brominated derivatives of PTMSP

Using conditions described in the literature,<sup>3</sup> PTMSP was brominated with N-bromosuccinimide in refluxing CCl<sub>4</sub> in the presence of benzoyl peroxide. An example for the synthesis of 20% brominated PTSMP is as follows. A PTMSP solution was prepared by dissolving PTMSP (1.0 g, 8.9 mmol) in 50 mL CCl<sub>4</sub> at room temperature under a

nitrogen atmosphere. N-bromosuccinimide (0.72 g, 4.5 mmol) was added to the PTMSP solution together with a catalytic amount of benzoyl peroxide. The mixture was stirred for 2 hours in the presence of light. After filtration of the reaction mixture, the brominated polymer was obtained by precipitating the polymer in an excess amount of methanol. The yield was nearly quantitative.

### **3.2.3. Synthesis of glycidyl-modified PTMSP from brominated PTMSP**

#### **3.2.3.1. Preparation through halides and lithium metal**

Using a Japanese patent<sup>7</sup> as a reference for the synthesis, dry 50% brominated poly[1-trimethylsilyl-1-propyne] (1.0 g, 4.4 mmol) was dissolved in 50 mL THF under a nitrogen atmosphere. Freshly cut lithium metal (62 mg, 8.9 mmol) was weighed and placed in a flask in a dry box. To this flask, a THF solution of brominated PTMSP was added slowly under a nitrogen atmosphere. After the lithium had reacted, the mixture was cooled to -20 °C (carbon tetrachloride-dry ice bath), and an excess of epichlorohydrin (dried over CaH<sub>2</sub>) was added. After 1 hour at -20 °C, the reaction was allowed to warm to room temperature and stirring was continued for 12 hours. The reaction mixture was then precipitated into methanol.

#### **3.2.3.2. Preparation through halides and lithium metal exchange**

Dry brominated poly[1-trimethylsilyl-1-propyne] (0.50 g, 2.2 mmol Br unit) was dissolved in 25 mL THF under a nitrogen atmosphere. This solution was cooled to -78 °C in an acetone-dry ice bath and a 1.6 M solution of BuLi in *n*-hexane (2.8 mL, 4.4

mmol) was injected into the solution from a syringe while flushing with nitrogen. After 2 hours at -78 °C, the reaction mixture was warmed to -20 °C. A excess amount of epichlorohydrin was then added. After 1 hour at -20 °C, the reaction was allowed to warm up to room temperature and stirring was continued for 12 hours. The reaction mixture was then precipitated into methanol.

#### 3.2.4. Synthesis of glycidyl-modified PTMSP from directly lithiated PTMSP

The direct lithiation of PTMSP was carried out according to the method described by Nagase et al.<sup>5</sup> A solution of PTMSP (0.10 g, 0.89 mmol) in 20 mL of dry THF was prepared under an argon atmosphere. To this solution, a 1.6 M solution of *n*-butyllithium (0.6 mL, 0.89 mmol) in *n*-hexane was added at 0 °C. After stirring for 2 hours at 0 °C, an excess amount of epichlorohydrin was added. The reaction mixture was precipitated into methanol to obtain the desired polymer.

#### 3.2.5. Synthesis of azido-modified PTMSP

*With phase transfer agent.* Brominated PTMSP (0.50 g, 2.2 mmol Br unit) was dissolved in either 25 mL benzene<sup>8</sup> or THF under a nitrogen atmosphere. NaN<sub>3</sub> (0.58 g, 8.9 mmol) or LiN<sub>3</sub> (0.44 g, 8.9 mmol) and a phase transfer reagent (18-crown-6, 29 mg, 0.11 mmol) were added at the desired temperature (50 °C for THF and 60 °C for benzene). The reaction mixture was sampled at different times (precipitated into methanol) and <sup>1</sup>H NMR was used to determine the conversion.



*With Zinc salt.* Brominated PTMSP (0.5 g, 2.2 mmol Br unit) was dissolved in 25 mL benzene or THF under a nitrogen atmosphere.  $\text{NaN}_3$  (0.58 g, 8.9 mmol) or  $\text{LiN}_3$  (0.44 g, 8.9 mmol),  $\text{ZnCl}_2$  (0.18 g, 0.73 mmol) and pyridine (2.2 mmol) were added at the desired temperature (50 °C for THF and 60 °C for benzene). The reaction mixture was sampled at different times (precipitated into methanol) and  $^1\text{H}$  NMR was used to determine the conversion.

### 3.3. Results and Discussion

It has been reported<sup>3</sup> that nearly quantitative yields of mono-brominated PTMSP were obtained for bromination levels up to 50%, but the maximum attainable bromination level was only 60%, even when a large excess of NBS was used. This behavior was attributed to extreme steric crowding at the allylic methyl group in the polymer structure. The accessibility of the allyl sites is so limited that monobromination is observed exclusively, and the presence of a bulky halogen at one site was thought to reduced the likelihood of bromination at adjacent allylic sites.<sup>3</sup>

20% and 50% brominated PTMSP were synthesized using the literature methods. Figure 3.1 shows  $^1\text{H}$  NMR of PTMSP and brominated PTMSP. The trimethylsilyl group resonance remained unchanged with bromination, consistent with no bromination at those sites. On the other hand, the resonance from the allyl methyl group (1.8 ppm) shifted slightly downfield (to 2.2 ppm) due to the presence of Br. Compared to PTMSP, the IR spectrum of brominated PTMSP (Figure 3.2) showed additional peaks caused by

bromination. For example, the peak at  $1219\text{ cm}^{-1}$  is due to a strong  $\text{CH}_2$  wagging band for  $\text{CH}_2\text{Br}$  group. Brominated PTMSP is pale yellow compared to colorless PTMSP, and TGA scans (Figure 3.3) showed decreasing thermal stability with bromination. DSC runs (Figure 3.4) showed no evidence of glass transition before decomposition occurred. The brominated polymer degraded at lower temperature, as shown by a exothermic transition near  $270\text{ }^\circ\text{C}$  in DSC traces, and an onset of weight loss in TGA runs at the same temperature.

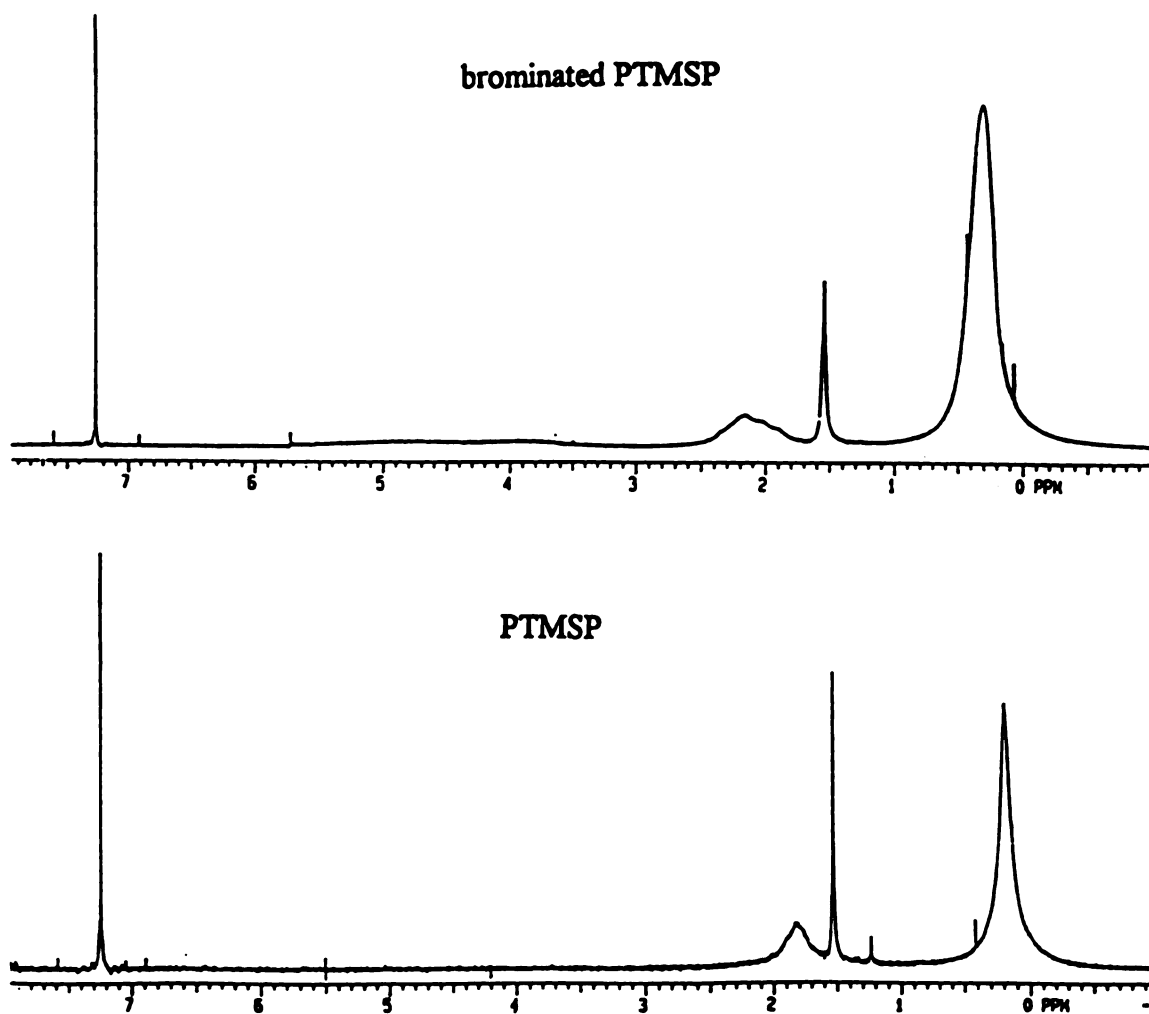


**Figure 3.1**  $^1\text{H}$  NMR of PTMSP and brominated PTMSP

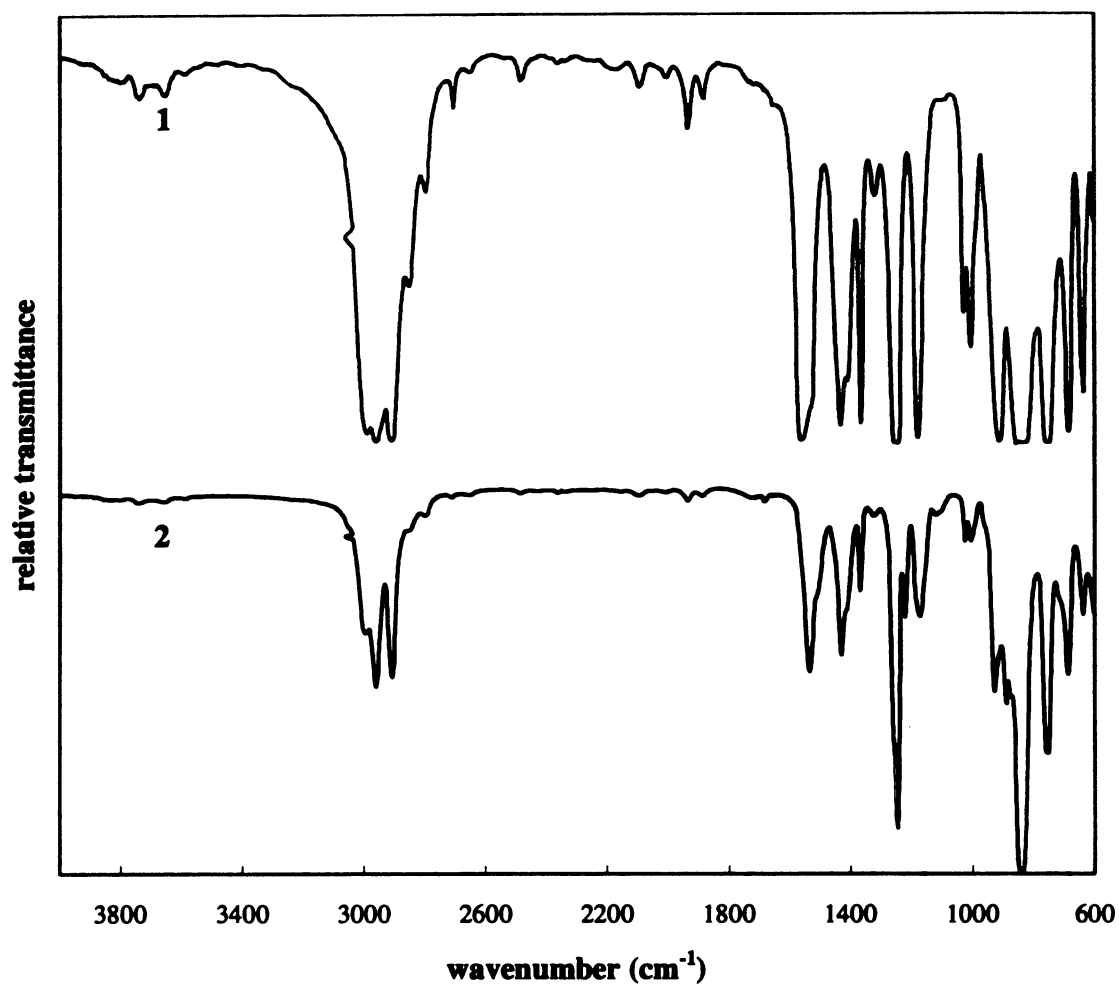


**Figure 3.2 . IR spectra of PTMSP and brominated PTMSP:**

**1, PTMSP; 2, 50% Brominated PTMSP.**

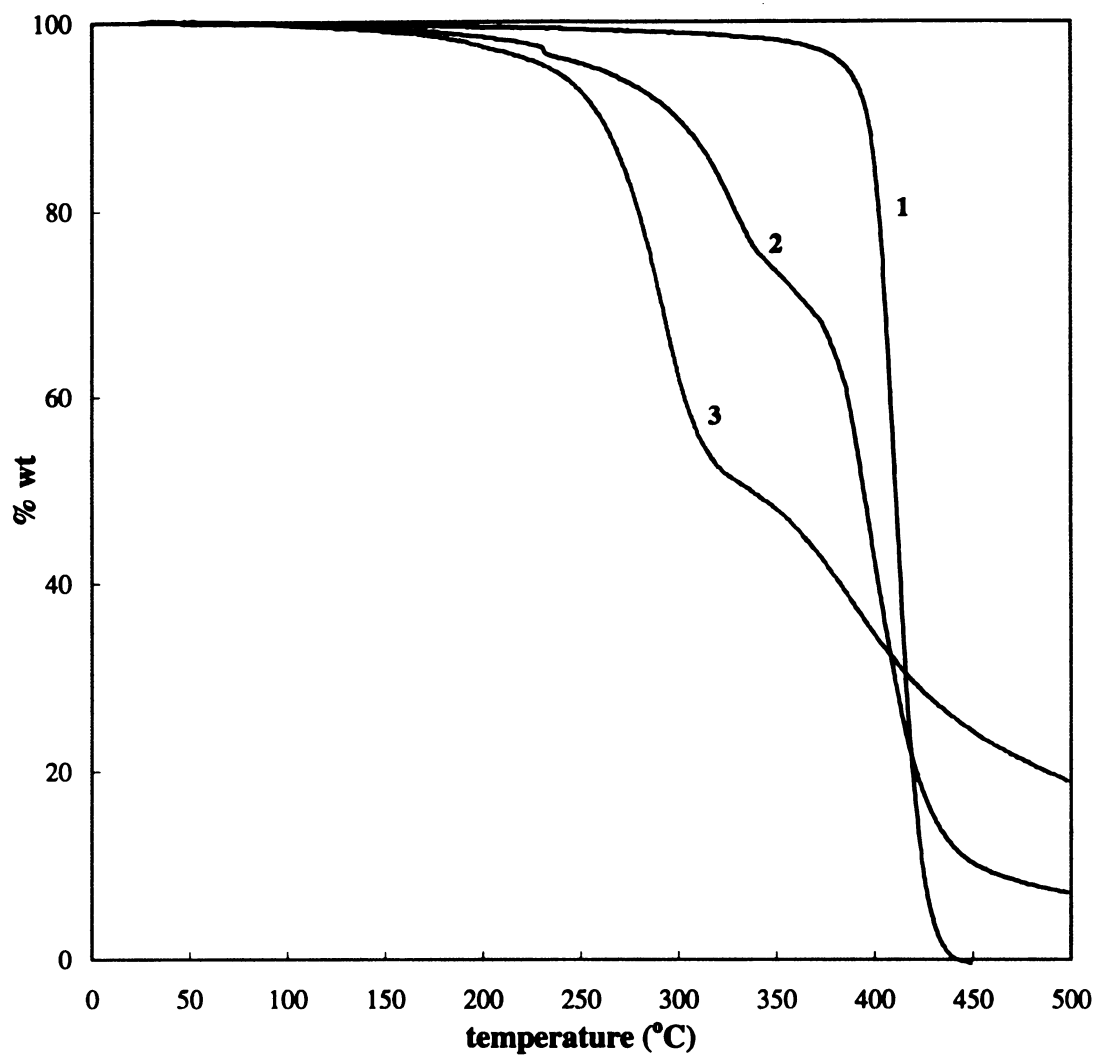


**Figure 3.3.** Thermogravimetric analysis of PTMSP and brominated PTMSP:

**1, PTMSP; 2, 20% Brominated PTMSP; 3, 50% Brominated PTMSP.**

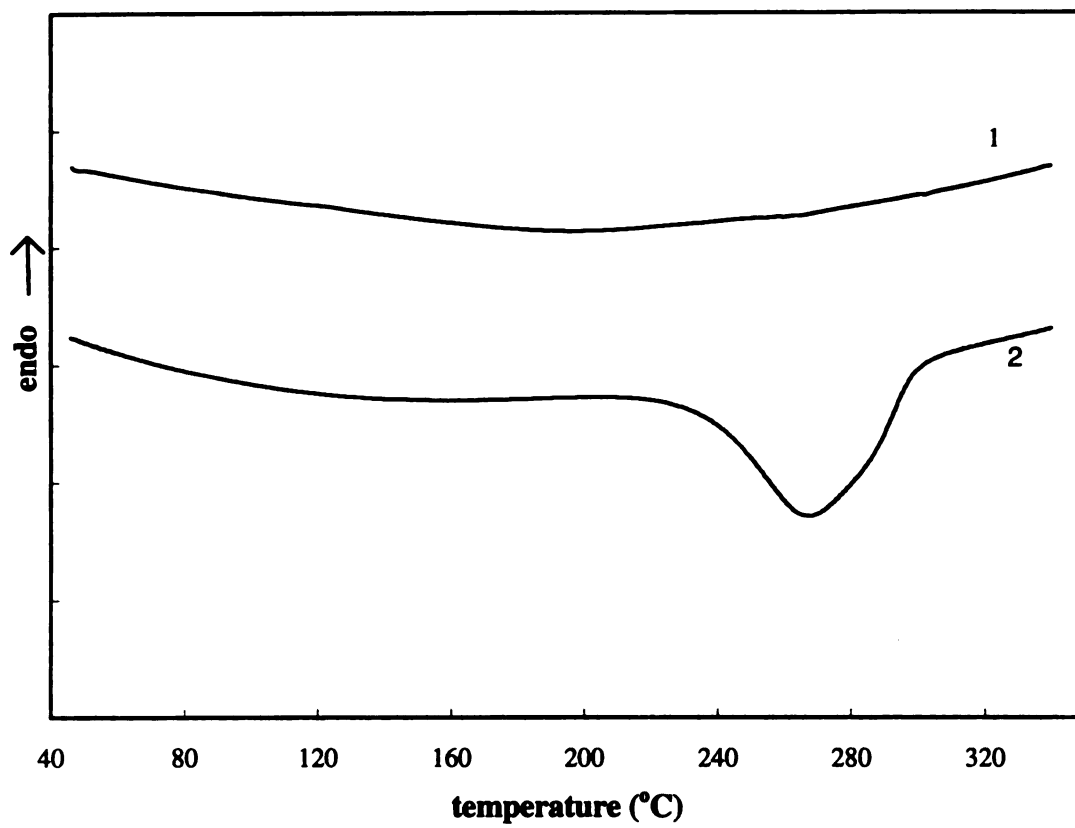


**Figure 3.4.** DSC of PTMSP and brominated PTMSP:

**1,** PTMSP; **2,** 50% Brominated PTMSP.

Our attempts to synthesize glycidyl-modified PTMSP from brominated PTMSP, **Scheme 3-I** did not produced the desired polymer. During the metalation, gelation was observed, and the resulting polymer became insoluble and unprocessable. This is a well-known problem in the preparation of allyl derivatives of active metals. Coupling of the allylmetalated polymer with remaining allylic halide sites (Wurtz coupling) is a significant side reaction which leads to gelation. For reactions using *n*-BuLi, adding *n*-BuLi solution to the polymer solution (normal addition), also led to gelation. When polymer solution was slowly added to *n*-BuLi solution (reverse addition), the butyl group apparently was incorporated into the polymer (coupling between brominated polymer and BuLi) instead of the epoxide group. If epoxides were introduced into the polymer, there should be a noticeable peak in  $^1\text{H}$  NMR spectrum around 3.3 ppm from the -CH of the epoxide group.<sup>9</sup> Figure 3.5a shows the  $^1\text{H}$  NMR spectrum of the modified polymer obtained by reacting brominated PTMSP with *n*-BuLi and epichlorohydrin. No peaks near 3.3 ppm were found, and instead broad peaks at 0.9 ppm and 1.3 ppm appeared that can be attributed to *n*-butyl group. Further evidence of alkylation were seen when brominated PTMSP was reacted with *t*-BuLi and epichlorohydrin.  $^1\text{H}$  NMR (Figure 3.5.b) of the product shows an additional peak around 0.9 ppm which could be attributed to protons on the added *t*-butyl group. Alkylation reactions dominated the lithiation chemistry even when a very low temperature (-78 °C) was used for the reaction.

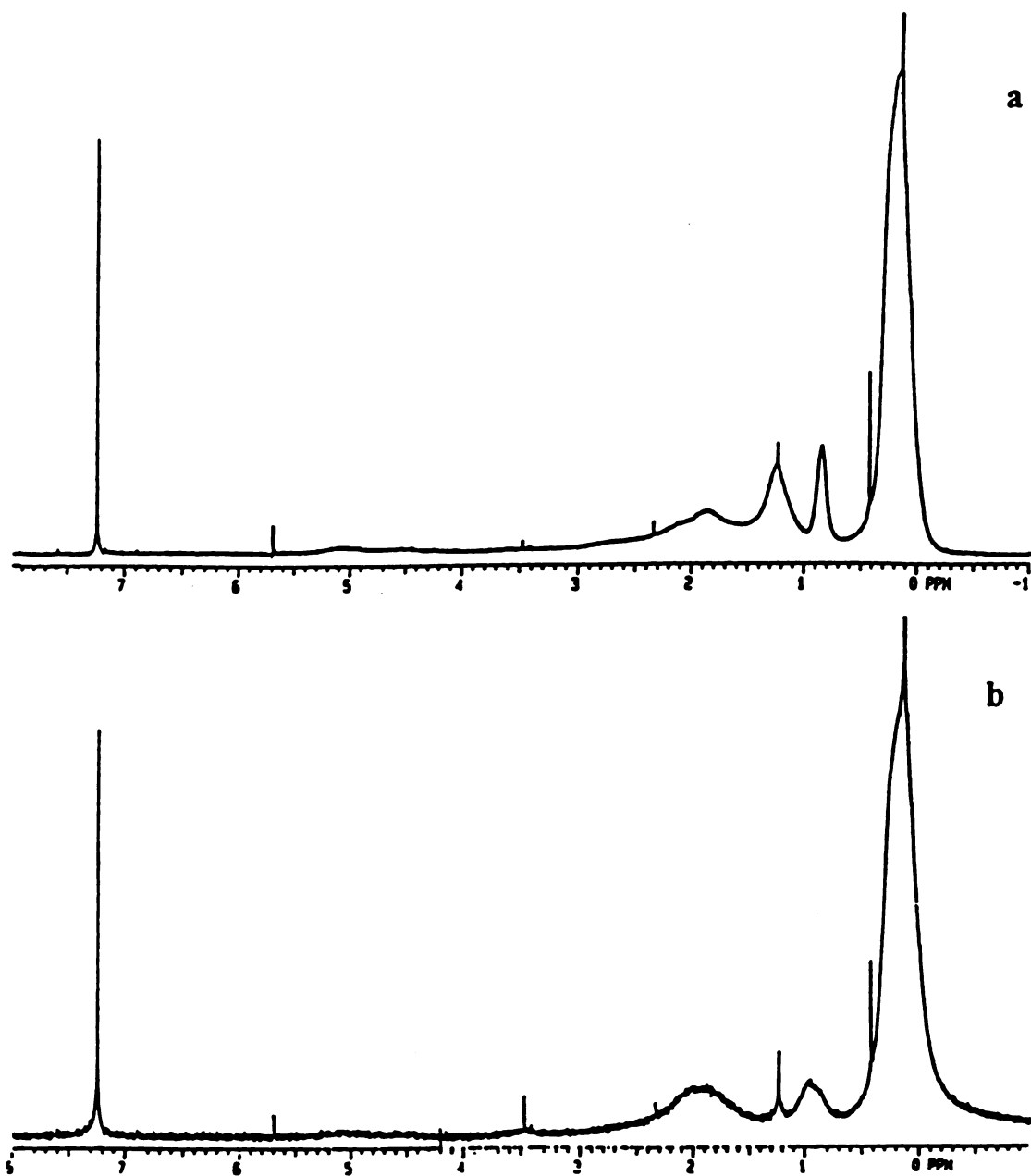


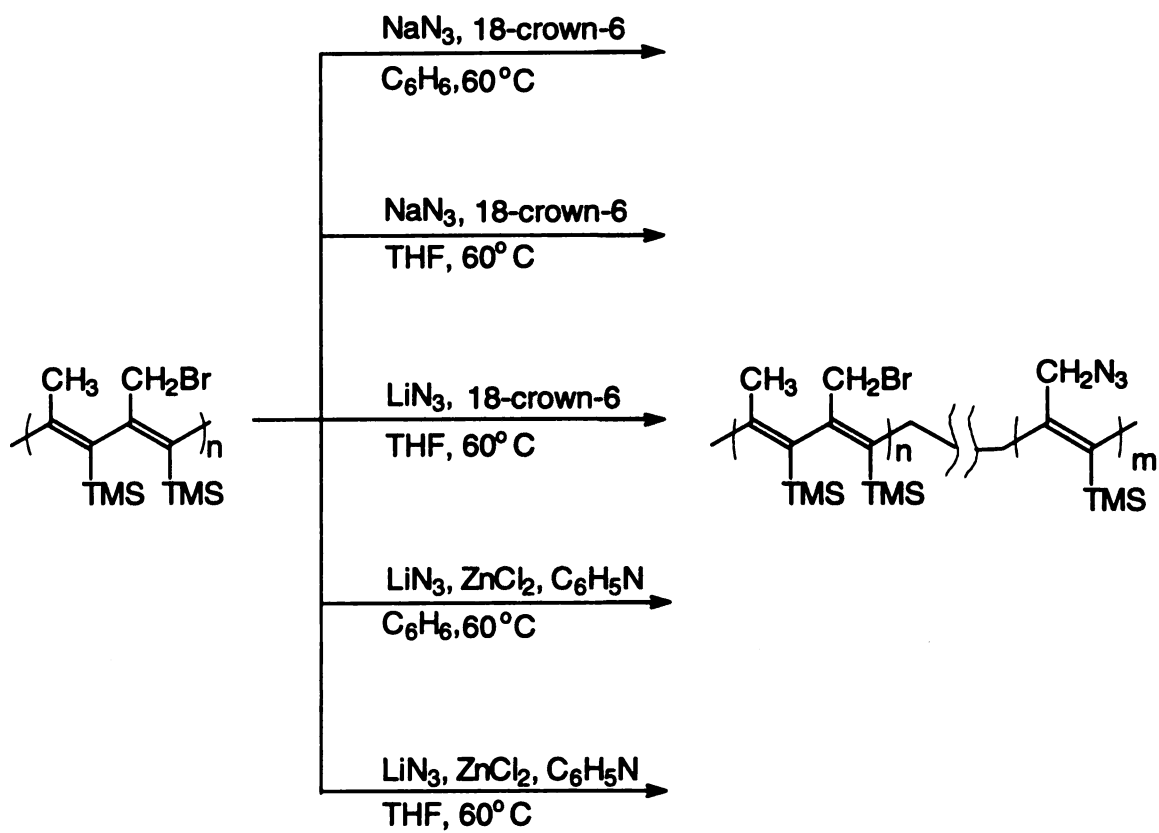
**Figure 3.5.**  $^1\text{H}$  NMR spectra of: **a.** product from the reaction of brominated PTMSP with *n*-BuLi and epichlorohydrin; **b.** product from the reaction of brominated PTMSP with *t*-BuLi and epichlorohydrin.

Although it has been reported that PTMSP/PDMS graft copolymer was synthesized via metallization of PTMSP with *n*-butyllithium,<sup>5</sup> our study showed no evidence of functional groups being introduced into the polymer under the reported conditions. We attribute the unreactive character of the allylic methyl group to the extreme steric crowding in the polymer structure.

Since we showed that PTMSP can be crosslinked with azide additives, including an azido group ( $-N_3$ ) in the PTMSP structure should give a polymer that can be crosslinked in a subsequent step. The most common synthetic approach to azides, especially alkyl azides, is displacement of halide by azide ion.<sup>10</sup> The reaction can be improved by using a phase-transfer agent.<sup>11</sup>  $S_N1$  active allyl azides (as well as tertiary and benzyl azides) have also been prepared from allyl bromide by the use of  $NaN_3/ZnCl_2$ <sup>12</sup> or trimethylsilyl azide.<sup>13</sup> Some polymeric halogen derivatives, such as poly(vinyl chloride) and poly(epichlorohydrin), have also been reported to be partially converted to polymeric azides.<sup>14,15</sup>

Scheme 3-III outlines the various conditions used in this study to introduce an azide group to brominated derivatives of PTMSP. Figure 3.6 and Figure 3.7 show typical NMR and IR spectra of the product. Using 50% brominated PTMSP, and under all conditions listed in Table 3.1, the products showed a small peak at  $\sim 2100\text{ cm}^{-1}$  in the IR spectra indicating the appearance of the  $N_3$  group. NMR data also are consistent with partial introduction of the azide. However, our best results show only partial conversion to azide derivatives after 5 days of reaction since IR spectra of the products showed a strong  $Br-CH_2-$  vibration at  $1219\text{ cm}^{-1}$ .





Schem 3-III.

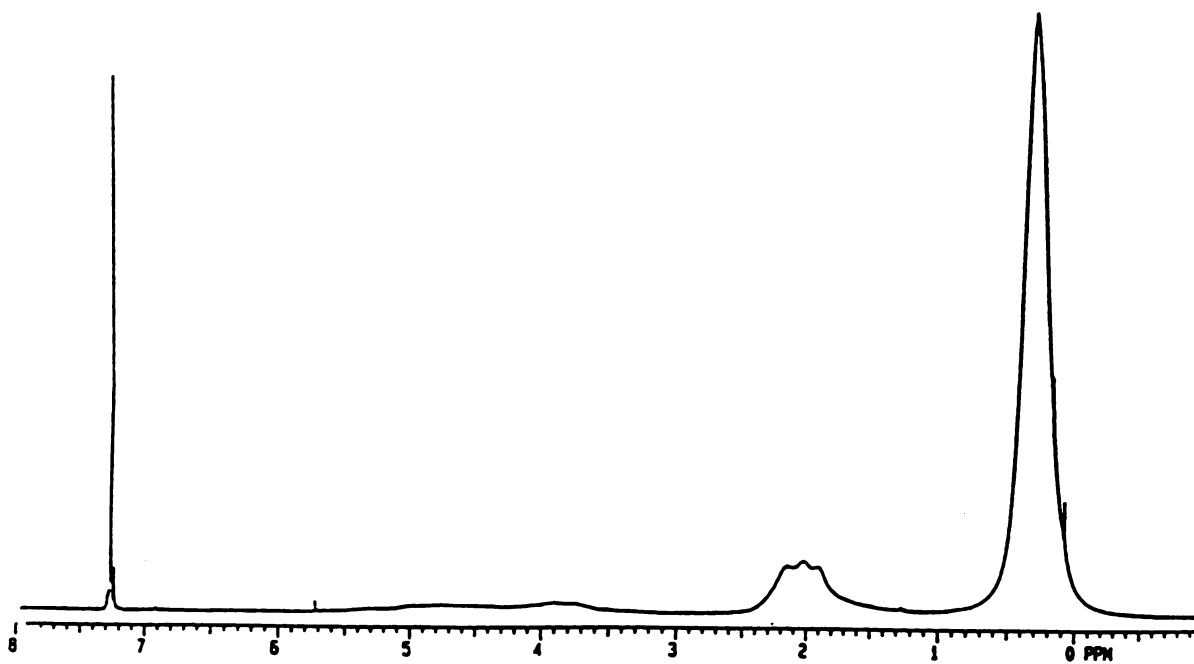


**Figure 3.6** NMR spectrum of polymer product obtained by reacting brominated PTMSP with azides.

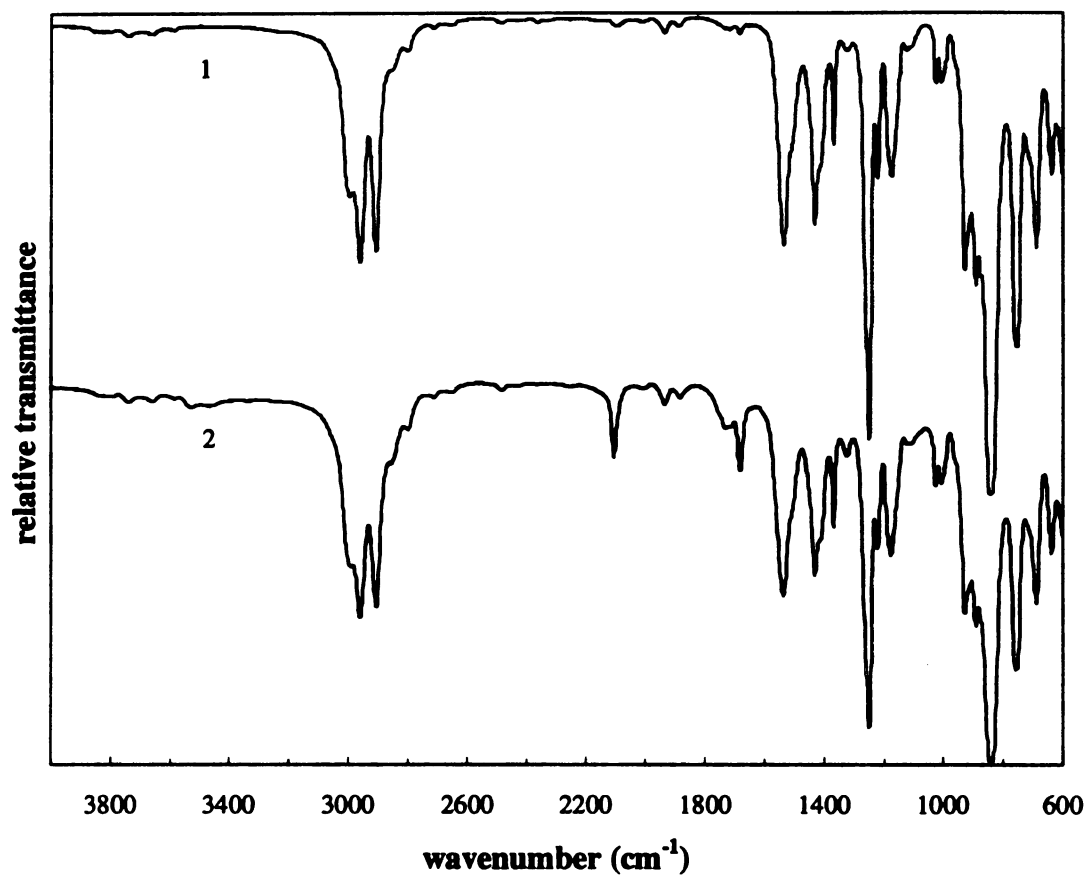


**Figure 3.7.** IR spectra of: 1, brominated PTMSP; 2, the polymer resulting from brominated PTMSP reacting with azides.

To compare different reaction conditions, the peaks at  $2100\text{ cm}^{-1}$  ( $\text{-N}_3$ ) and the peaks at  $3000\text{ cm}^{-1}$  ( $\text{CH}_3$  groups) were integrated, and the ratio of these two integrations was used to compare the relative conversion as seen in Table 3.1. Comparing **Run 1** with **Run 2** or **Run 4** with **Run 5** shows that the reaction rate is faster in THF than in benzene, because polar solvents are more effective for the solvation and ionization of the azide reactants as well as the solvation of  $\text{Br}^-$ . The relative effect of adding a phase-transfer agent (18-crown-6) or a catalyst  $\text{ZnCl}_2/\text{pyridine}$  is shown by comparing **Run 3** with **Run 7**. The reaction was faster when using  $\text{ZnCl}_2/\text{pyridine}$ , indicating that  $\text{ZnCl}_2$  reacts with Br on the polymer to accelerate the formation of the allylic cation. Neither the type of cation (**Run 5** and **Run 6**) nor concentration of nucleophile had a great effect on the reaction rate (**Run 7** and **Run 8**). Regardless of the conditions attempted, the conversion did not reach completion as indicated by the persistence of a strong  $\text{Br-CH}_2^-$  vibration at  $1219\text{ cm}^{-1}$  in IR spectra.

The presence of Br in the polymer will cause degradation during crosslinking by thermal treatment or photo irradiation. For the products of the above reaction to be useful as crosslinkable membranes, the remaining bromine needs to be displaced while retaining the azides. An effort was made to replace the remaining  $\text{-Br}$  with hydrogen by treating the azido derivatives with  $\text{Bu}_3\text{SnH/AIBN}$ . After reacting in toluene at  $75\text{ }^\circ\text{C}$  for 2 hours, IR spectra showed the disappearance of the  $\text{-N}_3$  and the  $\text{Br-CH}_2^-$  bands, indicating that the hydride not only replaced the bromide but also the azido group was lost.

Table 3.1. Summary of methods used for introducing azide into PTMSP at allylic position.

run	azide	-Br/N <sub>3</sub> ratio	phase- transfer agent		solvent	reaction time (hours)	relative* conversion
1	NaN <sub>3</sub>	1:4	18-crown-6		C <sub>6</sub> H <sub>6</sub>	65	0
2	NaN <sub>3</sub>	1:4	18-crown-6		THF	65	0.031
3	NaN <sub>3</sub>	1:4	18-crown-6		THF	120	0.040
4	LiN <sub>3</sub>	1:4		ZnCl <sub>2</sub> , Pyridine	C <sub>6</sub> H <sub>6</sub>	120	0.022
5	LiN <sub>3</sub>	1:4		ZnCl <sub>2</sub> , Pyridine	THF	65	0.030
6	NaN <sub>3</sub>	1:4		ZnCl <sub>2</sub> , Pyridine	THF	65	0.027
7	NaN <sub>3</sub>	1:4		ZnCl <sub>2</sub> , Pyridine	THF	120	0.055
8	NaN <sub>3</sub>	1:8		ZnCl <sub>2</sub> , Pyridine	THF	120	0.060

\* relative conversion: the integration of -N<sub>3</sub> absorption to the integration of CH<sub>3</sub> absorption.

### 3.4. Conclusions

Attempts to introduce epoxide crosslinking sites into PTMSP at allylic positions using substitution reactions were partially successful. Bromination of the polymer was achieved, but the introduction of pendant epoxide units via lithiation of the brominated polymer led to crosslinking. The reaction of lithiated PTMSP (prepared by reaction with lithium metal) with epichlorohydrin also did not yield the desired product. In contrast, the azido group has been introduced into PTMSP by reaction of brominated PTMSP with azide salts, although only partial conversion was achieved. Using tributyltin hydride to remove the remaining bromine in azide-containing PTMSP also reduced the azido group, which likely gave PTMSP as the product. Bromination of PTMSP and hydrogenolysis of PTMSP derivatives seems to be facile. Since both reactions involve radical pathways, it is not unreasonable to conclude that radical substitution reactions in PTMSP and its derivatives is easier than reactions that follow a  $S_{N1}$  or  $S_{N2}$  pathway. Introducing a longer functionalizable side chain through copolymerization should be a better route to crosslinkable PTMSP derivative.

### 3.5. References

1. Kunzler, J.; Percec, V. *Polym. Prepr.* **1988**, 28(1), 252.
2. Kunzler, J.; Percec, V. *New Polymer Mater.* **1990**, 1(4), 271.
3. Baker, G. L.; Klauser, C. F.; Gozdz, A. S.; Shelburne III, J. A.; Bowmer, T. N.  
in *Silicon-Based Polymer Science*, Ziegler, J. M.; Fearon, G. F. M., Eds.,  
*American Chemical Society*, Washington, DC, **1990**, p 663.
4. Bowmer, T. N.; Baker, G. L. *Polym. Preprints* **1986**, 27(2), 218.
5. Nagase, Y.; Ueda, T.; Matsui, K.; Uchikura, M. *J. Polym. Sci.: Part B: Polym. Phys.* **1991**, 29, 171.
6. Schlessinger, S. I. *Polym. Eng. and Sci.* **1974**, 14(7), 513.
7. Tanaka, H.; Morita, M. *Jpn. Kokai Tokkyo Koho JP* 61,105,544 [86,105,544]  
(Cl. G03C5/00), 23 May 1986, Appl. 84/225,989, 29 Oct **1984**: 5pp.
8. Markl, G.; Sommer, H. *Tetrahedron Lett.* **1993**, 34, 3107.
9. Mouzali, M.; Lacoste et M. J. M. Abadie *Eur. Polym. J.* **1989**, 25(5), 491.
10. Scriven, E. F. V.; Turnbull, K. *Chem. Rev.* **1988**, 88(2), 326.
11. Pfister, J. R.; Wymann, W. E. *Synthesis* **1983**, 1, 38.
12. Ravindranath, B.; Srinivas, P. *Indian J. of Chem.* **1985**, 24B, 1178.
13. Nishiyama, K.; Karigomi, H. *Chem. Lett.* **1982**, 9, 1477.
14. Cohen, H. L. *J. Polym. Sci.; Polym. Chem. Ed.* **1981**, 19, 3269.
15. Gilbert E. E. *J. Polym. Sci.; Polym. Chem. Ed.* **1984**, 22, 3603.

## Chapter 4

# Crosslinking of Poly[1-trimethylsilyl-1-propyne] Membranes by Introducing Crosslinking Sites through Copolymerization

### 4.1. Introduction

As mentioned in Chapter 3, three routes are available for functionalizing poly[1-trimethylsilyl-1-propyne]: reaction of main chain double bonds, reaction at allylic positions and copolymerization with acetylenic comonomers having pendant groups. Despite numerous attempts and the use of various reaction conditions, it has been shown that the double bonds of the polymer backbone are unreactive.<sup>1,2</sup> Functionalization of PTMSP through allylic bromination followed by introduction of crosslinking sites has been studied (Chapter 3), and there was only partial success in converting brominated polymer to PTMSP with crosslinking sites. No reaction went to completion, due to the difficulty of accessing the allylic group, a consequence of the steric hindrance created by the bulky side groups. Copolymerization with an acetylenic comonomer having a functionalizable pendant group should overcome this problem. The copolymerization of 1-trimethylsilyl-1-propyne with 1-(4-bromobutyldimethylsilyl)-1-propyne provides polymers having bromobutyl side groups which could be further functionalized.<sup>2,3</sup> Using the phase transfer catalyzed nucleophilic displacement reaction, the azide group can be introduced by replacing bromine on the copolymer.



## **4.2. Experimental**

### **4.2.1. Materials**

1,4-Dibromobutane, dimethylchlorosilane, tantalum pentachloride ( $\text{TaCl}_5$ ), and triphenylbismuth ( $(\text{C}_6\text{H}_5)_3\text{Bi}$ ) were purchased from Aldrich and were used without further purification. Monomers were degassed and dried under vacuum before use. Toluene used as solvent for polymerization was distilled from sodium to remove trace amounts of water. All other solvent and reagents were used as received.

### **4.2.2. Characterization**

Monomer and polymer structures were confirmed by 300 MHz  $^1\text{H}$ -NMR spectroscopy using a Varian Gemini-300, and IR spectroscopy using a Nicolet FT-IR 44. Molecular weights of polymers were determined by gel permeation chromatography (GPC) using a PLgel 20m Mixed A column and a Waters R401 Differential Refractometer detector at room temperature with THF as eluting solvent at a flow rate of 1 mL/min. Monodisperse polystyrene standards were used to calibrate the molecular weights. The concentration of the polymer solution was 1 mg/mL. Differential scanning calorimetry (DSC) and thermogravimetric analyses (TGA) of the polymers were performed under a nitrogen atmosphere at a heating rate 10  $^\circ\text{C}/\text{min}$  on a Perkin Elmer DSC 7 and a Perkin Elmer TGA 7 instrument, respectively. The temperature was calibrated with an indium standard. Elemental analyses were carried out by the Microanalysis Laboratory at

University of Illinois, Urbana-Champaign, using a CE440 Carbon, Hydrogen, Nitrogen Analyzer (Exter Analytical, Inc) and conventional Br analysis (titration).

#### 4.2.3. Monomer and polymer synthesis

The synthetic procedure used to prepared the copolymer is shown in Figure 4.1.

*4-bromo-1-butene.* The 4-bromo-1-butene was prepared according to the literature procedure.<sup>4</sup> Hexamethylphosphoric triamide (20 g, 0.11 mol) was slowly added to 1,4- dibromobutane (90 g, 0.42 mol) at 200 °C. The product, which was distilled into a dry ice cooled receiver, was washed with distilled water and redistilled at 98-100 °C/760 mm Hg to yield 21 g (37%) of 1,4-dibromobutane. The structure was confirmed with <sup>1</sup>H NMR (CDCl<sub>3</sub>, δ, ppm): 2.7 (q, -CH<sub>2</sub>-), 3.3 (t, -CH<sub>2</sub>Br), 5.1 (m, =CH-), 5.8 (m, CH<sub>2</sub>=).

*4-bromobutyldimethylchlorosilane.* Following the procedure of Kunzler and Percec,<sup>2</sup> hexachloroplatinic acid (0.040 g, 0.78 mmol) in a minimum of 2-propanol was dissolved in 75 mL of toluene under argon. The 2-propanol and water were removed by azeotropic distillation. To the above stirred solution was added 4-bromo-1-butene (12 g, 92 mmol) at 40 °C. Dimethylchlorosilane (8.6 g, 92 mol) was then added slowly and the solution was heated to 60 °C for 4 hours. The toluene was removed in vacuo and the product was obtained by vacuum distillation (b. p. 90-95 °C/23 mmHg. <sup>1</sup>H NMR (CDCl<sub>3</sub>, δ, ppm): 0.4 (s, -Si(CH<sub>3</sub>)<sub>2</sub>-), 0.8 (t, SiCH<sub>2</sub>-), 1.3 (m, SiCH<sub>2</sub>CH<sub>2</sub>-), 1.8 (m, -CH<sub>2</sub>CH<sub>2</sub> CH<sub>2</sub>-), 3.4 (t, -CH<sub>2</sub>Br).

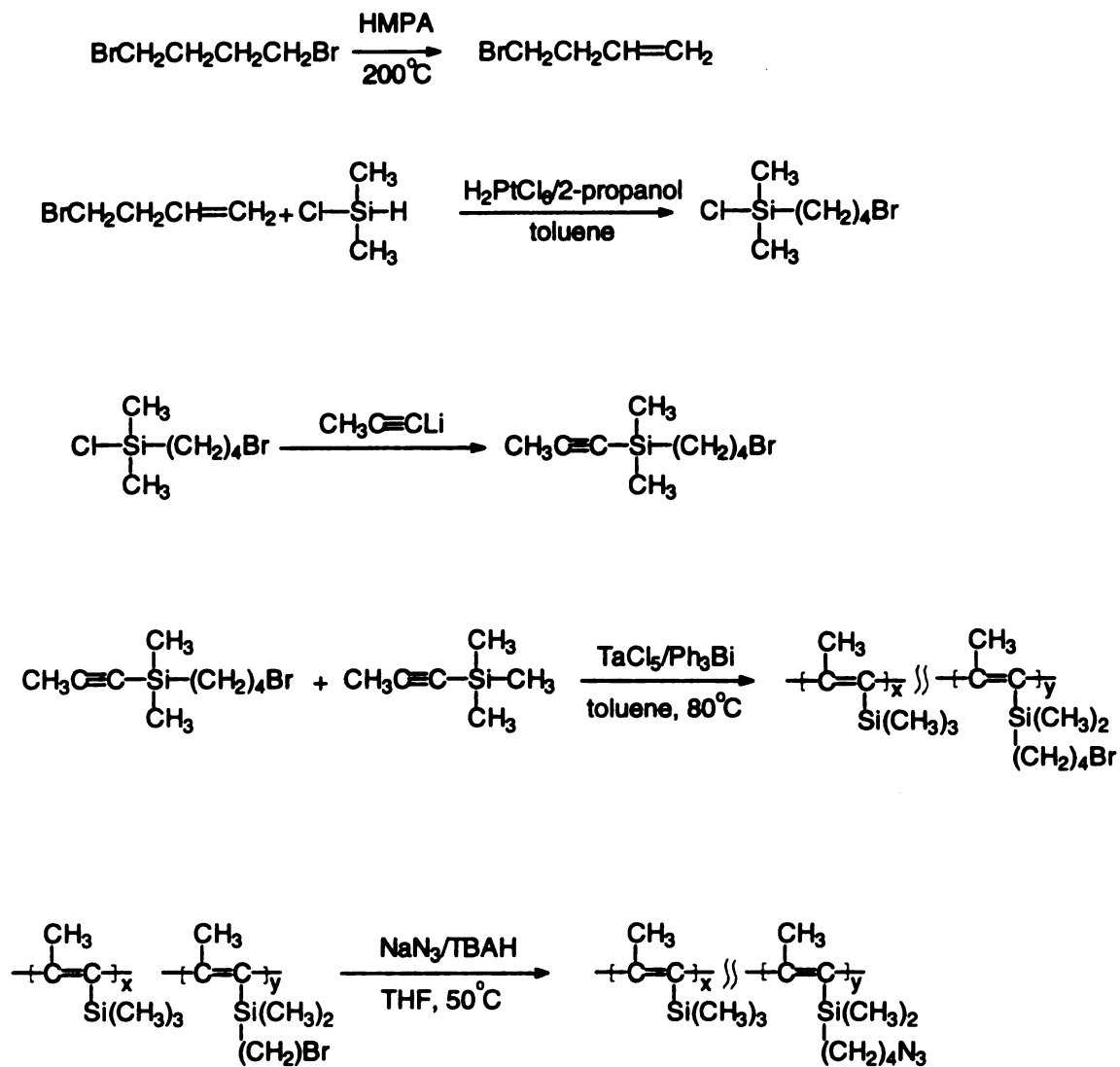


**Figure 4.1.** Synthetic procedure for preparing poly[1-trimethylsilyl-1-propyne-*co*-1-(4-azidobutyldimethylsilyl)-1-propyne] from 4-bromo-1-butene.

*1-(4-bromobutyldimethylsilyl)-1-propyne*. To a stirred solution of propynyllithium (1.34 g, 0.0292 mol) in 50 mL of dry diethylether (prepared by bubbling  $\text{CH}_3\text{C}\equiv\text{CH}$  gas through cold ether at  $-78\text{ }^\circ\text{C}$  and then adding a solution of BuLi dropwise to the cold propyne-ether solution), 4-bromobutyldimethylchlorosilane (6.7 g, 0.029 mol) was added dropwise at  $0\text{ }^\circ\text{C}$ . The reaction mixture then was stirred overnight at room temperature. The resultant solution was poured into 400 mL of ice water. The ether layer was collected and washed with distilled water, dried with  $\text{MgSO}_4$ , filtered and the diethyl ether was removed by rotoevaporation. The remaining oil was purified by vacuum distillation to yield 4.6 g (68%) of *1-(4-bromobutyldimethylsilyl)-1-propyne* (b.p.  $59\text{--}65\text{ }^\circ\text{C}/3\text{ mm Hg}$ ).  $^1\text{H}$  NMR (( $\text{CDCl}_3$ ,  $\delta$ , ppm): 0.25 (s,  $-\text{Si}(\text{CH}_3)_2-$ ), 0.5 (t,  $\text{SiCH}_2-$ ), 1.4 (m,  $\text{SiCH}_2\text{CH}_2-$ ), 1.75 (s,  $\text{CH}_3\text{C}$ ), 1.8 (m,  $-\text{CH}_2\text{CH}_2\text{CH}_2-$ ), 3.4 (t,  $-\text{CH}_2\text{Br}$ ).

*Poly[1-trimethylsilyl-1-propyne-co-1-(4-bromobutyldimethylsilyl)-1-propyne]*. A mixture of 1-trimethylsilyl-1-propyne (TMSP) and *1-(4-bromobutyldimethylsilyl)-1-propyne* were degassed on a vacuum line and dissolved in dry toluene. This monomer solution was then added to a stirred solution of tantalum pentachloride and triphenylbismuth (mole ratio  $\text{TaCl}_5$ :  $\text{Ph}_3\text{Bi}$  = 1:1) in toluene (monomers:catalyst ratio  $\approx 15$ :1). The reaction mixture was heated for 16 hours. The resulting gel-like product was dissolved by adding more toluene, centrifuged to remove most of the catalyst and precipitated by slow addition into an excess amount of methanol with rapid stirring. The polymer was purified by redissolving and reprecipitating to give an 80% yield of poly[1-trimethylsilyl-1-propyne-co-1-(4-bromobutyldimethylsilyl)-1-propyne]. GPC:  $M_n$

=809,000.  $M_w/M_n = 2.4$ .  $^1\text{H}$  NMR ( $\text{CDCl}_3$ ,  $\delta$ , ppm): 0.25 ( $-\text{Si}(\text{CH}_3)_3$  and  $-\text{Si}(\text{CH}_3)_2-$ ), 1.1-1.3 ( $-(\text{CH}_2)_3-$ ), 1.5-2.0 ( $-\text{CH}_3\text{C}$ ), 3.4 ( $-\text{CH}_2\text{Br}$ ).

*Poly[1-trimethylsilyl-1-propyne-co-1-(4-azidobutyldimethylsilyl)-1-propyne].*

To a stirred solution of 1.0 g poly[1-trimethylsilyl-1-propyne-co-1-(4-bromobutyldimethylsilyl)-1-propyne] (bromine content 20 %) in 100 mL of THF, sodium azide (0.65 g, 10 mmol) and a catalytic amount of tetrabutylammonium hydrogen sulfate (TBAH) (100 mg) were added. The reaction mixture was stirred 120 hours at 60 °C. The resulting polymer was dissolved in additional THF and centrifuged to remove most of the catalyst and other undissolved solids. The clear solution was precipitated into methanol, filtered, redissolved in THF and again precipitated from methanol. The collected polymer was vacuum dried at room temperature over night to obtain a 90% yield of poly[1-trimethylsilyl-1-propyne-co-1-(4-azidobutyldimethylsilyl)-1-propyne]. Elemental Analysis was used to determine the composition of the copolymers as shown in Table 4.1. GPC:  $M_n = 680,000$ ,  $M_w/M_n = 2.9$ .  $^1\text{H}$  NMR ( $\text{CDCl}_3$ ,  $\delta$ , ppm): 0.25 ( $-\text{Si}(\text{CH}_3)_3$  and  $-\text{Si}(\text{CH}_3)_2-$ ), 1.3-2.0 ( $-(\text{CH}_2)_3-$  and  $-\text{CH}_3\text{C}$ ), 3.25 ( $-\text{CH}_2\text{N}_3$ ).

#### 4.2.4. Membrane crosslinking

The crosslinking of the co-polymer membranes was induced by either UV irradiation or thermal treatment. Photo crosslinking of the membranes was carried out at 254 nm using an Ace-Hanovia high-pressure quartz mercury-vapor lamp for a half hour. Thermal crosslinking of the membranes was achieved by heating the membranes in vacuum at 250 °C for 2-4 hours depending on the content of azide group in the

membranes. The completion of the crosslinking was determined by monitoring the intensity of  $-N_3$  absorption at  $2100\text{ cm}^{-1}$  (Figure 4.8). After crosslinking, the membranes became insoluble in the solvents which are normally good solvents for PTMSP and the copolymer, such as THF, cyclohexane and toluene.

**Table 4.1** Elemental analysis results of poly[1-trimethylsilyl-1-propyne-*co*-1-(4-azidobutyldimethylsilyl)-1-propyne] with various contents of  $N_3$ .

theo. $N_3$ (mol%) <sup>a</sup>	20		10		5		3	
	calc.	found	calc.	found	calc.	found	calc.	found
C%	61.59	60.61	62.84	62.8	63.5	63.26	63.86	63.25
H%	10.11	7.68	10.39	10.25	10.55	10.02	10.57	9.82
N%	6.53	5.45	3.49	2.71	1.81	1.36	1.1	1.26
Si%	21.79	24.95	23.28	27.79	24.11	b	24.45	22.45
found $N_3$ (mol%) <sup>c,d</sup>	19.5		9.1		4.4		4.0	

a. calculated by assuming ideal copolymerization and 100% conversion to poly[1-trimethylsilyl-1-propyne-*co*-1-(4-azidobutyldimethylsilyl)-1-propyne].

b. not analyzed

c. calculated from elemental analysis results.

d. Br was not detected using titration method.

### 4.3. Results and discussion

#### 4.3.1. Analysis of the synthesized poly[1-trimethylsilyl-1-propyne-co-1-(4-azidobutyldimethylsilyl)-1-propyne]

Poly[1-trimethylsilyl-1-propyne-co-1-(4-azidobutyldimethylsilyl)-1-propyne] was prepared with azide contents in the range of 2-20 mol % by the reaction of poly[1-trimethylsilyl-1-propyne-co-1-(4-bromobutyldimethylsilyl)-1-propyne] with sodium azide. The reaction was sampled at different reaction times, and NMR and FTIR spectra were taken to determine the conversion. Figure 4.2 and Figure 4.3 show the  $^1\text{H}$  NMR and FTIR spectra of poly[1-trimethylsilyl-1-propyne-co-1-(4-bromobutyldimethylsilyl)-1-propyne] and the reaction mixture at different reaction time. During the reaction, the NMR peak at 3.4 ppm which is assigned to  $-\text{CH}_2\text{Br}$  in poly[1-trimethylsilyl-1-propyne-co-1-(4-bromobutyldimethylsilyl)-1-propyne] decreased while the peak at 3.25 ppm assigned to  $-\text{CH}_2\text{N}_3$  in poly[1-trimethylsilyl-1-propyne-co-1-(4-azidobutyldimethylsilyl)-1-propyne] increased. In IR spectra, a new band appeared at  $2100\text{ cm}^{-1}$  due to the  $-\text{N}_3$  group in poly[1-trimethylsilyl-1-propyne-co-1-(4-azidobutyldimethylsilyl)-1-propyne] and the band near  $1219\text{ cm}^{-1}$  ( $\text{CH}_2$  wagging from the  $\text{CH}_2\text{Br}$  group) decreased. That the peak at 3.4 ppm in NMR spectra and the absorption band at  $1219\text{ cm}^{-1}$  decreased to baseline demonstrates that complete displacement of the bromide was achieved. Elemental analysis of these copolymers (Table 4.1) showed an undetectable amount of Br.

The UV-visible spectra of poly[1-trimethylsilyl-1-propyne-*co*-1-(4-azidobutyldimethylsilyl)-1-propyne] copolymers (Figure 4.4) exhibit a peak in the UV region with an absorption maximum around 230 nm, slightly shifted to longer wavelength compared with PTMSP. Like PTMSP, the azide copolymers are white solids.

Differential scanning calorimetry (DSC) spectra of both poly[1-trimethylsilyl-1-propyne-*co*-1-(4-bromobutyldimethylsilyl)-1-propyne] and poly[1-trimethylsilyl-1-propyne-*co*-1-(4-azidobutyldimethylsilyl)-1-propyne] (Figure 4.5) showed no thermal transitions below the decomposition temperature, indicating that neither poly[1-trimethylsilyl-1-propyne-*co*-1-(4-bromobutyldimethylsilyl)-1-propyne] nor poly[1-trimethylsilyl-1-propyne-*co*-1-(4-azidobutyldimethylsilyl)-1-propyne] has a glass transition temperature in this region. The exothermic peaks at 380 °C are due to the decomposition of the copolymers. This is consistent with the thermal gravimetric analyses of the copolymers shown in Figure 4.6. The exothermic peak in DSC at 270 °C of poly[1-trimethylsilyl-1-propyne-*co*-1-(4-azidobutyldimethylsilyl)-1-propyne] is attributed to the thermal decomposition of N<sub>3</sub> and release of nitrogen gas in the azide copolymer.



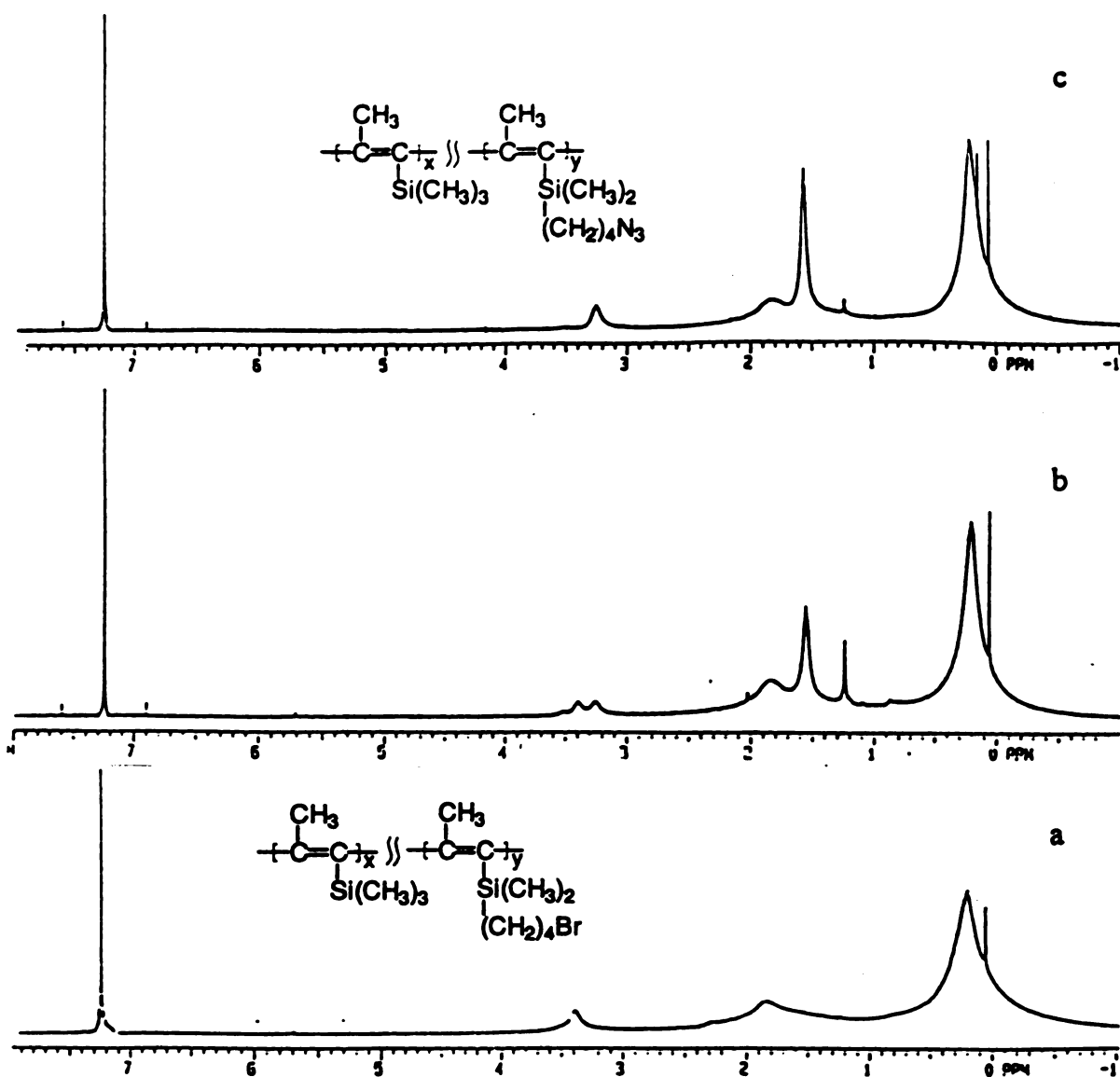


**Figure 4.2.**  $^1\text{H}$  NMR spectra of reaction mixtures during the reaction of poly[1-trimethylsilyl-1-propyne-co-1-(4-bromobutyldimethylsilyl)-1-propyne] (10 mol% Br) to poly[1-trimethylsilyl-1-propyne-co-1-(4-azidobutyldimethylsilyl)-1-propyne] (10 mol%  $\text{N}_3$ ). **a.** poly[1-trimethylsilyl-1-propyne-co-1-(4-bromobutyldimethylsilyl)-1-propyne]; **b.** after 80 hours at 60 °C; **c.** after 120 hours reaction at 60 °C, poly[1-trimethylsilyl-1-propyne-co-1-(4-azidobutyldimethylsilyl)-1-propyne] (10 mol%  $\text{N}_3$ ).

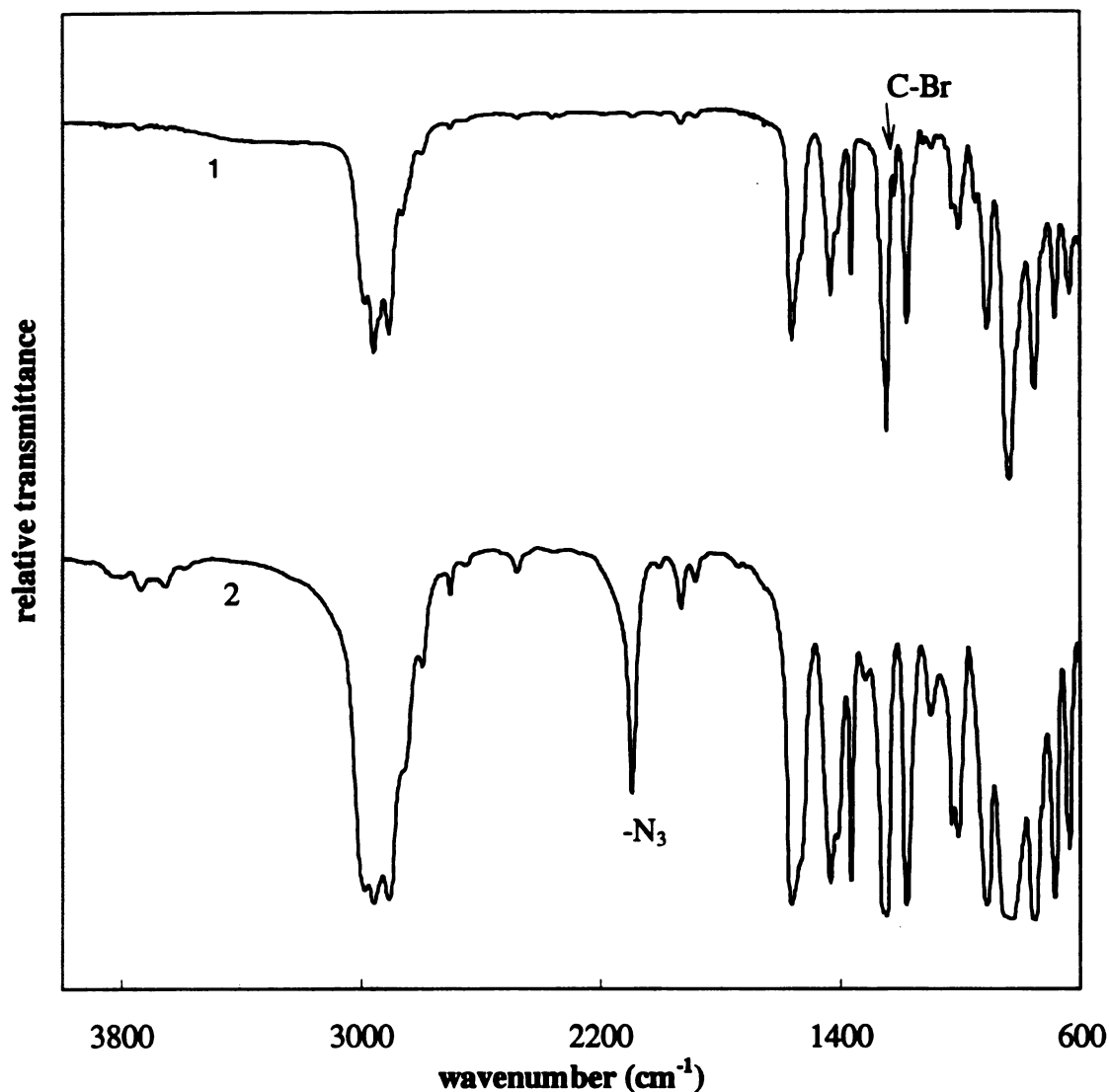


**Figure 4.3.** FTIR spectra of poly[1-trimethylsilyl-1-propyne-co-1-(4-bromobutyldimethylsilyl)-1-propyne] (10 mol % Br) and poly[1-trimethylsilyl-1-propyne-co-1-(4-azidobutyldimethylsilyl)-1-propyne] (10 mol% N<sub>3</sub>). 1. poly[1-trimethylsilyl-1-propyne-co-1-(4-bromobutyldimethylsilyl)-1-propyne]; 2. after 120 hours at 60 °C, poly[1-trimethylsilyl-1-propyne-co-1-(4-azidobutyldimethylsilyl)-1-propyne] (10 mol% N<sub>3</sub>).

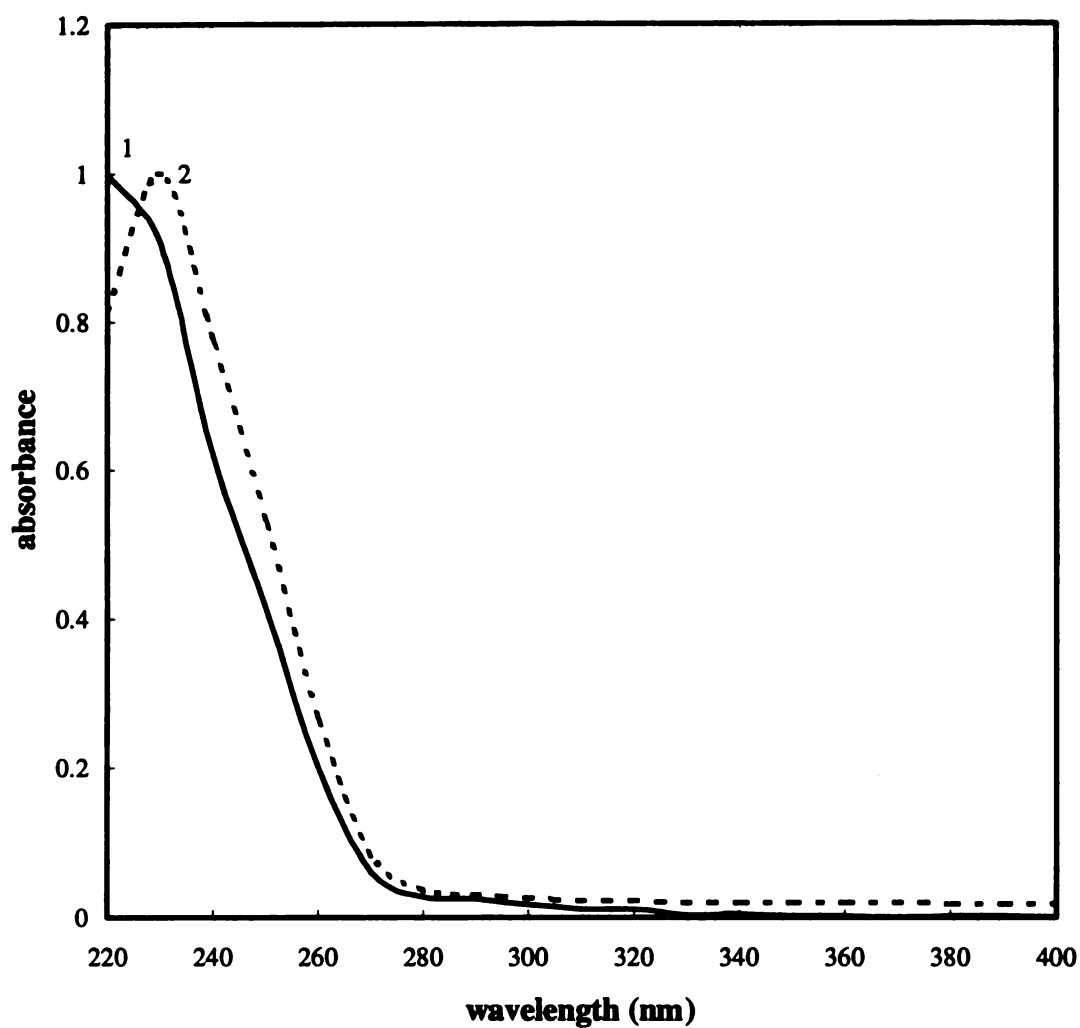


**Figure 4.4.** UV-visible spectra of: **1**, poly[1-trimethylsilyl-1-propyne]; **2**, poly[1-trimethylsilyl-1-propyne-*co*-1-(4-bromobutyldimethylsilyl)-1-propyne] (10 mol% N<sub>3</sub>) (in cyclohexane).

In DSC curves, the peak areas can be quantitatively related to enthalpic changes. In particular, the area of the peak at 270 °C is related to the heat released during the thermal degradation of  $-N_3$  in the copolymer. In other words, the area of the peak is proportional to the amount of  $-N_3$  present in the copolymer. Figure 4.7 shows the enthalpy change of the copolymers containing different amount of  $-N_3$  vs. the theoretical content of  $-N_3$  in the copolymers. The nearly linear plot demonstrates that azide copolymers have  $-N_3$  contents close to their theoretical values, and that the copolymerization must have been ideal. In addition, one can determine the absolute  $N_3$  content of a poly[1-trimethylsilyl-1-propyne-*co*-1-(4-azidobutyldimethylsilyl)-1-propyne] by combining DSC and elemental analysis results. Plotting the  $N_3$  content (obtained from elemental analysis) of a series of azide copolymers vs. the measured enthalpy changes will yield the value for the enthalpy change per azide, which can be used to determine the amount of azide groups in poly[1-trimethylsilyl-1-propyne-*co*-1-(4-azidobutyldimethylsilyl)-1-propyne] with unknown compositions.

TGA curves and IR spectra of poly[1-trimethylsilyl-1-propyne-*co*-1-(4-azidobutyldimethylsilyl)-1-propyne] also provide information that can be used for the quantitative determination of  $N_3$  contents in the copolymers. A comparison of TGA and DSC of the copolymers shows that the weight loss starting at 270 °C is due to the release of nitrogen which can be used to calculate the amount of  $N_3$  in the copolymers. In IR spectra, the  $N_3$  content can be determined by integration of the  $N_3$  absorption band. The quantitation also requires a calibration curve which can be obtained from elemental analysis.

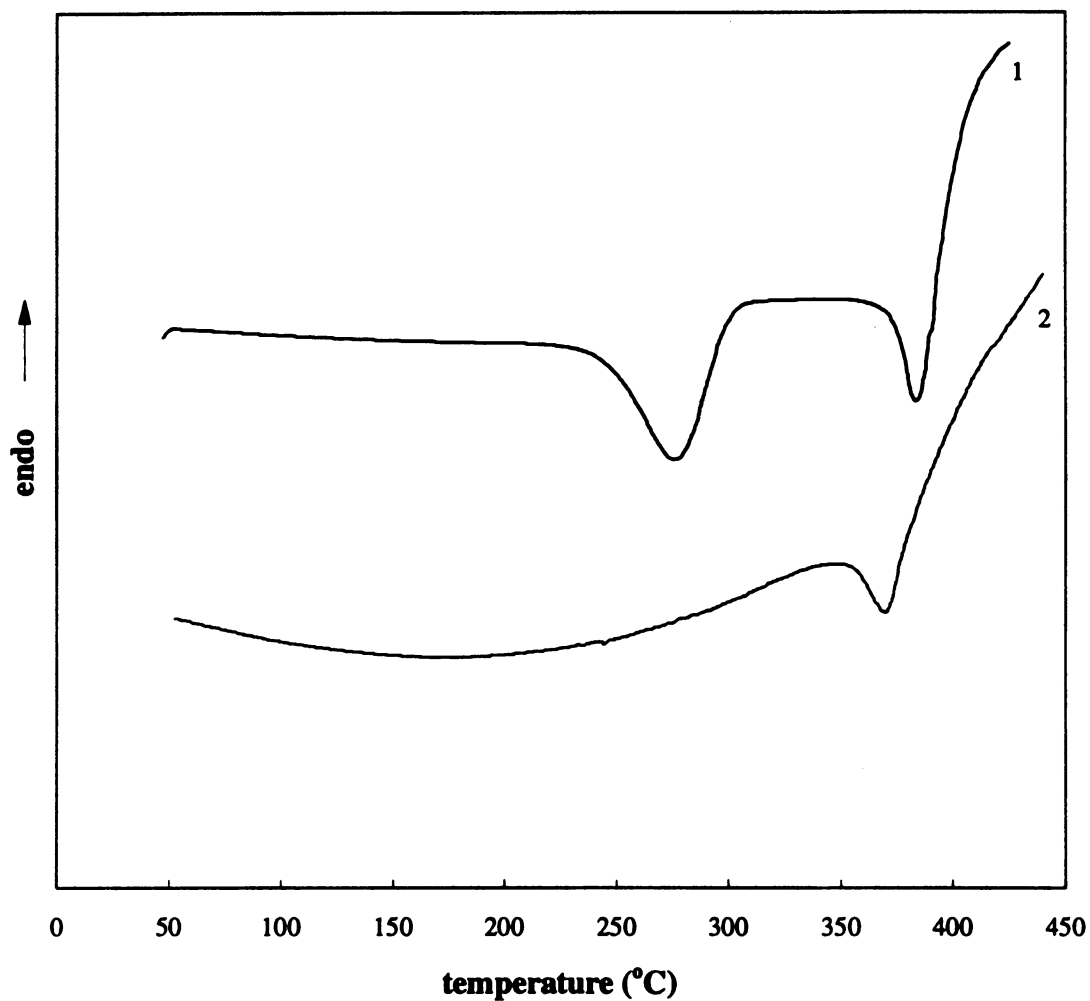


**Figure 4.5.** DSC curves: 1, poly[1-trimethylsilyl-1-propyne-*co*-1-(4-azidobutyldimethylsilyl)-1-propyne]; 2, poly[1-trimethylsilyl-1-propyne-*co*-1-(4-bromobutyldimethylsilyl)-1-propyne] ( in nitrogen, heating rate: 20 °C/min).

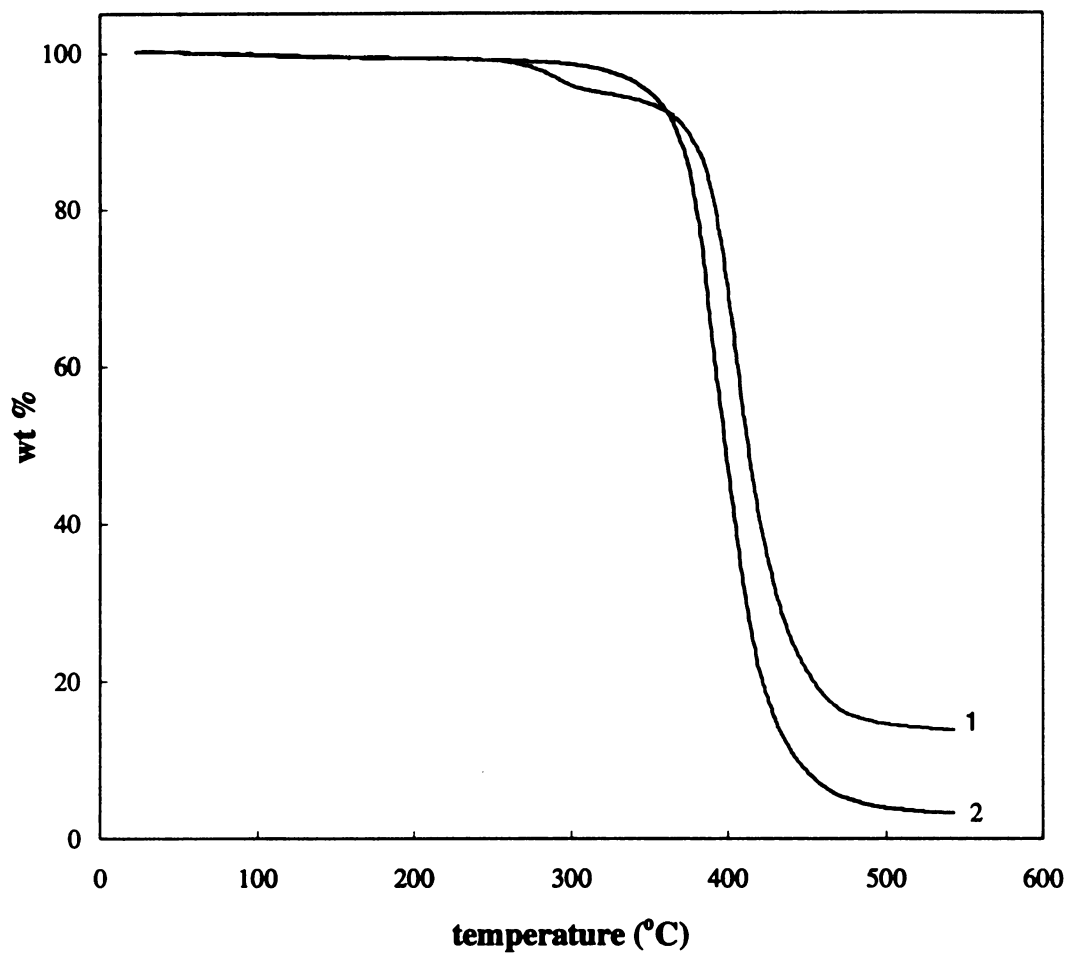


**Figure 4.6.** TGA curves: 1, poly[1-trimethylsilyl-1-propyne-*co*-1-(4-azidobutyldimethylsilyl)-1-propyne]; 2, poly[1-trimethylsilyl-1-propyne-*co*-1-(4-bromobutyldimethylsilyl)-1-propyne] ( in nitrogen, heating rate: 10° C/min).

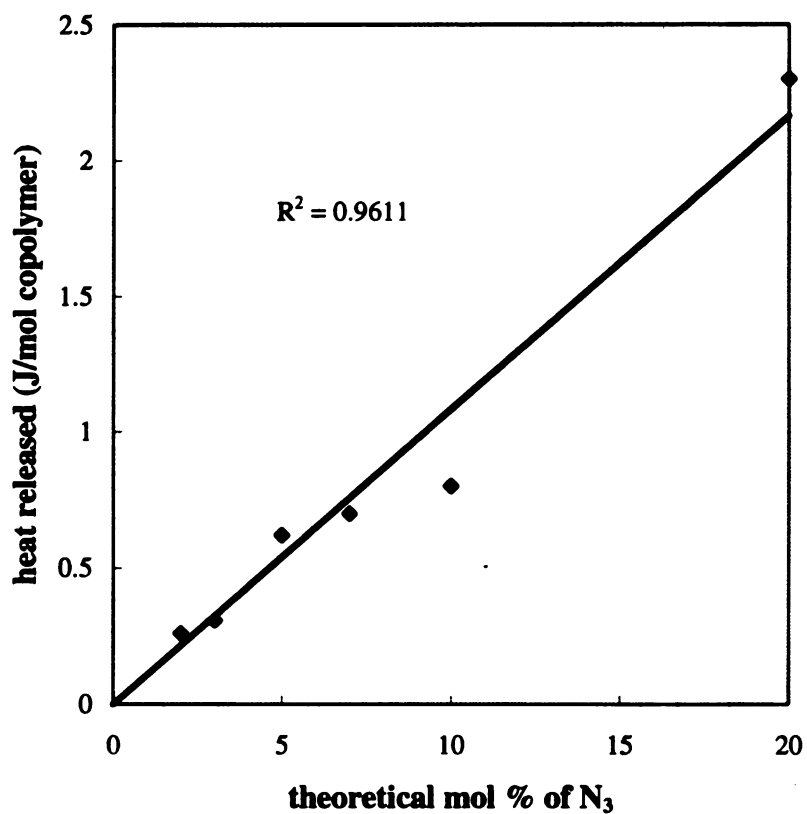


**Figure 4.7.** The plot of the measured enthalpy change of various poly[1-trimethylsilyl-1-propyne-*co*-1-(4-azidobutyldimethylsilyl)-1-propyne] copolymers vs. the theoretical  $N_3$  content in the copolymers.

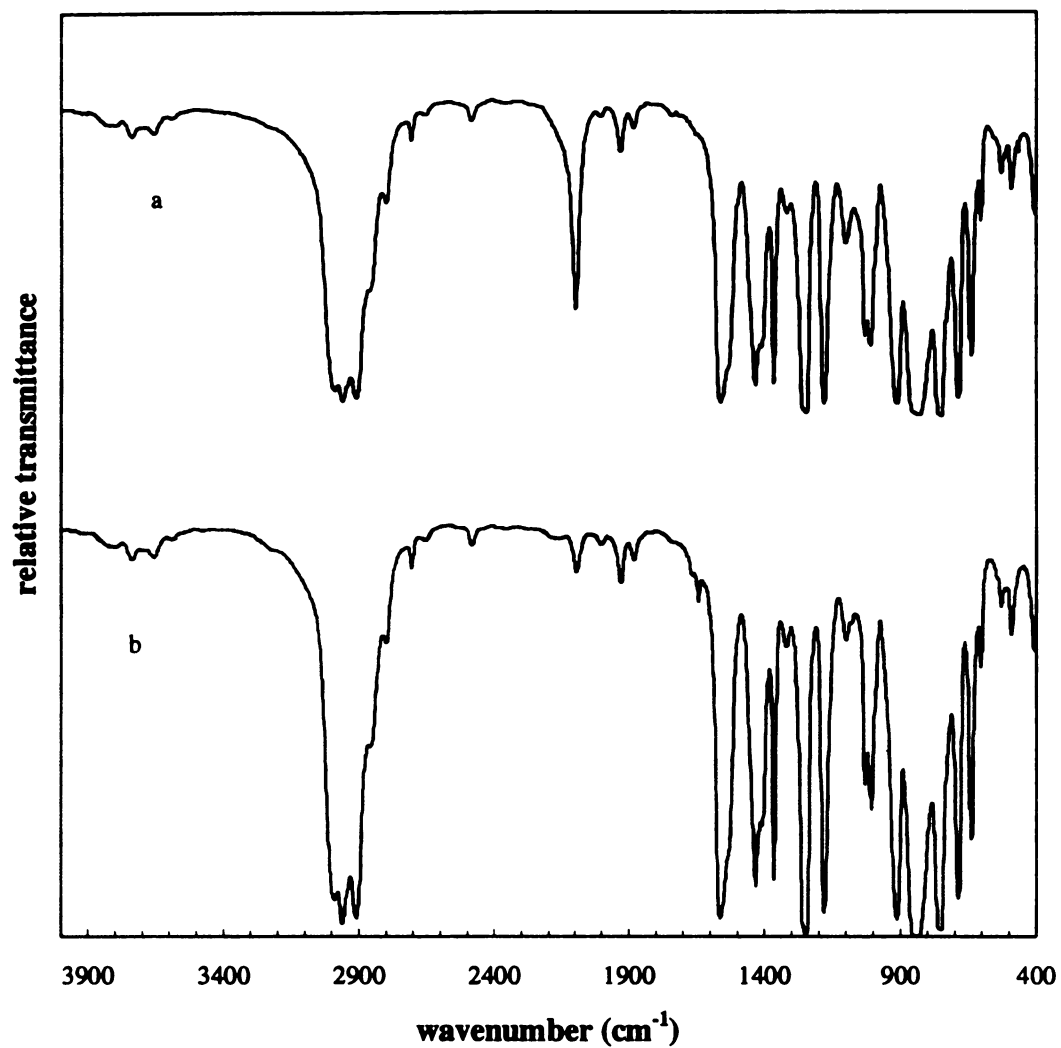


**Figure 4.8.** FTIR spectra of poly[1-trimethylsilyl-1-propyne-*co*-1-(4-azidobutyldimethylsilyl)-1-propyne](10 mol% N<sub>3</sub>): a, before crosslinking; b, after crosslinking.



#### 4.3.2. Properties of thermally and photo-crosslinked PTMSP copolymer membranes

The permeability of thermo- and photo-crosslinked azide copolymer membranes are given in Table 4.2 and Table 4.3, respectively. The permeability of untreated azide copolymer membranes showed lower permeability than PTMSP membranes. The filling of the free volume in PTMSP by the longer azidobutyldimethylsilyl side chain in the copolymers results in the lower gas permeability. Thermal crosslinking caused slight enhancement in the selectivity and a reduction in the permeability of poly[1-trimethylsilyl-1-propyne-*co*-1-(4-azidobutyldimethylsilyl)-1-propyne] membranes. For copolymer membranes containing the same amount of azide groups, photo crosslinking resulted in larger O<sub>2</sub>/N<sub>2</sub> separation factors and decreases in permeability. As discussed in Chapter 2, the different behavior of thermal and photo crosslinked films may be due to more free volume in the thermally crosslinked membranes (possibly due to the thermal expansion of the membranes during the crosslinking process) or a lower degree of crosslinking.

For comparison, a PTMSP membrane was also irradiated under the same conditions used for crosslinking the azide copolymers (254 nm). As discussed in Chapter 2, PTMSP membranes irradiated at 254 nm show enhanced selectivity, but remained soluble. In contrast, UV irradiation of poly[1-trimethylsilyl-1-propyne-*co*-1-(4-azidobutyldimethylsilyl)-1-propyne] membranes gave insoluble membranes with better mechanical properties.

Ideally, a greater content of azides group in the copolymer should produce a higher degree of crosslinking after photo treatment. However, higher crosslinking did not lead to higher separation factors as shown in Figure 4.3. This observation shows that

there is a limit to modification by cross-linking beyond which the selectivity is not affected while the permeability continues to decrease. This is believed to be due to excessive filling of free volume by the long azidobutyldimethylsilyl side chain.

It is worth comparing the crosslinking of copolymer membranes and that of bis(aryl azide) containing membranes. The UV-vis spectra of PTMSP membranes containing bis(aryl azides) have two absorption maxima with one from PTMSP (220 nm) and a second from the bis(aryl azide) (300 nm for 4,4'-diazidobenzophenone--azide-BAA, 250 nm for azide-HFBAA). The UV absorption maximum of poly[1-trimethylsilyl-1-propyne-*co*-1-(4-azidobutyldimethylsilyl)-1-propyne] is at 230 nm which is only slightly shifted from that of PTMSP. Irradiation at 300 nm led to crosslinking of PTMSP/BAA films but had little effect on the PTMSP main chain, while irradiation of PTMSP or poly[1-trimethylsilyl-1-propyne-*co*-1-(4-azidobutyldimethylsilyl)-1-propyne] at 254 nm may alter the structure of PTMSP during crosslinking. Higher temperatures (260 °C) are required to initiate the thermal reaction of the azide groups in poly[1-trimethylsilyl-1-propyne-*co*-1-(4-azidobutyldimethylsilyl)-1-propyne] compared to bis(aryl azide) containing PTMSP (175 °C), since the decomposition temperature of alkyl azides is higher than that of aryl azides.<sup>5</sup>

**Table 4.2.** Permeability coefficients of oxygen,  $P(O_2)$ , nitrogen,  $P(N_2)$ , and the oxygen/nitrogen separation factor,  $\alpha$ , at  $23 \pm 1$  °C, for thermally crosslinked poly[1-trimethylsilyl-1-propyne-*co*-1-(4-azidobutyldimethylsilyl)-1-propyne] copolymer membranes.

mol % N <sub>2</sub> in membrane	before crosslinking		after crosslinking	
	$P(O_2)$	$\alpha(O_2/N_2)$	$P(O_2)$	$\alpha(O_2/N_2)$
PTMSP	7.05	1.7	6.03 <sup>a</sup>	1.6
2	5.44	1.7	3.53	1.7
3	5.19	1.7	2.99	1.9
5	3.51	1.7	2.14	2.1
7	3.33	1.5	2.05	2.1
10	3.7	1.6	2.15	2.1

$P(O_2)$  and  $P(N_2)$  are in units of  $10^{-7} \text{ cm}^3(\text{STP}) \cdot \text{cm}/\text{cm}^2 \cdot \text{s} \cdot \text{cm Hg}$

a. control experiment, membrane is still soluble.

**Table 4.3.** Permeability coefficients of oxygen,  $P(O_2)$ , nitrogen,  $P(N_2)$ , and the oxygen/nitrogen separation factor,  $\alpha$ , at  $23 \pm 1$  °C, of photo-crosslinked poly[1-trimethylsilyl-1-propyne-*co*-1-(4-azidobutyldimethylsilyl)-1-propyne] copolymer membranes.

mol % $N_3$ in membrane	before crosslinking		after crosslinking	
	$P(O_2)$	$\alpha(O_2/N_2)$	$P(O_2)$	$\alpha(O_2/N_2)$
PTMSP	7.91	1.4	0.70 <sup>a</sup>	3.2
2	5.62	1.8	0.46	3.8
5	4.18	1.5	0.374	3.7
7	3.37	1.5	0.296	3.9

$P(O_2)$  and  $P(N_2)$  are in units of  $10^{-7} \text{ cm}^3(\text{STP}) \cdot \text{cm}/\text{cm}^2 \cdot \text{s} \cdot \text{cm Hg}$

a. control experiment, membrane is still soluble.

Table 4.4 lists the pycnometric densities of the copolymer membranes measured by the sink-float technique (ASTM D3800-B)<sup>6</sup> with water-methanol mixtures. The density data reveal that photo crosslinking resulted in the decrease of free volume but thermal crosslinking caused much smaller changes. These free volume changes are associated with the changes in the permeability properties of corresponding membranes.

The temporal stability of crosslinked copolymer membranes stored under vacuum at 10 mtorr are shown in table 4.5. The permeabilities of crosslinked membranes declined less than PTMSP when stored under vacuum. If we assume that the interchain diffusion causes densification and a decrease in the free volume and permeability, this suggests that crosslinking of PTMSP inhibits the interchain diffusion and stabilizes the gas permeability.

**Table 4.4.** The pycnometric densities of poly[1-trimethylsilyl-1-propyne-*co*-1-(4-azidobutyldimethylsilyl)-1-propyne] copolymer membranes under various treatment.

<b>mol % N<sub>3</sub></b>	<b>crosslinking method</b>	<b>Density (g/cm<sup>3</sup>)</b>
2 %	as cast	0.9270
	thermal	0.9285
	photo	0.9340
3%	as cast	0.9313
	thermal	0.9310
	photo	0.9382
5%	as cast	0.9315
	thermal	0.9335
	photo	0.9382
7%	as cast	0.9325
	thermal	0.9330
	photo	0.9405

**Table 4.5.** Temporal stability of the crosslinked copolymer membranes stored under vacuum.

Membranes	Days in vacuum	P(O <sub>2</sub> )	Normalized P(O <sub>2</sub> )
PTMSP**	0	8	1
	20	3	0.38
PTMSP*	0	6.95	1
	18	4.94	0.71
2-N <sub>3</sub> -thermal	0	4.55	1
	21	5.07	1.1
2-N <sub>3</sub> -photo	0	3.53	1
	20	3.69	1.04
3-N <sub>3</sub> -thermal	0	3.00	1
	31	3.17	1.05
5-N <sub>3</sub> -photo	0	0.47	1
	20	0.46	0.98
7-N <sub>3</sub> -thermal	0	2.05	1
	22	1.99	0.93
10-N <sub>3</sub> -thermal	0	2.10	1
	18	2.14	1.02

P(O<sub>2</sub>) and P(N<sub>2</sub>) are in units of 10<sup>-7</sup> cm<sup>3</sup>(STP)•cm/cm<sup>2</sup>•s•cmHg

\*\*Data from Nagai, K.; Higuchi, A.; Nakagawa, T. *J. Polym. Sci. Part B: Polym. Phys.*, **1995**, 33, 289.

\*Data from this work.

#### 4.4. Conclusions

Copolymers of 1-(4-azidobutyldimethylsilyl)-1-propyne with 1-trimethylsilyl-1-propyne were prepared by functionalizing the bromobutyl side chain of poly[1-trimethylsilyl-1-propyne-*co*-1-(4-bromobutyldimethylsilyl)-1-propyne] copolymers. The amount of N<sub>3</sub> in the copolymer can be determined quantitatively by elemental analysis, thermal gravimetric analysis, or by combining elemental analysis with differential scanning calorimetry or IR spectroscopy. Membranes of poly[1-trimethylsilyl-1-propyne-*co*-1-(4-azidobutyldimethylsilyl)-1-propyne] with various azide contents were crosslinked by photo and thermal treatment. Thermally crosslinked copolymer membranes showed slight improvements in selectivity with small decreases in permeability while photo-crosslinked copolymer membranes led to greater selectivity but with reduced permeabilities. Compared to crosslinking by the physical addition of bis(aryl azides) into PTMSP membranes, copolymerization allowed incorporation of higher levels of crosslinking sites. Our data shows signs of limiting behavior. For example, thermal- crosslinked films with  $\geq 5\%$  of azide have the same permeability and selectivity. In contrast, photochemically crosslinked films continue to show decreases in permeability as the azide content is increased. This behavior is likely related to the UV-induced permeability changes seen in pure PTMSP films. The permeabilities of crosslinked copolymer membranes stored in vacuum were stable, while the permeability of PTMSP membranes when stored under the same conditions dropped to 70% of their original value. We believe the crosslinking limits



physical aging by inhibiting the interchain diffusion which was believed accelerated by the small molecules such as pump oil.<sup>7,8</sup>

#### 4.5. References

1. Kunzler, J.; Percec, V. *Polym. Prepr.* **1988**, 28(1), 252.
2. Kunzler, J.; Percec, V. *New Polymer Mater.* **1990**, 1(4), 271.
3. Kunzler, J.; Percec, V. Eur. Pat. Appl. EP 303,480 (Cl. C08/00), 15, Feb. 1989.
4. Kraus, G.; Landgrebe, K. *Synthesis* **1984**, 10, 885.
5. Abramovitch, R. A.; Kyba, A. P. "Decomposition of Organic Azides" in *The Chemistry of the Azido Group*, ed. Patai, S., Interscience Publishers, **1971**.
6. ASTM, D3800-79 (reapproved 1990), *American Society for Testing and Materials*.
7. Nagai, K.; Higuchi, A.; Nakagawa, T. *J. Polym. Sci. Part B: Polym. Phys.* **1995**, 33, 289.
8. Langsam, M.; Robeson, L. M. *Polym. Eng. and Sci.* **1989**, 29, 44.

## Chapter 5

### Study of Ethanol / Water Pervaporation Through Modified PTMSP Membranes

#### 5.1. Introduction

Fermentation alcohol represents one of the more important resources of renewable energy. Therefore, the recovery of alcohol from aqueous mixtures has received much attention recently.<sup>1-4</sup> Fermentation is normally carried out as a batch process, but because the produced alcohol acts as an inhibitor for the microorganisms producing it, both the final alcohol concentration and the alcohol productivity are low.<sup>5</sup> Microorganisms usually experience strong inhibition at approximately 5 to 8 wt% of ethanol.<sup>3</sup> In order to achieve a high ethanol productivity, an ethanol selective membrane can be coupled to the fermentor. The fermentation broth is continuously pumped through a membrane filtration unit, the rejected microorganisms are recycled to the fermentor while the inhibitory end-products permeate through the membrane.

Pervaporation is a useful technique for removing water from alcohol-rich mixtures.<sup>6-9</sup> The separation of alcohol from dilute mixtures, however, is more difficult since it requires alcohol-selective membranes. Several other types of alcohol-selective membrane materials are mentioned in the literature, for instance nitrile-butadiene rubber, styrene-butadiene rubber,<sup>10</sup> and poly(*tert*-butyl methacrylate-*co*-styrene).<sup>11</sup> Most of the

investigations use silicone rubber (polydimethylsiloxane, PDMS) membranes,<sup>1,12</sup> but its selectivity is low and it is not a practical membrane because defect-free ultrathin membranes cannot be prepared from this material.

Poly(1-trimethylsilyl-1-propyne) (PTMSP) membranes selectively permeate ethanol in pervaporation of aqueous ethanol solutions.<sup>13,14</sup> PTMSP forms good membranes, and because of its extremely high molecular weight, very thin membranes can be prepared.<sup>15</sup> However, PTMSP membranes also suffer from relatively low selectivity for the separation of ethanol/water mixtures. PTMSP membranes have been modified by several methods in order to attain higher permselectivity for alcohol. It has been reported that the preparation of PTMSP/PDMS graft copolymer,<sup>15</sup> the introduction of fluoroalkyl groups into PTMSP,<sup>16</sup> and alkylsilylation of PTMSP<sup>17</sup> all improve the separation factor without loss in permeability at certain compositions. It was concluded that the higher selectivity toward ethanol is probably due to the increased hydrophobicity of modified PTMSP membranes.

Because of the higher diffusivity of water (smaller size) compared to ethanol, it is important to enhance the solubility of ethanol over water during the design of a polymer membrane. The solubility parameter,  $\delta$ , is the square root of the cohesive energy density and is widely used to predict the solubility of polymers in various solvents.<sup>18,19</sup> When the  $\delta$  values for a polymer and solvent are similar, the polymer usually is soluble in the solvent. For PTMSP, the calculated value of  $\delta$  is  $17.6 \text{ (J/cm}^3\text{)}^{1/2}$ ,<sup>12</sup> and the values for ethanol and water are 26.0 and 47.8, respectively.<sup>19</sup> It will be difficult to predict whether increasing or decreasing the solubility parameter of PTMSP can lead to a better separation, since the solubility parameters of both ethanol and water are much higher than that of PTMSP. In

order to use solubility parameters as a guide in the synthesis and modification of ethanol-selective membranes, we attempted to establish a quantitative relationship between ethanol/water permeation rate/selectivity and the solubility parameter,  $\delta$ .

### 5.1.1. Calculation of solubility parameters for polymers by inverse gas chromatography (IGC)

The solubility parameter,  $\delta$  (unit of  $(\text{cal}/\text{cm}^3)^{1/2}$  or  $(\text{J}/\text{cm}^3)^{1/2}$ ), is derived from the cohesive energy density.  $\delta^2$  is a measure of intermolecular forces and may be defined<sup>20</sup> as

$$\delta^2 = \frac{\Delta E}{V^\circ} \quad (5.1)$$

where  $\Delta E$  is the energy of vaporization and  $V^\circ$  is the molar volume of the liquids. It is apparent that it is necessary to determine both the vaporization energy and the molar volume of a liquid in order to evaluate its solubility parameter. There is rarely much difficulty in finding a reliable value for the molar volume and vaporization energy, but frequently there are problems in obtaining the vaporization energy of solids, such as polymers. Alternative methods must be used in order to determine solubility parameters for polymers. Dipaola-Baranyi and Guillet<sup>21</sup> have developed a chromatographic method for the calculation of the solubility parameter of polymeric stationary phases,  $\delta_2$ , from measurement of Flory-Huggins polymer-solvent interaction parameters,  $\chi$ .

The Flory-Huggins interaction parameter,  $\chi$ , has been widely used to characterize a variety of polymer-solvent and polymer-polymer interactions. Defined empirically as

shown in Equation 5.2<sup>22</sup>,  $\chi$ , is a general dimensionless interaction parameter reflecting the intermolecular forces between the molecules in a particular polymer-liquid system

$$\chi = (\mu_1 - \mu_1^0)/(RT\phi_2^2) - [\ln \phi_1 + (1 - V_1/V_2) \phi_2]/\phi^2 \quad (5.2)$$

where  $\mu$  is the chemical potential;  $V$  is molar volume; 0 refers to pure liquid state; 1 and 2 refer to the liquid and polymer, respectively;  $\phi$  is volume fraction; and  $R$  and  $T$  are gas constant and temperature, respectively.

The interpretation of the Flory-Huggins interaction parameter,  $\chi$ , as a residual free energy function<sup>23</sup> rather than the original enthalpy parameter allows separation into enthalpic and entropic contributions

$$\chi = \chi_H + \chi_S \quad (5.3)$$

The solubility parameters of solvent,  $\delta_1$ , and polymer,  $\delta_2$ , are introduced in the form of Regular Solution theory<sup>20</sup> to account for enthalpy effects:

$$\chi^\infty = (V_1/RT)(\delta_1 - \delta_2)^2 + \chi_s^\infty \quad (5.4)$$

where the superscript  $\infty$  indicates that IGC data are measured at infinite dilution of solvent in the polymer and  $V_1$  is the molar volume of the solvent. Expansion of the term in parentheses and rearrangement yields

$$(\delta_1^2/RT) - \chi/V_1 = (2\delta_2/RT)\delta_1 - (\delta_2^2/RT + \chi_s/V_1) \quad (5.5)$$

A plot of the function of the left hand side of Equation 5.4 versus  $\delta_1$  should give a linear graph and the value of  $\delta_2$  can be calculated from the slope.

To obtain the solubility parameter of a polymer, the interaction parameter  $\chi$  has to be calculated from chromatography measurements:

$$\chi = \ln(273.16Rv_2/p_1^0V_g V_1) - 1 - p_1^0(B_{11} - V_1)/RT \quad (5.6)$$

where  $V_g$  is specific retention volume,  $v_2$  is the specific volume of the polymer,  $p_1^0$  is the probe vapor pressure,  $V_1$  is the molar volume of the probe and  $B_{11}$  is the second virial coefficient of the probe.

Specific retention volumes,  $V_g$ , were computed from the relation<sup>24</sup>

$$V_g = \frac{273.2}{T} \cdot \frac{(t_p - t_0)}{W} \cdot F \cdot J \cdot C \quad (5.7)$$

where

$$C = 1 - \frac{(P_{H_2O})}{P_0} \quad (5.8)$$

and

$$J = 1.5 [ (P_i/P_0)^2 - 1 ] / [ (P_i/P_0)^3 - 1 ] \quad (5.9)$$

In these equations,  $T$  is the temperature of the flowmeter, which measures the carrier gas flow rate  $F$ ;  $W$  is the weight of polymer on the column;  $t_p$  is the retention time of the probe molecule;  $t_0$  is the retention time of a noninteracting marker such as air;  $J$  is the correction for the pressure drop across the column;  $C$  is the correction for the vapor pressure of water in the soap bubble flowmeter;  $P_0$  is the pressure of the carrier gas at the outlet of the column;  $P_i$  is the pressure at the inlet; and  $P_{H_2O}$  is the vapor pressure of water at the temperature of the flowmeter.

Probe vapor pressures ( $p_i^0$ ) are found in the CRC Handbook or obtained from the Antoine equation

$$\log p_i^0 = A - B/(t + C) \quad (5.10)$$

where  $t$  is the temperature in  $^{\circ}C$ , and  $A$ ,  $B$  and  $C$  are constants from standard sources.<sup>25</sup>

Second virial coefficients ( $B_{11}$ ) are computed from<sup>26</sup>

$$B_{11}/V_c = 0.0430 - 0.886 T_c/T - 0.694 (T_c/T)^2 - 0.0375(n-1)(T_c/T)^{4.5} \quad (5.11)$$

where  $V_c$  and  $T_c$  are the critical volume and temperature of the probe,  $T$  is the temperature (K), and  $n$  is the number of carbon atoms of the  $n$ -alkane. For the other hydrocarbons, an effective number of carbon atoms,  $n_a$ , is estimated and replaces  $n$  in eq. 5.11.<sup>27</sup>

### **5.1.2. Calculation of solubility parameters for crosslinked polymer by swelling measurement**

The solubility parameter of a crosslinked polymer may be determined by swelling experiments.<sup>28</sup> The best solvent is defined for the purposes of the experiment as the one with the closest solubility parameter to the polymer. This solvent also swells the polymer most. Several solvents with a range of solubility parameters are selected, and the crosslinked polymer is swelled to equilibrium in each of them. The swelling coefficient,  $Q$ , is plotted against the solubility parameter of the solvents with the maximum defining the solubility parameter of the polymer.

The swelling coefficient,  $Q$ , is defined by

$$Q = \frac{m - m_0}{m_0} \times \frac{1}{\rho_s} \quad (5.12)$$

where  $m$  is the weight of the swollen sample,  $m_0$  is the dry weight, and  $\rho_s$  is the density of the swelling agent.

### **5.1.3. Calculation of solubility parameters by the group contribution method**

Solubility parameters may be calculated from a knowledge of the chemical structure of the polymer.<sup>29</sup> Use is made of the group molar attraction constant,  $G$ , for each group,



$$\delta = \frac{\rho \Sigma G}{M} \quad (5.13)$$

where  $\rho$  represents the density and  $M$  is the mer molecular weight. Group molar attraction constants  $G$ , the contribution of each group to the vaporization energy, have been calculated by Small<sup>30</sup> and Hoy from measurement of heat of evaporation.<sup>31</sup> A wide range of values of  $G$  for chemical groups is listed in **Appendix 1**.

## 5.2. Experimental

Membranes were prepared by casting a dilute solution (1-2 wt%) of PTMSP in toluene on a glass plate at room temperature. The solution was allowed to evaporate to dryness for 48 hours, and the membranes were then dried under vacuum for 12 hours. To prepare modified membranes, PTMSP and a small amount of the appropriate azide were co-dissolved in toluene, and membranes were then cast from the solution after filtration.

The crosslinking of the azide containing membranes was induced by either UV irradiation or thermal treatment. Photo crosslinking of membranes with azide **BAA**, was carried out at 300 nm in a Rayonet photoreactor with membranes sealed in a wide cylindrical Pyrex container under a nitrogen atmosphere for 3 hours or until the  $N_3$  absorption in the IR disappeared. Photo crosslinking of membranes with fluorinated azide **HFBA**, was carried out under nitrogen atmosphere for a half hour at 254 nm using an

Ace-Hanovia high-pressure quartz mercury-vapor lamp with membranes sealed in a wide diameter cylindrical quartz container. Thermal crosslinking of the membranes was achieved by heating the flat membranes in a vacuum oven at 175 °C for 3-7 hours depending on the amount of azide in the membranes. The crosslinking of the co-polymer membranes was also induced by either UV irradiation or thermal treatment. Photo crosslinking of the membranes was carried out at 254 nm while thermal crosslinking of the membranes was achieved by heating the membranes in vacuum at 250 °C for 2-4 hours depending on the content of azide group in the membranes. After photo treatment, membranes were curled toward the side that was exposed to UV light. Thermally treated membranes remained flat after crosslinking.

Pervaporation of aqueous organic solutions (ethanol/water) through the membranes was carried out in an apparatus illustrated in Fig. 5.1 and 5.2. The feed solution was circulated on the upper side of the membrane, and the pressure of the lower side was kept less than 0.5 mm Hg. The amount of permeate was determined by gravimetry. The composition and flux of the permeating mixture were determined by gas chromatography with a Porapak Q column. The separation factor can be calculated by equation 5.14.

$$\alpha_{ij} = [X_{i1}/X_{j1}]/[X_{i2}/X_{j2}] \quad (5.14)$$

The permeation rate,  $R$  in  $\text{g} \cdot \text{m}/\text{m}^2 \cdot \text{hr}$ , is calculated by equation 5.15

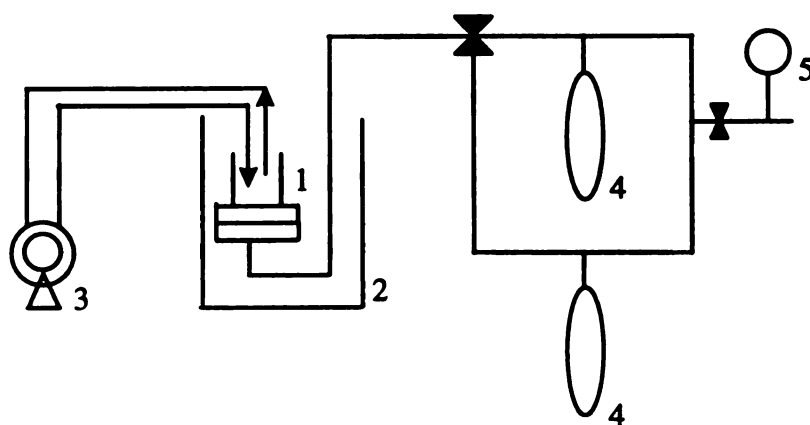


**Figure 5.1.** Pervaporation apparatus. 1. pervaporation cell,  
2. temperature-controlled bath, 3. circulating pump, 4. traps.  
5. vacuum gauge.

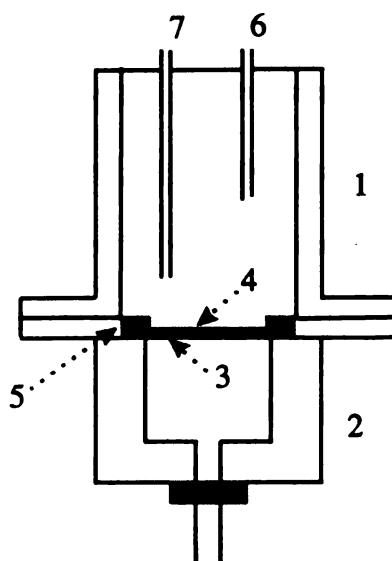


**Figure 5.2.** Pervaporation cell. 1. upper compartment (feed), 2. lower compartment (permeate), 3. perforated stainless disk, 4. polymer membrane, 5. Teflon O-ring, 6. circulation outlet, 7. circulation inlet.

$$R = \frac{(F \cdot \theta)}{(a \cdot t)} \quad (5.15)$$

where  $F$ ,  $q$ ,  $a$  and  $t$  are the permeate flux (g), membrane thickness (m), membrane area ( $\text{m}^2$ ), and time (h), respectively.

Solute probes used for IGC measurement, *n*-hexane, *n*-heptane, *n*-octane, benzene, toluene, and methanol, were obtained from Aldrich and used without further purification. PTMSP and partially 20% allyl brominated PTMSP were used to prepare the columns.

Shown in Table 5.1 are the parameters of the chromatographic columns prepared for IGC measurement. The polymers were dissolved in methylene chloride and deposited

on an inert chromatographic support (AW DMCS Chromosorb W) by slow evaporation of methylene chloride on a rotary evaporator. After vacuum drying for 48 hours with slight heating, the polymer coated chromatographic support was packed into a 1 m  $\times$  1/8" stainless steel column. The actual weight percent of the polymer on the chromatographic support was determined by Thermal Gravimetric Analysis.

**Table 5.1.** Stationary Phases and Column Parameters.

Polymer	Solvent	Support	Packing and column		
			Loading %	polymer mass g	length m
PTMSP	CH <sub>2</sub> Cl <sub>2</sub>	Chromsorb W, AW, DMCS, 80/100	10	0.125	1.0
20%Br-PTMSP	CH <sub>2</sub> Cl <sub>2</sub>	Chromsorb W, AW, DMCS, 80/100	15	0.155	1.0

IGC measurements were carried on a Perkin Elmer 5800 gas chromatograph, equipped with a thermal detector. Helium was used as carrier gas. The air peak was used as a noninteracting marker to correct for dead volume in the column. Pressures at the inlet and outlet of the column were read from the pressure gauge. Flow rates were measured from the end of the column with a soap bubble flow meter.

The swelling measurements for crosslinked PTMSP membranes were carried out by immersing the membranes in the solvents chosen for 12 hours. The swollen membranes were weighed after immediately wiping off the solvent on the surface.

### 5.3. Results and Discussion

#### 5.3.1. Pervaporation of ethanol / water mixtures with PTMSP membrane

Pervaporation of aqueous ethanol solutions of different concentration was carried out at 25 °C. Figure 5.3 shows the permeation composition curve. Comparison of the permeation composition curve with vapor-liquid equilibrium curve<sup>32</sup> shows that separation of ethanol/water solution through PTMSP membranes is comparable to distillation in terms of selectivity. If higher selectivity membranes could be made, pervaporation could easily compete with distillation.

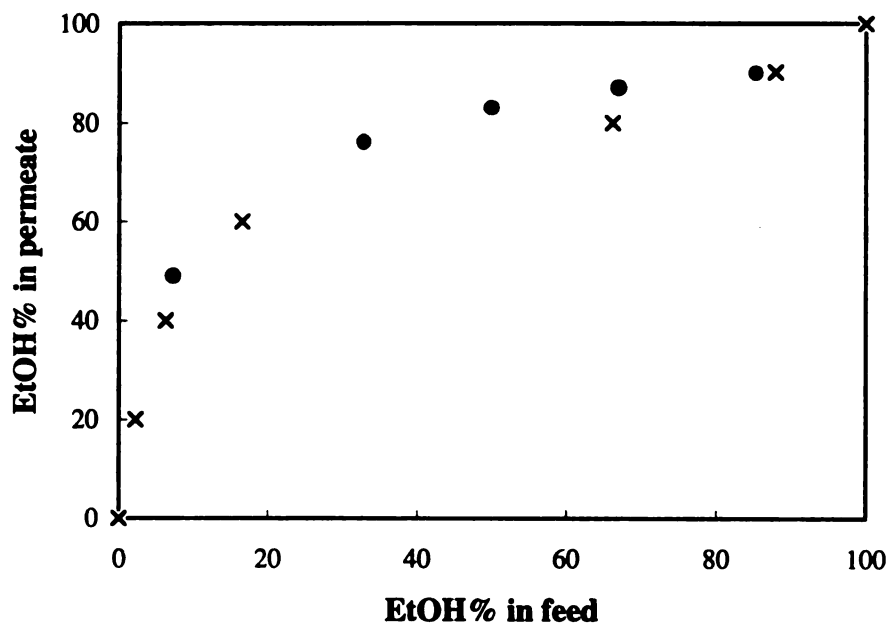


**Figure 5.3.** Composition curves for separation of ethanol/water mixture:

• pervaporation with a PTMSP membrane; × distillation.

### 5.3.2. Pervaporation of dilute aqueous ethanol solution through modified PTMSP membranes

Table 5.2 lists the results for ethanol/water separation through PTMSP and the modified membranes described in Chapters 2, and 4. Compared to PTMSP, the allyl brominated PTMSP membrane (20% Br-PTMSP) had a slightly lower permeation rate and separation factor for ethanol. For the crosslinked membranes with the same amount of added crosslinking agents, thermally crosslinked membranes exhibited higher permeation rates and better separation factors than photo-crosslinked membranes. For the poly[1-trimethylsilyl-1-propyne-*co*-1-(4-bromobutyldimethylsilyl)-1-propyne] membranes, the permeation rate and separation factor are improved at lower contents (e.g. 2%) of bromobutyldimethylsilylpropyne while higher contents (e.g. 7%) caused a decrease of the permeation rate and separation factor. The same behavior was observed for poly[1-trimethylsilyl-1-propyne-*co*-1-(4-azidobutyldimethylsilyl)-1-propyne] membranes. It seems that small amount of bromobutyldimethylsilyl or azidobutyldimethylsilyl side chains increased the solubility of ethanol while the diffusion coefficient was largely unchanged. Increasing the amount of these long side chains likely resulted in the filling of the space between chains, and therefore decreased the free volume. As expected, the uncrosslinked copolymer membranes showed higher permeation rates and separation factors than both thermally crosslinked and photochemically crosslinked membranes. Comparing  $R$  and  $\alpha$  values for different membranes, higher permeation rates are generally associated with a higher separation factor.

**Table 5.2.** Pervaporation results of dilute aqueous ethanol solution through PTMSP and modified membranes at 25 °C.

Membrane		EtOH composition (wt. %)		R(EtOH) (g·m/m <sup>2</sup> ·h) ×10 <sup>3</sup>	$\alpha$ (EtOH/H <sub>2</sub> O)
		feed	permeate		
PTMSP		6.95	46.0	0.926	11.4
20%Allyl-Br-PTMSP		6.27	20.0	0.843	3.14
crosslinked via bis(aryl azides)	2%-BAA-th	4.56	25.9	0.292	7.32
	2%-BAA-ph	6.66	12.7	0.238	2.03
	2%-HFBAA-th	9.95	42.9	0.413	6.79
	2%-HFBAA-ph	7.32	3.34	0.052	0.44
	3%-HFBAA-th	8.3	31.0	0.478	4.96
	3%-HFBAA-ph	7.96	5.83	0.0525	0.715
copolymer membranes	2%-Br-co	4.57	46.7	9.10	18.2
	7%-Br-co	4.79	37.9	6.29	12.7
	2%-N <sub>3</sub> -as cast	5.01	44.2	1.10	14.5
	2%-N <sub>3</sub> -th	4.53	32.23	0.675	9.14
	2%-N <sub>3</sub> -ph	4.52	5.33	0.092	1.19
	7%-N <sub>3</sub> -as cast	4.97	40.75	0.698	13.6
	7%-N <sub>3</sub> -th	4.49	32.81	0.557	9.78
	7%-N <sub>3</sub> -ph	4.40	4.61	0.04	1.05

In membrane entries, number percent represents the mole percent of N<sub>3</sub> in polymer; 'BAA' and 'HFBAA' refer to membranes containing two azides shown in Figure 2.3; 'Br-co' represents brominated copolymer while '-N<sub>3</sub>-' represents azide copolymer; 'th' and 'ph' are thermal-crosslinking and photo-crosslinking, respectively.



### 5.3.3. Determination of the solubility parameter of PTMSP and brominated PTMSP

There has been no report of the experimental value of the solubility parameter of PTMSP, and estimating the solubility parameter of PTMSP by IGC seems to be attempted in the present work for the first time. The obtained values will be compared to the values calculated by the group contribution method later in this chapter with Equation 5.13. For PTMSP, the calculated value of  $\delta$  is  $17.6 \text{ (J/cm}^3\text{)}^{1/2}$ ; the values for ethanol and water are 26.0 and 47.8, respectively.<sup>19</sup> In order to use the solubility parameter,  $\delta$ , to explain ethanol/water permeation rate and selectivity, inverse gas chromatography was used to determine the solubility parameter of pure PTMSP and brominated PTMSP. The parameters of the chromatographic columns prepared with these polymer are described in the Experimental.

The probes used in the study were *n*-hexane, *n*-heptane, *n*-nonane and *n*-decane (abbreviated as *n*-C<sub>6</sub>, *n*-C<sub>7</sub>, *n*-C<sub>9</sub> and *n*-C<sub>10</sub>). Specific retention volumes measured as a function of temperature for the four probes are shown in Table 5.3. The specific retention volumes of probes on both PTMSP and brominated PTMSP are temperature dependent and decreased with the increasing of temperature for each probe. Similar results had been obtained for the other polymer-probe systems.<sup>33, 34</sup>

The probe parameters including the vapor pressures  $p_i^0$ , the molar volume  $V_i$  and solubility parameters  $\delta_i$  at different temperatures were taken from literature sources, as listed in Table 5.4.

**Table 5.3.** Specific retention volumes of probes as a function of temperature for PTMSP and 20 % brominated PTMSP.

		$V_g^0(\text{cm}^3/\text{g})$			
	T(K)	<i>n</i> -C <sub>6</sub>	<i>n</i> -C <sub>7</sub>	<i>n</i> -C <sub>9</sub>	<i>n</i> -C <sub>10</sub>
PTMSP	433	4445.0	97.0	489	1132
	443	33.9	68.4	341	814
	453	25.3	53.1	244	536
20%Br-PTMSP	433	15.2	31.9	147	324
	443	11.3	22.7	96.3	196
	453	7.61	15.2	60.9	122

**Table 5.4.** Probe parameters as a function of temperature.

T	probes	$p_1^0(\text{mm Hg})$	$V_1(\text{cm}^3/\text{mol})$	$\delta_1(\text{cal}/\text{cm}^3)^{1/2}$
433K	<i>n</i> -C <sub>6</sub>	6739	168	4.9
	<i>n</i> -C <sub>7</sub>	3432	181	5.4
	<i>n</i> -C <sub>9</sub>	959	209	6.1
	<i>n</i> -C <sub>10</sub>	520	231	6.2
443K	<i>n</i> -C <sub>6</sub>	8053	173	4.6
	<i>n</i> -C <sub>7</sub>	4192	185	5.2
	<i>n</i> -C <sub>9</sub>	1225	213	5.9
	<i>n</i> -C <sub>10</sub>	680	234	6.1
453K	<i>n</i> -C <sub>6</sub>	9359	177	4.4
	<i>n</i> -C <sub>7</sub>	5069	189	5.0
	<i>n</i> -C <sub>9</sub>	1545	217	5.8
	<i>n</i> -C <sub>10</sub>	877	238	5.9

The Flory-Huggins interaction parameter,  $\chi$ , was calculated as a function of temperature for each probe using equation 5.6, and the values are tabulated in Table 5.5. The polymer-liquid system exhibited unusual behavior: Flory-Huggins interaction parameters for all polymer-liquid pairs under all temperatures tested are negative and increase with increasing temperature. Negative Flory-Huggins interaction parameter values have been reported for cellulose nitrate-propylacetate,<sup>35</sup> cellulose nitrate-acetone and cellulose acetate-acetone systems.<sup>36</sup> Although the polymer-liquid interaction parameter was expected to be inversely dependent on absolute temperature as originally formulated, as now empirically defined it depends in an unspecific way on temperature.<sup>18</sup> The solubility parameters  $\delta_2$  for PTMSP and brominated PTMSP were evaluated from Equation 5.5. Using the solubility parameters,  $\delta_1$ , of the probes at the same temperature from Table 5.4, values of  $\delta_2$  for the polymers at different temperatures were obtained from the slopes of the plots of  $(\delta_1^2/RT - \chi/V_1)$  against  $\delta_1$  (Figure 5.4) and are listed in Table 5.6. However, most values of solubility parameters are measured and reported at room temperature. A correction must therefore be made to bring  $\chi$  and  $\delta_2$  to room temperature.

The temperature dependence of  $\chi$  in the temperature range tested fits an equation of the form

$$\chi = \alpha + \beta/T \quad (5.16)$$

where  $\alpha$  and  $\beta$  are the intercept and slope of the line and T is the absolute temperature. The constants were evaluated from a least-squares analysis of the data and are summarized

in Table 5.7. If one assumes that this relationship remains valid at low temperatures (which is reasonable), then  $\chi$  at 20 °C can be estimated from extrapolation of the high temperature data. The  $\chi$  values so obtained are also listed in Table 5.7. The regression in most cases were good. Using the solubility parameters and the molar volumes for the probes at 20 °C from literatures,<sup>37,38</sup> the plots of  $(\delta_1^2/RT-\chi/V_1)$  against  $\delta_1$  did not yield a good linear correlation. For long polymer chains the solubility parameter is independent of temperature.<sup>18</sup> Thus solubility parameters at 433K will be used to represent the values at room temperature.

**Table 5.5.** Calculated Flory-Huggins interaction parameters  $\chi$  of probes for PTMSP and 20% allyl brominated PTMSP.

		$\chi$			
	T(K)	<i>n</i> -C <sub>6</sub>	<i>n</i> -C <sub>7</sub>	<i>n</i> -C <sub>9</sub>	<i>n</i> -C <sub>10</sub>
PTMSP	433	-1.59	-1.83	-2.39	-2.74
	443	-1.47	-1.68	-2.28	-2.68
	453	-1.34	-1.61	-2.19	-2.53
Br-PTMSP	433	-0.51	-0.71	-1.18	-1.49
	443	-0.39	-0.57	-1.01	-1.26
	453	-0.14	-0.36	-0.80	-1.04

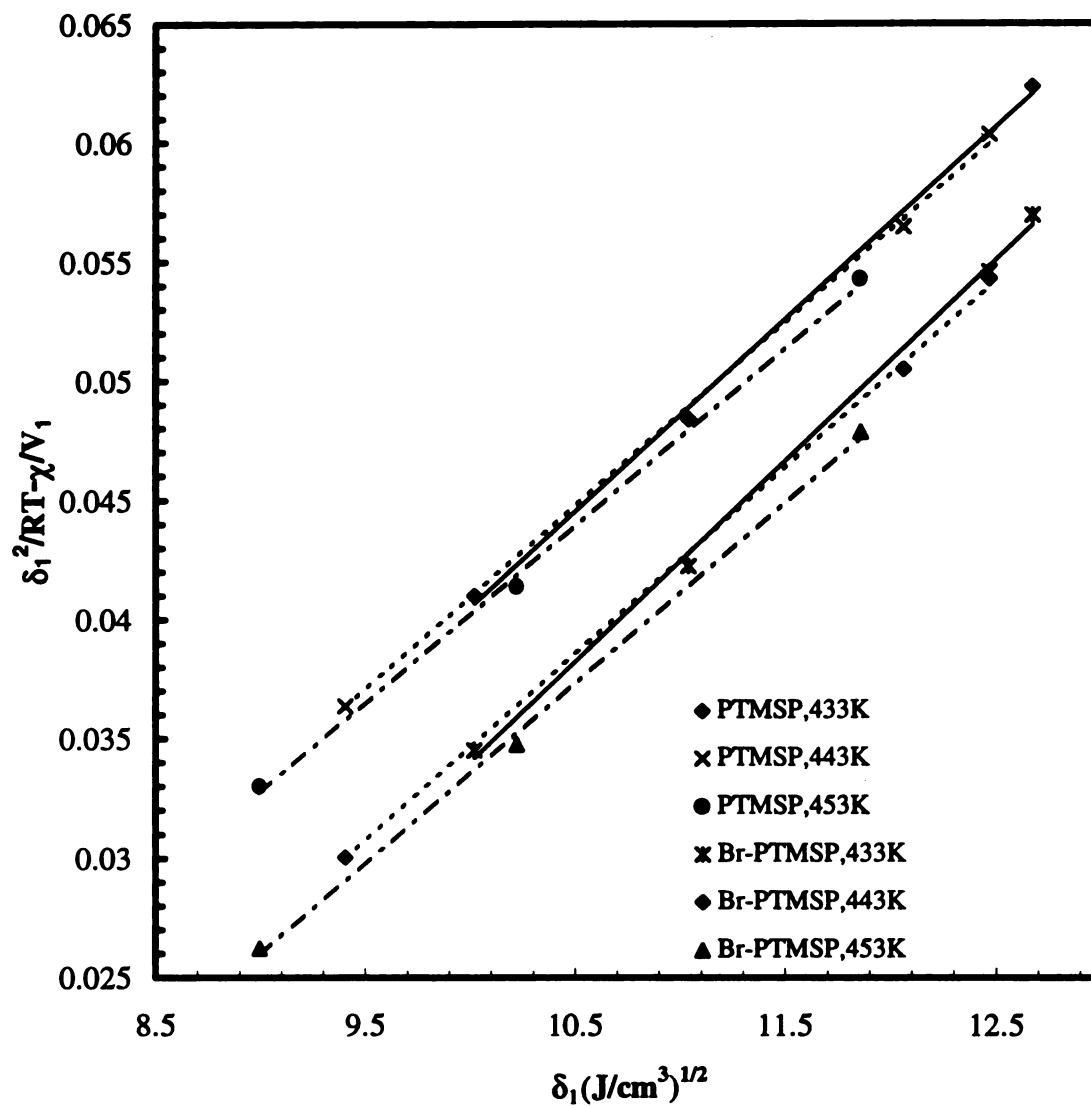


**Figure 5.4.** Estimation of the solubility parameters of PTMSP and 20% brominated PTMSP from Flory-Huggins parameters.

**Table 5.6.** The solubility parameters  $\delta_2$  of PTMSP and 20% allyl brominated PTMSP at different temperatures.

$\delta_2(\text{J/ cm}^3)^{1/2}$			
T (K)	433	443	453
PTMSP	14.5	14.4	14.3
Br-PTMSP	15.1	14.6	14.6

**Table 5.7.** Temperature dependence of probe parameters in PTMSP and 20 % allyl brominated PTMSP.

polymer	probes	slope	intercept	correlation coefficient	$\chi(20^\circ\text{C})$
PTMSP	<i>n</i> -C <sub>6</sub>	-2412.84	3.976411	0.989	-4.25854
	<i>n</i> -C <sub>7</sub>	-2101.18	3.038822	0.9548	-4.13243
	<i>n</i> -C <sub>9</sub>	-2018.81	2.271761	0.9999	-4.61838
	<i>n</i> -C <sub>10</sub>	-2119.85	2.136208	0.929	-5.09876
Br-PTMSP	<i>n</i> -C <sub>6</sub>	-3543.41	7.656518	0.9518	-4.43705
	<i>n</i> -C <sub>7</sub>	-3421.5	7.176286	0.9845	-4.50119
	<i>n</i> -C <sub>9</sub>	-3863.8	7.724014	0.9929	-5.46301
	<i>n</i> -C <sub>10</sub>	-4400.52	8.670446	1	-6.3484

#### **5.3.4. Estimation of the solubility parameter of the crosslinked membranes by swelling experiments**

To investigate the relationship of the solubility parameter of the crosslinked polymers to the results of ethanol/water separation by pervaporation, the solubility parameters of the crosslinked membranes were estimated by swelling experiments. Figure 5.5 and Figure 5.6 show typical results. All crosslinked polymers exhibited two peaks; the peak at low values of  $\delta$  correspond to swelling by good solvents, while the peak of higher  $\delta$  seems to be pore-size related. Considerable scatter in equilibrium swelling plots has been reported for a large number of polymers.<sup>39</sup> Despite this limitation, the swelling coefficients of thermally crosslinked membranes and photo-crosslinked membranes with same degree of crosslinking reach a swelling maxima around the same solubility value. However, as seen in Table 5.1, the separation factors of ethanol/water pervaporation are significantly different. Considering the higher density of photo-crosslinked membranes compared to thermally crosslinked membranes (Table 2.3 and Table 4.4), the free volume in the membranes seems to play more important role where the solubility parameters are not considerably different. In another words, the diffusion selectivities are different for photo-crosslinked and thermal-crosslinked membranes while the solubility selectivities are similar. The overall selectivity, which is the product of diffusion selectivity and solubility selectivity, is therefore different for the two classes of membranes.

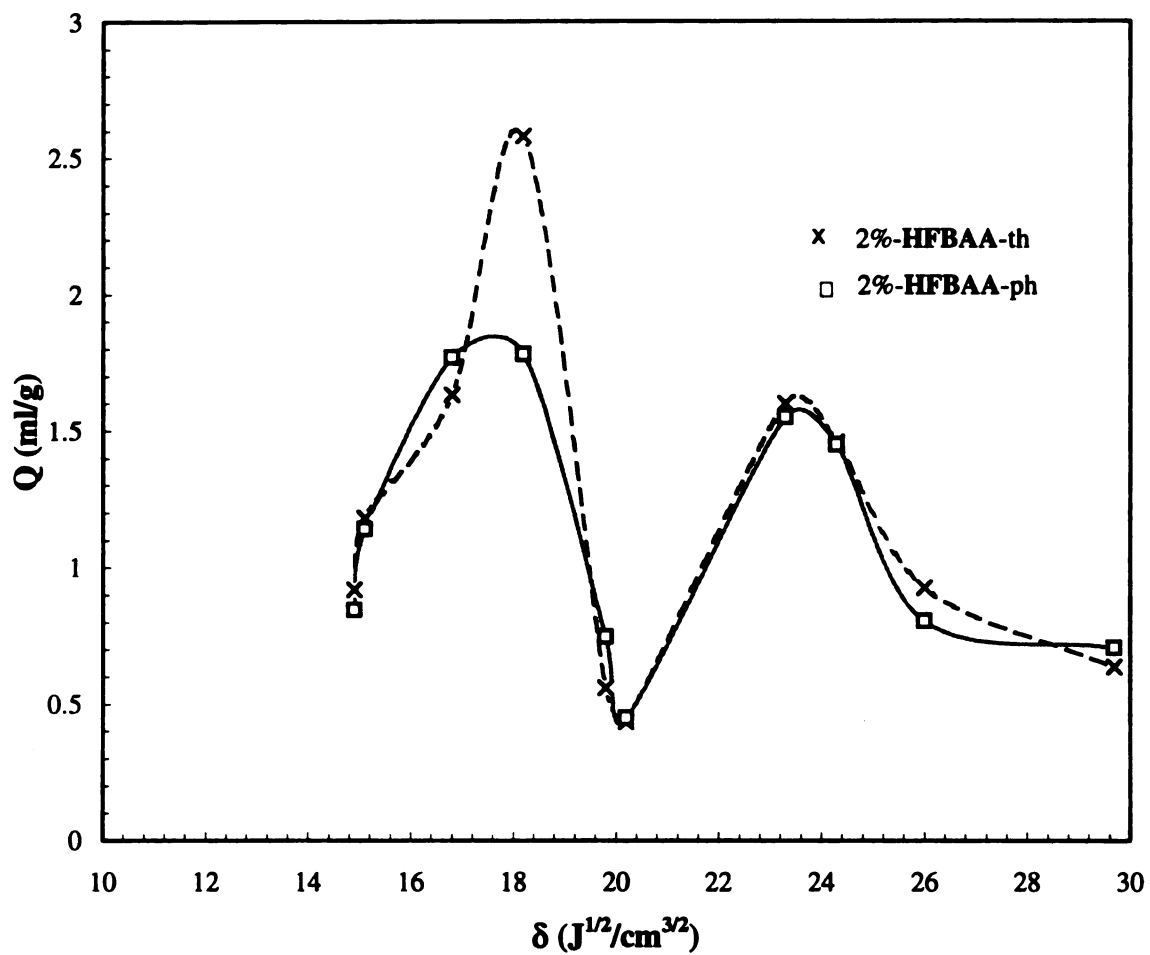


**Figure 5.5.** The plot of the swelling coefficient,  $Q$ , for **HFBAA** (2%) crosslinked PTMSP as a function of the solubility parameter of various solvents.



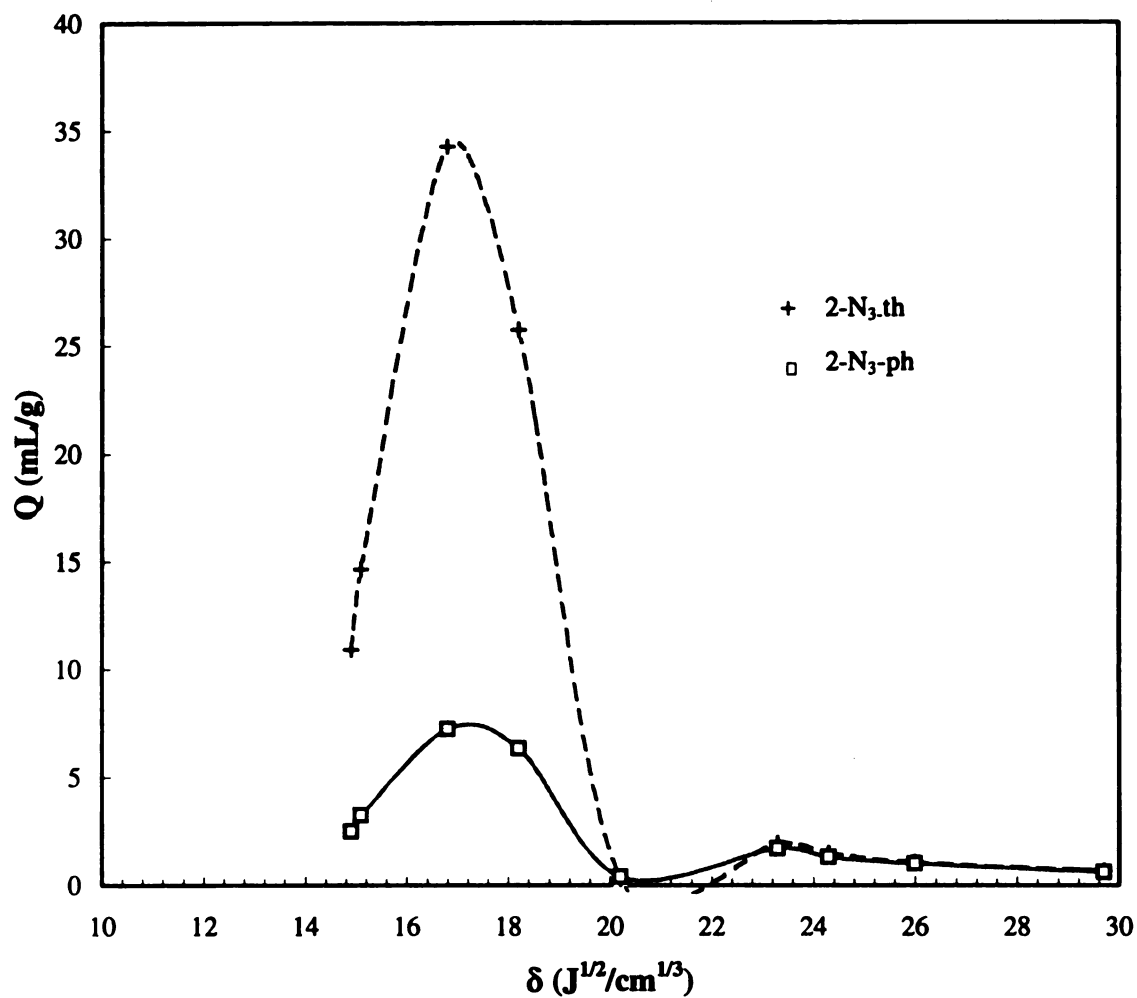


**Figure 5.6.** The plot of swelling coefficient  $Q$  of crosslinked poly[1-trimethylsilyl-1-propyne-*co*-1-4-azidobutyldimethylsilyl-1-propyne] (2%  $\text{N}_3$ ) as a function of the solubility parameter of various solvents.

### **5.3.5. Estimation of the solubility parameter of some membranes by group contribution method**

The solubility parameters of pervaporation membranes were also calculated by group contribution method with Equation 5.13 using the group molar attraction constants in Appendix I. The results are listed in Table 5.8, along with those estimated from inverse gas chromatography and swelling measurements. One can see differences between the values of the solubility parameters calculated by different methods. Given the variability, the solubility parameter alone cannot be used to predict the separation factor in pervaporation with PTMSP films.

**Table 5.8.** Solubility parameters of polymer membranes used for ethanol/water pervaporation.

membrane		density (g/cm <sup>3</sup> )	$\delta$ (J <sup>1/2</sup> /cm <sup>3/2</sup> )			$\alpha$ (EtOH/H <sub>2</sub> O)
			IGC	Swell	Group	
PTMSP		0.9260	14.5	**	17.6	11.4
20% Allyl Br-PTMSP		0.9415	15.1	**	16.3	3.14
crosslinked via bis(aryl azide)s	2%-BAA-th	0.9330	**	**	***	7.32
	2%-a-ph	0.9350	**	**	***	2.03
	2%-HFBA-th	0.9380	**	18.0	***	6.79
	2%-HFBA-ph	0.9470	**	17.6	***	0.44
	3%-HFBA-th	0.9470	**	18.2	***	4.96
	3%-HFBA-ph	0.9490	**	18.0	***	0.715
copolymer membranes	2%-Br-co	0.9340	*	**	17.6	18.2
	7%-Br-co	0.9270	*	**	17.4	12.7
	2%-N <sub>3</sub> -as cast	0.9285	*	**	***	14.5
	2%-N <sub>3</sub> -th	0.9340	**	17.0	***	9.14
	2%-N <sub>3</sub> -ph	0.9390	**	17.0	***	1.19
	7%-N <sub>3</sub> -as cast	0.9325	*	**	***	13.6
	7%-N <sub>3</sub> -th	0.9330	**	17.8	***	9.78
	7%-N <sub>3</sub> -ph	0.9405	**	17.8	***	1.05

\* Experiment not performed

\*\* Unable to measure

\*\*\*Data used for calculation not available

In membrane entries, number percent represents the mole percent of N<sub>3</sub> in polymer; 'BAA' and 'HFBA' refer to membranes containing two azides shown in Figure 2.3; 'Br-co' represents brominated copolymer while '-N<sub>3</sub>-' represents azide copolymer; 'th' and 'ph' are thermal-crosslinking and photo-crosslinking, respectively.

## 5.4. Conclusions

The separation of ethanol from water in the dilute aqueous solution by pervaporation has been performed on PTMSP and a variety of modified PTMSP membranes. Of the modified membranes, poly[1-trimethylsilyl-1-propyne-co-1-(4-bromobutyldimethylsilyl)-1-propyne] membranes and poly[1-trimethylsilyl-1-propyne-co-1-(4-azidobutyldimethylsilyl)-1-propyne] membranes showed improved separation factors compared to PTMSP while all crosslinked membranes showed lower separation factors. The solubility parameters of some membranes were estimated with inverse gas chromatography, swelling measurements and by the group contribution method. It is not possible to obtain a quantitative relationship between the solubility parameter and selectivity for ethanol/water separation. One has to consider the free volume of the polymer membranes together with the solubility parameter of the polymer.

## 5.5. References

1. Hennepe, H. J. C.; Bargeman, D.; Mulder, M. H. V.; Smolders, C. A. J. *Membr. Sci.* **1987**, 35, 39.
2. Hickery, P. J.; Slater, C. S. *Separation and Purification Methods* **1990**, 19(1), 93.
3. Park, C.-H.; Geng, Q. *Separation and Purification Methods* **1992**, 21(2), 127.

4. Hickery, P. J.; Juricic, F. P.; Slater, C. S. *Separation Science and Technology* **1992**, 27(7), 843.
5. Maiorella, B. L.; Blanch, H. W.; Wilke, C. R. *Biotechnol. Bioeng.* **1984**, 26, 1003.
6. Itoh, T.M.; Toya, H.; Ishihara, K.; Shinohara, I. *J. Appl. Polym. Sci.* **1985**, 30,179.
7. Yoshikawa, M.; Yukoshi, T.; Sanui, K.; Ogata, N. *J. Polym. Sci.: Part A: Polym Chem.* **1986**, 24, 1585.
8. Huang, R. Y. M., Feng, X. *Separation Science and Technology* **1992**, 27(12), 1583.
9. Yoshikawa, M.; Hara, H.; Tanigaki, M.; Guiver, M., Matsuura, T. *Polymer* **1992**, 33(22), 4805.
10. Brun, J.-P.; Larchet, C.; Bluvestre, G.; Auclair, B. *J. Membrane Sci.* **1985**, 25, 55.
11. Yoshikawa, M.; Ohsawa, T., Tanigaki, M., Eguchi, W. *J. Appl. Polym. Sci.* **1989**, 37, 299.
12. Kimura, S.; Nomura, T. *Membrane* **1983**, 8, 177.
13. Ishihara, K.; Nagase, Y.; Matsui, K. *Makromol. Chem., Rapid Commun.* **1986**, 7, 43.
14. Masuda, T.; Tang, B., Higashimura, T. *Polym. J.* **1986**, 18, 565.
15. Nagase, Y.; Ishihara, K.; Matsui, K. *J. Polym. Sci.: Part B: Polym. Phys.* **1990**, 28, 377.

16. Nagase, Y.; Sugimoto, K.; Takamura, Y.; Matsui, K. *J Polym. Sci.* **1991**, *43*, 1227.
17. Nagase, Y. ; Takamura, Y.; Matsui, K. *J Polym. Sci.* **1991**, *42*, 185.
18. *CRC Handbook of Solubility Parameters and Other Cohesion Parameters*, Barton, Allan F. M., CRC Press, **1991**.
19. Sperling, L. H. *Introduction to Physical Polymer Science*, John Wiley & Sons, Inc., **1992**.
20. Hilderbrand, J. H.; Scott, R. W.; Prausnitz, J. M. *Regular and Related Solutions*, Van Nostrand: New York, **1972**.
21. Dipaola-Baranyi, G.; Guillet, J. E. *Macromolecules* **1978**, *11*, 228.
22. Orwoll, R. A. *The Polymer-Solvent Interaction Parameter*, Rubber Chem. Technol., **1977**, *50*, 451.
23. Flory, P. J. *Disc. Farad. Soc.* **1970**, *2*, 672.
24. Bolvari, A. E.; Ward, T. C.; Koning, P. A.; Sheehy, D. P. "Experimental Techniques for Inverse Gas Chromatography" in *Inverse Gas Chromatography*, American Chemical Society, Washington DC, 1989.
25. Dreishach, D. R. *Adv. Chem. Ser.* **1959**, *No. 15*; **1959**, *No. 22*; and **1961**, *No. 29*.
26. McGlashan, M. L.; Potter, D. J. B. *Proc. R. Soc. London. Ser. A.* **1962**, *267*, 478.
27. Guggenheim, F. A.; Wormald, C. J. *J. Chem. Phys.* **1965**, *42*, 3775.
28. Bristow, G. M.; Watson, W. F. *Trans Farady Soc.* **1958**, *54*, 1731.
29. Sperling, L. H. *Introduction to Physical Polymer Science* ; John Wiley & Sons, Inc., **1992**, p 68.

30. Small, P. A. *J. Appl. Chem.* **1953**, 3, 71.
31. Hoy, K. L. *J. Paint Technol.* **1970**, 46, 76.
32. Baker, R. W. et al. *Membrane Separation Systems*, Noyes Data Corporation, Park Ridge, **1991**.
33. Yampolskii, Yu. P.; Kaliuzhnyi, N. E., Durgarjan, S. G. *Macromolecules* **1986**, 19, 846.
34. Özdemir, E.; Açikses, Coskun, M. *Macromolecular Reports* **1992**, A29(suppl. 1), 63.
35. Sperling, L. H. *Introduction to Physical Polymer Science*, John Wiley & Sons, Inc., **1992**, p 77.
36. *CRC Handbook of Solubility Parameters and Other Cohesion Parameters*, Barton, Allan F. M., CRC press, **1991** p 380.
37. Barton, A. F. M. *Chem. Rev.* **1975**, 75, 731.
38. Stephenson, R. M.; Malanowski, S., *Handbook of Thermoodynamics of Organic Compounds*, Elsevier, **1987**.
39. *CRC Handbook of Solubility Parameters and Other Cohesion Parameters*, Barton, Allan F. M.; CRC Press, **1991**, p 418.

## **Chapter 6**

### **Summary and Future Work**

#### **6.1. Summary**

The major objective of the current study has been to understand the structural origins of decline of the high gas permeability of poly[1-trimethylsilyl]-1-propyne] and to find a way to inhibit the decline. The study demonstrated that the permeability decline was limited by crosslinking the PTMSP membranes after the membranes were formed, which supports the model we proposed for the mechanism of permeability decline. When PTMSP is dissolved in a solvent to cast a film, the polymer-polymer interaction is largely replaced by the polymer-solvent interaction, which increases the interpolymer distance in solution. During the film formation, the solvent molecules vaporize and the polymer-polymer interaction again replaces the polymer-solvent interaction. During the last stage of film formation, the solution becomes extremely viscous and the rate of solvent vaporization is so fast that excess free volume is frozen in the polymer matrix.

Our understanding is that the permeability decrease is caused by the slow interdiffusion of polymer coils in the solid state. From solution, the polymer is deposited under kinetic control as an ensemble of spheres. With time, the chains interdiffuse causing an increase in the density and decrease in free-volume and the permeability. Crosslinking



the polymer chains after the membrane formation suppressed the chain-chain interdiffusion and stabilized the permeability of the membranes.

Among the methods attempted to introduce a crosslinker into PTMSP films, physical addition of bis(aryl azides) and copolymerization of 1-trimethylsilyl-1-propyne with 1-(4-bromobutyldimethyl)-1-propyne were two routes which led to effective crosslinking upon thermal or photo treatment. On the other hand, attempts to introduce crosslinking sites through allylic substitution failed despite a variety of approaches, although functionalization of PTMSP through free radical reaction has been shown to yield brominated polymer. The poor reactivity of the allylic methyl group in PTMSP again demonstrated the effect of the unique structure of this polymer. The rigid, nonlinear and irregular main-chain conformation achieved during polymerization reaction is caused by the large side-chain groups. These groups shield the main-chain as well as the allylic methyl groups, which results in the limited accessibility of these groups.

Compared to PTMSP, crosslinking stabilized the gas permeability at a lower value. For all film modifications investigated in this study, the gas permeabilities decreased while the selectivities increased upon crosslinking. These results tend to follow design arguments that have been recognized in the past decade, that is, the separation factor for gas pairs varies inversely with the permeability of the more permeable gas of the specific pair. In another words, one always has to sacrifice permeability in order to improve the selectivity. Lloyd Robeson demonstrated the “upper bound” concept for the limits of separation factor for specific value of permeability by collecting data from over 300 references.<sup>1</sup> Figure 6.1 shows the data for O<sub>2</sub>/N<sub>2</sub> separation cited in reference 1. Although

crosslinking PTMSP decreased gas permeability, some of the crosslinked PTMSP membranes are located above the upper bound which represents the present state of the technology as stated by the author.

The replacement of one of the methyl groups on the silicon atom of PTMSP by longer alkyl groups decreases  $P_{O_2}$  and increases  $O_2/N_2$  selectivity.<sup>2</sup> This is believed to be due to filling of the micropores by the alkyl groups, the crosslinker in this case, which leads to an overall loss of free volume and decrease in average micropore size. The phenomenon is usually not encountered for polymers in which the alkyl groups are attached to carbons on the polymer backbone. In such cases the alkyl groups tend to act as a permanent spacer which increase interchain spacing and hence free volume and gas permeability. Presumably the higher mobility of Si relative to C allows the pendent chains to twist and fill the interchain spaces instead of forcing the parallel chain segments farther apart. However, this effect could not be tested since our attempts to add a crosslinker to a carbon attached to the polymer backbone, that is, to introduce a crosslinker to the allylic methyl on the PTMSP polymer chain, has proved unsuccessful. One possible solution is to use a monomer that has a crosslinker attached to the allylic methyl of the monomer, that upon polymerization will yield the desired functionalized polymer. However, highly crowded disubstituted acetylene monomers, such as  $EtC\equiv CSiMe_3$ , have not yet been polymerized.<sup>3</sup> Exploring catalysts for the polymerization of those highly crowded disubstituted acetylene monomers will be of continuing interest in this field.

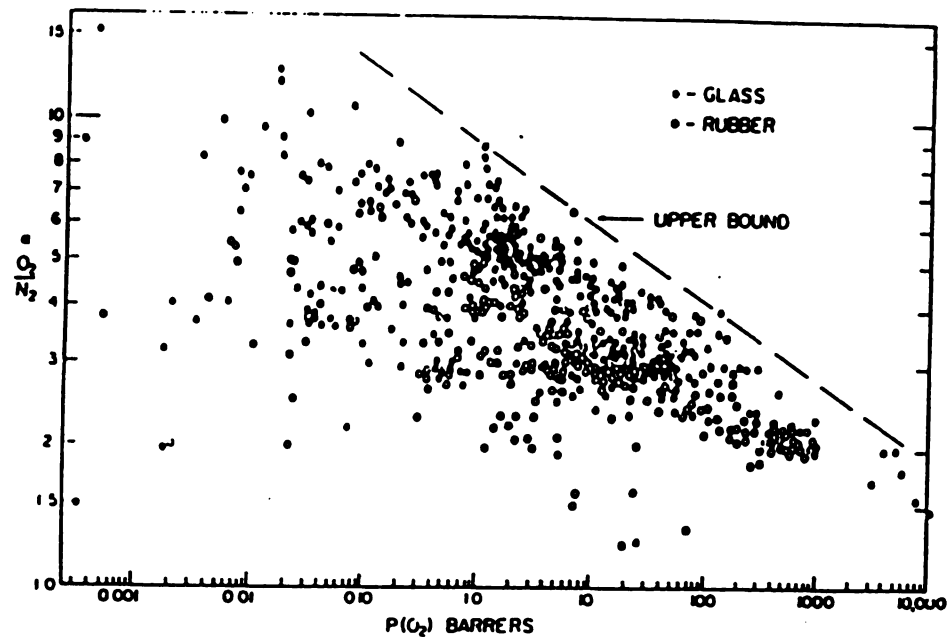
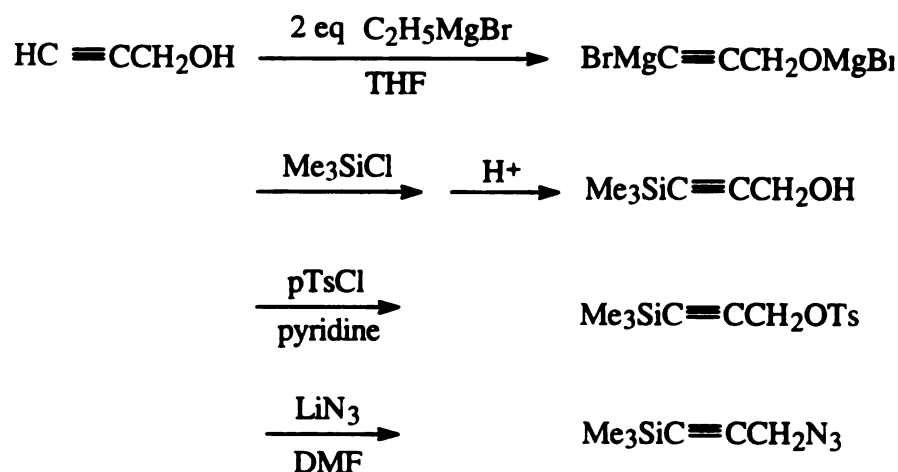


Figure 6.1. Literature data for  $O_2/N_2$  separation factor versus  $O_2$  permeability.

## 6.2. Future work

Introducing the azide group  $-N_3$  into PTMSP is a successful method that leads to crosslinked PTMSP. The current study showed that azide group can be added to the polymer through two routes: the physical addition of additives containing azide groups, and via copolymerization where  $-N_3$  is attached to one of the alkyl groups on the silicon atom. It would be very interesting if  $-N_3$  can be added to the carbon attached to the PTMSP backbone, assuming a catalyst is available to polymerize  $N_3CH_2C\equiv CSiMe_3$ . Figure 6.2 illustrates a scheme that might be used to obtain the monomer  $N_3CH_2C\equiv CSiMe_3$ .



**Figure 6.2.** Possible synthetic routes to  $N_3CH_2C\equiv CSiMe_3$ .

Although the pervaporation of ethanol/water with the PTMSP and modified membranes has been studied in this work, most attention has been focused on the gas permeability of modified membranes. More work could be done on the pervaporation of organic solvent mixtures with crosslinked membranes. PTMSP is believed to be an organic-selective membrane considering that ethanol is more permeable than water through the membrane. However, PTMSP is not a good candidate for separation of organic mixtures because PTMSP is soluble in most organic solvents. Compared to PTMSP, crosslinked PTMSP membranes are better in terms of solvent-resistance, and they could be used to investigate a broad range of liquid-liquid separations.

### 6.3. References

1. Robeson, L. M. *J. Membr. Sci.* **1991**, *62*, 165.
2. Takada, K.; Matsuya, H.; Musuda, T.; Higashimura, T. *J. Appl. Polym. Sci.* **1985**, *30*, 1605.
3. Masuda, T.; Higashimura T. *Adv. Polym. Sci.* **1986**, *81*, 121.

Appendix I. Group molar attraction constants at 25 °C.

Group	G	Group	G	Group	G		
—CH <sub>3</sub>	214	Ring	5-membered	105–115	Br	single	340
—CH <sub>2</sub> —	133	Ring	6-membered	95–105	I	single	425
—CH <	28	Conjugation		20–30	CF <sub>2</sub>	n-fluorocarbons only	150
> C <	–93	H	(variable)	80–100	CF <sub>3</sub>		274
CH <sub>2</sub> =	190	O	ethers	70	S	sulfides	225
—CH =	111	CO	ketones	275	SH	thiols	315
> C =	19	COO	esters	310	ONO	nitrates	~ 440
—CH=C<	285	CN		410	NO <sub>2</sub>	(aliphatic nitro-compounds)	~ 440
—C=C—	222	Cl	(mean)	260	PO <sub>4</sub>	(organic phosphates)	~ 500
Phenyl	735	Cl	single	270	Si	(in silicones)	– 38
Phenylene	658	(o,m,p)	twinned as in	> CCl <sub>2</sub>	260		
Naphthyl	1146	Cl	triple as in	≡ CCl <sub>3</sub>	250		

Source: P. A. Small, *J. Appl. Chem.*, 3, 71(1953).

MICHIGAN STATE UNIV. LIBRARIES



31293015796026